AFOSR-TR- 81-0073

LEVEL ⑤

FINAL TECHNICAL REPORT

15 DECEMBER 1977 TO 30 SEPTEMBER 1980

AD A094644

REGIONAL SEISMIC WAVE PROPAGATION

A079982

30 NOVEMBER 1980

RONDOUT ASSOCIATES, INCORPORATED
P.O. BOX 224
STONE RIDGE, NY 12484

Sponsored by
Advanced Research Projects Agency (DOD)
ARPA Order No. 3291-13
Monitored by AFOSR under Contract F49620-78-C-0043

81 2 2 064

UNCLASSIFIED

SECURITY CLASSIFICATION OF THIS PAGE UNCLASSIFIED

REPORT DOCUMENTATION PAGE — READ INSTRUCTIONS BEFORE COMPLETING FORM

1. REPORT NUMBER: 18 19 AFOSR-TR-81-0073
2. GOVT ACCESSION NO.: AD-A094644
3. RECIPIENT'S CATALOG NUMBER: 12 96

4. TITLE (and Subtitle): 6 Regional Seismic Wave Propagation.

5. TYPE OF REPORT & PERIOD COVERED: 9 Final rept. 15 Dec [redacted]77-30 Sep[redacted]80

6. PERFORMING ORG. REPORT NUMBER: 14 03-80-3

7. AUTHOR(s): 10 Paul W. Pomeroy [redacted] Thomas C. Chen

8. CONTRACT OR GRANT NUMBER(s): 15 F49620-78-C-0043, ARPA Order-3291

9. PERFORMING ORGANIZATION NAME AND ADDRESS:
Rondout Associates, Incorporated
P.O. Box 224
Stone Ridge, NY 12484

10. PROGRAM ELEMENT, PROJECT, TASK AREA & WORK UNIT NUMBERS: 61102F 3291/30

11. CONTROLLING OFFICE NAME AND ADDRESS:
AFOSR /NP
Bolling AFB, DC 20332

12. REPORT DATE: 11 30 Nove[redacted]980

13. NUMBER OF PAGES: 87

14. MONITORING AGENCY NAME & ADDRESS (if different from Controlling Office): 16 3291 17 30

15. SECURITY CLASS. (of this report): Unclassified

15a. DECLASSIFICATION/DOWNGRADING SCHEDULE

16. DISTRIBUTION STATEMENT (of this Report)
Approved for public release; distribution unlimited.

17. DISTRIBUTION STATEMENT (of the abstract entered in Block 20, if different from Report)

18. SUPPLEMENTARY NOTES

19. KEY WORDS (Continue on reverse side if necessary and identify by block number)

Regional Distance Wave Propagation
Seismic Discrimination Methods
Propagation Characteristics-Comparative Study
Lg Wave-Review
Attenuation-Lg, Intermediate-Period Rayleigh Waves
Seismic Noise-Review
Magnitude-Yield Relation
Yield-Related Parameters

20. ABSTRACT (Continue on reverse side if necessary and identify by block number)

In a review of studies on the seismic phase Lg, we describe its particle motion, dispersion, spectral content, mode of propagation, and magnitude-scale; we also tabulate the regional velocity, attenuation, and propagation efficiency for this seismic phase.

The characteristics of Lg-wave propagation in the eastern and western United States are compared with those in different regions of the Soviet Union. Possible discriminants such as (i) Lg vs. P

DD FORM 1 JAN 73 1473

393833

UNCLASSIFIED

SECURITY CLASSIFICATION OF THIS PAGE (When Data Entered)

amplitudes, (ii) Lg/P amplitude ratios as a function of distance, (iii) group velocities of Lg at amplitude maxima, and (iv) Lg energy ratios are found, similar to attenuation and group velocity, to be highly dependent on the propagation path. The valid application of these quantities to the problem of earthquake-explosion discrimination will therefore require regional studies more detailed than previously assumed.

As a preliminary effort to quantify the propagation characteristics of seismic waves on a regional basis, we have measured the attenuation rates of Lg waves for the eastern United States, and the western and central portions of the Soviet Union. We have also proposed two magnitude scales for Lg waves and intermediate-period (8-13 sec) Rayleigh waves in the eastern U.S. A plotting of M_S (from 8-13 sec Rayleigh waves) vs. M_{Lg} (from 0.3-1.0 sec Lg waves) for eight earthquakes and one underground nuclear explosion in the eastern U.S. shows no separation between the two populations.

A re-evaluation of the magnitude-yield relation and an examination of physical parameters which may be relevant to the estimated yield of underground nuclear explosions were performed. The preliminary results indicate that (i) the m_b vs. yield relation shows regional differences and dependence on the source medium, and (ii) the collapse volume and the diameter of the collapsed crater are usually proportional to the estimated yield.

Table of Contents

Table of Illustrations

Table of Illustrations

Table of Illustrations

List of Tables

Abstract

In a review of studies on the seismic phase Lg, we describe its particle motion, dispersion, spectral content, mode of propagation, and magnitude-scale; we also tabulate the regional velocity, attenuation, and propagation efficiency for this seismic phase.

The characteristics of Lg-wave propagation in the eastern and western United States are compared with those in different regions of the Soviet Union. Possible discriminants such as (i) Lg vs. P amplitudes, (ii) Lg/P amplitude ratios as a function of distance, (iii) group velocities of Lg at amplitude maxima, and (iv) Lg energy ratios are found, similar to attenuation and group velocity, to be highly dependent on the propagation path. The valid application of these quantities to the problem of earthquake-explosion discrimination will therefore require regional studies more detailed than previously assumed.

As a preliminary effort to quantify the propagation characteristics of seismic waves on a regional basis, we have measured the attenuation rates of Lg waves for the eastern United States, and the western and central portions of the Soviet Union. We have also proposed two magnitude scales for Lg waves and intermediate-period (8-13 sec) Rayleigh waves in the eastern U.S. A plotting of M_S (from 8-13 sec Rayleigh waves) vs. M_{Lg} (from 0.3-1.0 sec Lg waves) for eight earthquakes and one underground nuclear explosion in the eastern U.S. shows no separation between the two populations.

A re-evaluation of the magnitude-yield relation and an examination of physical parameters which may be relevant to the estimated yield of underground nuclear explosions were performed. The preliminary results indicate that (i) the m_b vs. yield relation shows regional differences and dependence on the source medium, and (ii) the collapse volume and the diameter of the collapsed crater are usually proportional to the estimated yield.

Introduction

During this contract period we conducted research on five topics which are directly related to the problems of regional seismic wave propagation and earthquake-explosion discrimination. The topics are: (i) a review of the available studies on the seismic phase *Lg*, (ii) a comparison of seismic discrimination methods at regional distances in the U.S. and the USSR, (iii) a preliminary study on the attenuation and magnitude-scale of Lg and intermediate-period (8-13 sec) Rayleigh waves, (iv) a preliminary re-evaluation of the magnitude-yield relation and an examination of the physical parameters which may be relevant to the estimated yield of underground nuclear explosions, and (v) a review on the nature and reduction of seismic noise, applicable to the design of marine seismic systems.

Through the review on the properties of Lg waves, we hope to achieve three goals: (i) to compile and categorize the available observations into accessible format, (ii) to summarize the theoretical development in an overview fashion, and (iii) to emphasize the features that are related to the problems of earthquake-explosion discrimination. In this report, we will present a review on the seismic phase Lg. The review is subdivided into seven topics: (A) particle motion and dispersion, (B) regional velocity, (C) spectral content, (D) wave guide and mode of propagation, (E) attenuation and propagation efficiency, (F) magnitude-scale based on Lg, and (G) others (Sn-to-Lg conversion, application to the earthquake-explosion discrimination problem, and search for oceanic Lg).

A comparative study of regional wave propagation in the eastern United States and different regions of the Soviet Union is presented in the second part of this Final Technical Report. Four topics were selected to assess the feasibility of directly comparing the characteristics of regional seismic waves in the US and the USSR, and to evaluate their relative importance to the problem of earthquake-explosion

discrimination. The topics are: (i) Lg vs. P amplitudes, (ii) Lg/P amplitude ratios as a function of distance, (iii) Lg group velocity at amplitude maxima, and (iv) Lg energy ratios.

To improve our ability to discriminate earthquakes from explosions on a regional basis, we initiated a study to quantify the attenuation rates of Lg waves in the eastern U.S. and the western and central portions of the USSR. In addition, we have suggested a magnitude-scale formula for Lg waves in the eastern U.S.; the formula is very similar to the one proposed by Nuttli (1973) for the central U.S. Since underground nuclear explosions are more efficient at generating short-period waves than long-period waves, we have begun to explore the possibility of using intermediate-period (8-13 sec) surface waves as a seismic discriminant. In this preliminary effort, we have determined the attenuation rate and a magnitude formula appropriate for intermediate-period Rayleigh waves in the eastern U.S. We have also tested, with negative result, the potential of using M_S (from intermediate-period Rayleigh waves) vs. M_{Lg} as a discriminant. Since only one explosion (SALMON) was used in the comparison, the result is quite inconclusive.

In studying regional seismic wave propagation, we often encounter the problem of how to calibrate a magnitude-yield relation at regional distances. This problem, although quite fundamental in nature, is by no means an easy one because a well-determined magnitude-yield relation requires a clear knowledge of (i) the source size, (ii) the amplitudes of seismic waves at different distances, (iii) the effects of crustal structure at the source and the receiver, and (iv) the effects of the propagation path. The last part of this report re-examines this relation; it also describes the preliminary results from analyses of several physical parameters that are related to the yield of underground nuclear explosions.

A good understanding on the nature of the microseismic noise is crucial to the optimization of signal-to-noise ratios for a marine seismic system. In the appendix of RAI's Semi-Annual Technical Report, No. 4, Pomeroy (1980) has addressed to this need by reviewing the

available seismological literature on the subject. In the review, he has focused on (i) the causal mechanisms and depth-distributions of propagating and non-propagating seismic noise, (ii) the effects of local topography and geologic structure on noise amplification, (iii) the feasibility of installing a vertical array, and (iv) recommendations for the selection of station sites. The aforementioned review is not reproduced in this Final Technical Report.

Part I. Review of Lg

The purpose of this review is threefold: (i) to provide a summary of the available observations on Lg, (ii) to present the theoretical developments in an overview fashion, and (iii) to clarify or comment on what appears to us to be confusing concerning the interpretation of Lg.

The name Lg was assigned by Press and Ewing (1952) in their pioneering study on this seismic phase. "L" because the particle motion was predominantly of Love or transverse type, and "g" because the wave was believed to propagate in the granitic layer of the crust, and was therefore considered a surface-wave counterpart of the near-earthquake body waves Pg and Sg. These authors summarized the properties of Lg (for propagation paths in North America) succinctly in the abstract of their 1952 paper:

"Surface shear waves (Lg) with initial period 1/2 to 6 seconds with sharp commencements and amplitudes larger than any conventional phase have been recorded for continental paths at distances up to 6000 km. These waves have a group velocity of 3.51 $\pm$ 0.07 km/sec and for distances greater than 20° they have reverse dispersion. For distances less than about 10° the periods shorten and Lg merges into the recognized near-earthquake phase Sg."

This and later investigations of Lg also point out that (i) the wave is not observed after approximately 100 km of propagation in the oceanic crust, (ii) the particle motion may contain a substantial amount of longitudinal and vertical components, and (iii) the observations may be explained by a collection of Airy phases of higher mode Love and Rayleigh waves.

The terms of Sg and Lg were used to refer to different waves in some earlier studies. Although both terms referred to high-frequency shear waves in the continental crust, the distinctions

were based on differences in the observed frequency content, the distances of observation, and the interpretation in their mode of propagation. Sg, which is analogous to its compressional-wave counterpart Pg, referred to the direct shear arrival at short epicenter distances; while Lg referred to the superposition of normal modes, with frequencies slightly lower than those of Sg, at epicentral distances greater than about 10° (Press and Ewing, 1952). [There has been considerable confusion concerning the definitions of Pg and Sg. These terms replaced the $\overline{P}$ and $\overline{S}$ of Mohorovicic (1914) for typographical convenience (page 86 of Jeffreys, 1976) and the supposed association with the granitic layer of the crust. While the definition of $\overline{P}$ referred to the direct compressional arrival at short distances with a velocity of about 5.5 km/sec (cf. Figure 18-1 of Richter, 1958), the original data was obtained at distances over 150 km. Explosion data from California indicated that direct compressional arrivals at 120 km within the epicenter had a velocity near 6.34 km/sec. The Californian researchers consequently suggested the notation "p" for the direct wave at short distances and "$\overline{P}$" for the compressional wave with a velocity around 5.5 km/sec (page 286-287 of Richter, 1958). The consensus at the present seems to be the use of the nomenclature P for direct compressional waves and the terms "Pn" and "Pg" for occasions when two distinct arrivals with velocities around 8.0-8.4 km/sec and 5.4-5.7 km/sec are observed.] In view of the consensus on the terminology of P-, Pg-, and Pn- waves and the arbitrary distinction between Sg and Lg, we are in favor of calling the direct shear arrival "S" and reserving the term "Lg" for shear waves with group velocities around 3.5 km/sec at epicentral distances where Sn (or the mantle-refracted S) becomes the first shear arrival. In this report, the term "Lg" will refer to both the "Lg" and the "Sg" cited in earlier seismological literature. In the following sections, we will attempt to summarize and discuss previous studies on the observations and interpretations of the Lg phase. We have divided the literature available to us into 7 topics: (A) particle motion and dispersion, (B) regional velocity, (C) spectral content, (D) wave guide and mode of excitation, (E) attenuation and propagation efficiency, (F) magnitude-scale based on Lg, and (G) others.

A. Particle Motion and Dispersion

Press and Ewing (1952) describe the particle motion of Lg in the following words:

"...During the first cycles the waves have approximately equal amplitudes on all three components, but the transverse horizontal rapidly gains amplitude and becomes several times larger than the other two within about 30 seconds. Approximately one minute after the commencement of the phase, the amplitude on the transverse component, having reached a value many times larger than that of S or SS on any component, begins to decrease gradually, but does not drop to a value comparable with that of SS until about 30 minutes later, the period then being of the order 10-14 seconds. The group velocity for the latter part of this phase is certainly less than about 2 km/sec , the lower limit being uncertain...". As for Eurasian events recorded at Uppsala and Kiruna, Båth (1954) reports that the particle motion of Lg was primarily transverse and was often observed at two different group velocity windows: Lg_1, at 3.54 $\pm$ 0.06 km/sec and Lg_2 at 3.37 $\pm$ 0.04 km/sec. Lehmann (1953) states that there was "considerable" vertical motion involved. All the authors mentioned above agreed that both the horizontal and the vertical components of particle motion were present in the Lg phase. Herrin and Richmond (1960) used a ray-approach analysis to explain the particle motion of Lg. Their calculations indicate that a strong SV type motion (i.e. with longitudinal and vertical components of motion) would be present with the SH-type motion intially; but during the later part of the wave train where the angle of incidence for the rays presumably becomes less steep, energy leakage to the bottom layers due to Sv-to-P conversion would occur and the SV-motion tends to decrease faster than that of the SH-motion. The results of this analysis are in agreement with the observations of Oliver et al. (1955), but do not agree with their own observations at Dallas for earthquakes in southwestern United States and Mexico where strong SV-motion continued throughout the Lg wave-train.

Herrin and Richmond also estimated the partitioning of energy between SV and P waves at different angles of incidence; Herrin (1961) pointed out some errors in their partitioning of energy and corrected them. By correlating the verical component to the longitudinal component of the Lg particle motion, Sutton et al. (1967) found out that the particle motion of Lg from underground nuclear explosions and small earthquakes tended to be either transverse or mixed.

Aside from the qualitative comparison of Press and Ewing between the vertical and horizontal components of displacement, there are several other reports on their relative amplitudes. For the Lg amplitudes generated by the nuclear explosion GNOME in a salt mine of New Mexico, Romney et al. (1962) note that the displacements on all three components were approximately equal. But for earthquakes in the northeastern U.S.--southeastern Canada regions recorded at North American stations, Street (1976) reports that the maximum sustained horizontal component of Lg consistently exceeded the vertical component by a factor of 3. For all epicentral distances in Iran, the resultant horizontal motion of Lg at 1 sec was usually twice that of the vertical component (Nuttli, 1980a). Båth (1956), however, found some Lg waves with no vertical particle motion at all.

Although Press and Ewing (1952) suggested the possibility of using higher mode surface waves to interpret the Lg phase, Oliver and Ewing (1957) were the first to calculate the dispersion curves of higher mode Rayleigh waves and use them to explain the longitudinal and vertical components of Lg particle motion. In a later paper, Oliver and Ewing (1958) computed the dispersion curves from simple earth models for higher mode Love and Rayleigh waves and found that the M_2-mode (1st shear mode) and the second Love mode had similar velocities at the same period, which may explain the simultaneous arrivals of the vertical, longitudinal, and transverse components of ground motion for Lg. Dispersion curves and particle motions of higher mode Love and Rayleigh waves were computed for realistic earth models by Brune and Dorman (1963), and later including the

effects of sphericity into the earth models by Kovach and Anderson (1964). Brune and Dorman also computed synthetic seismograms for the transverse component of Lg. The results of these authors confirm the hypothesis of Oliver and Ewing. Knopoff et al. (1973) presented further evidence to identify the transverse component of Lg motion as higher mode Love waves by (i) computing the relative spectral excitations for double-couple sources at different depths, and (ii) constructing synthetic seismograms for the higher mode Rayleigh waves and identified them as the longitudinal and vertical components of Lg motion.

The particle motion of the 1st shear mode (M_2) was computed by Oliver and Ewing (1957) to be retrograde elliptical; the same authors later reported that observations from an Arctic event (5/25/1950, 8:34:32; 65.5°N, 151.5°W) recorded at Palisades, confirmed their previous theoretical results on the particle motion (Oliver and Ewing, 1958). Barley (1978) traced the particle motion of higher mode Rayleigh waves (2.0 sec $\leq T \leq$ 3.5 sec) for the group velocity window 3.0 to 3.5 km/sec , and found it to be retrograde elliptical. This result was predicted by the theoretical calculations of Panza et al. (1972) for the first three higher Rayleigh modes; these authors also found that at a given period the ellipticity (defined as the ratio of the longitudinal component of particle motion to the vertical component) increased with decreasing mode number. For a shield structure with a low velocity channel (LVC) in the upper mantle, they found that at periods less than 4 sec the ellipticity for the third higher Rayleigh mode was greater or equal to 0.7, whereas the ellipticity for the fundamental and the first two higher Rayleigh modes was greater or equal to 1.0.

B. Regional Velocity

Table I is a summary of Lg velocities which were published in journals and reports available to us. Whenever possible, we tried to include information pertaining to the measurements of the velocity,

such as the location of the seismic events and recording stations, the type of instrument used to record the events (horizontal or vertical component, short or long period, etc.), and the period of the Lg waves at which the measurement was made. Although the majority of the references cited did not specify their method of measurement, we deduced from their figures that most reported velocities were measured at the initial stage of the coda when a visible change in wave frequency or amplitude could be observed, either on the long- or short-period instruments. The measurements of Pomeroy and Nowak (1978), however, were made at the amplitude maxima of the Lg coda which seemed to be more unstable. Differences in the method of measurement and the recording instrument may account for the apparent discrepancy between the various reports. While measurements at the beginning of the coda probably correspond to the Airy phase(s) of higher mode surface waves with the fastest group velocity, measurements at the amplitude maxima probably coincide with the group velocity window where several Airy phases overlap. Whereas the former is indicative of the average properties of the wave guide, the latter which tends to be slower than the former, is probably not only more diagnostic of the detailed structure of the wave guide but also informative concerning the relative excitation of the various modes at the source (Knopoff et al., 1974). We would like to explore this possible aspect of Lg in a future study.

C. Spectral Content

The only sources known to us on the spectral content of Lg are derived from Street et al. (1976) and the Soviet seismological literatures (e.g. Antonova et al, 1978; Nurmagambetov, 1974). The studies on Lg propagation in the USSR were compiled and summarized in a report by Shishkevish (1979).

Street et al. derived their data from over 300 short-period, vertical component recordings of 78 earthquakes in the central U.S. In the period range they analyzed (approximately 0.05 - 10 sec),

the amplitude spectra generally indicate a falloff of (omega) between the flat portions at the long- and short-period ends. Their spectra were corrected for the effects of instrument response, but not for the anelastic attenuation of the path.

The frequency selection seismograph stations (ChISS) of the USSR have enabled the spectral analysis of Lg to become a routine procedure. Their results, commonly plotted as log (A/T) vs. log (1/T), generally display peaks at short epicentral distances. The peak is shifted towards lower frequencies as epicentral distance increases. This dependency of spectral peak on epicentral distance is also a function of propagation path. In these studies, the frequency ranged from 0.3 to approximately 20 Hz while the epicentral distance spanned from 30 to 3000 km. The falloff in their velocity amplitude spectra (i.e. displacement amplitude spectra multiplied by frequency) is also dependent on epicentral distances: at epicentral distances around 350 km, the falloff ranges from slightly greater than one to approximately two; whereas at epicentral distances greater than about 1000 km, the falloff remains less than 3. Since these measurements of Lg spectral content did not take the effects of geometrical spreading and anelastic attenuation into account, the spectral characteristics measured at short epicentral distances were probably more representative of the source spectra and a spectral falloff of about 2 could be taken as representative of the source falloff for the displacement amplitude spectra of Lg waves. The high-frequency spectral peaks observed in the USSR is probably an artifact of the velocity spectra plot; that is, the spectral peak will disappear if the plot is converted into a displacement amplitude spectra.

D. Wave Guide and Mode of Excitation

Press and Ewing (1952) are, again, the first ones to point out that "...Lg is a wave which is confined to a surface or near-surface layer by wave-guide action..." based on the observed velocity and large amplitudes. Subsequent theoretical studies tend to support

their claim although this conclusion is not reached without its share of confusion. In a study of Lg waves in Eurasia, Båth (1954) observed a correlation between hypocentral depth and the energies contained in Lg_1 and Lg_2. That is, the energy of Lg_1 generally decreased with increasing hypocentral depth, whereas the energy for Lg_2 reached a maximum when the source depth was around 45 km. He attributes the difference in energy distribution to several crustal channels or layers which transmitted waves at different group velocities. This claim, although sound when interpreted in terms of Airy phases with different group velocities, led to two unexpected results when viewed from the perspective of channel waves. Firstly, terminologies for waves which supposedly propagated in different channels of the crust and upper mantle proliferated (e.g. Båth, 1958). Secondly, several low-velocity channels in the crust and upper mantle came to be used as explanations for the efficient propagation of the various channel waves (Gutenberg, 1955; Båth, 1956, 1958).

Based on the dispersion curves of higher mode Love and Rayleigh waves, Oliver and Ewing (1957, 1958), Brune and Dorman (1963), and Kovach and Anderson (1964) found it possible to explain the frequency content and the group velocity of Lg waves by using the Airy phases of the higher modes. Kovach and Anderson (1964) also point out that the modes observed "...depend on the period range being studied and the depth of the source..." and that variations in the velocity and period of the observed Lg depended on the positions of the Airy phase, which in turn depended on the elastic parameters of the propagation path. If the interpretation of Lg waves as superpositions of higher mode surface waves is correct, then we would expect an additional dependence on the source radiation pattern. At periods greater or equal to 5 sec , radiation patterns of the first higher Love and Rayleigh modes compare favorable with calculated results (Mitchell, 1973, a,b). The observations of Sutton et al. (1967) on short-period (0.5-2.0 sec) Lg waves, however, indicate that "...there seems to be no systematic difference in the short-period energy radiation pattern be-

tween the underground nuclear explosions and the earthquakes..." and that the pattern of the energy-contours (or contours based on the maximum amplitude) could be better explained by a correlation with the major tectonic provinces of the United States. Since the modal composition of Lg at short periods is a combination of many higher modes, the observed amplitudes may not be diagnostic of the radiation pattern of the individual modes. Also, scattering is probably more important for short-period waves and its effects more likely to mask any azimuthal pattern that may be present.

Panza et al. (1972) showed that the collection of higher mode Rayleigh waves could be separated into a family of crustal waves and a family of channel waves in a structure containing even a slight low-velocity channel (LVC) in the upper mantle. As it is implied by the name, channel waves have most of the energy in the LVC and have essentially zero energy at the surface. Crustal waves, on the other hand, have most of their energy in the crust; consequently, only the fundamental mode and the crustal waves need to be considered for the excitation of Rayleigh waves. Knopoff et al. (1973) demonstrated that higher mode Love waves could similarly be divided into crustal waves and channel waves. For a structure without any LVC, the whole suite of higher mode Love and Rayleigh waves has to be taken into account for the ground motion of the Lg waves.

Knopoff et al. (1974) further establish that the group velocity and the periods of the Lg stationary phase could be diagnostic for the crustal thickness and the shear velocity in the crust and the upper mantle. In general, as the crustal thickness increased, both the group velocity of the late-arriving Lg stationary phases, U_{min}, and the period at U_{min}, T_{min}, tended to increase. Increasing the crustal velocity while keeping all other parameters constant would tend to decrease T_{min}, but increase U_{min}, the magnitude of Lg-excitation, and the general period-content of the Lg waves. These authors also demonstrate that (i) for thick-

nesses of the upper mantle lid greater than 20-25 km, Lg is insensitive to changes in its thickness, and (ii) Lg is insensitive to the velocity in the upper mantle LVC. Panza and Calcannile (1975) point out that higher mode contribution becomes more significant as the period decreases and/or as the hypocentral depth increases.

As for the low-velocity channel in the crust and/or upper mantle, Oliver and Ewing (1958) concluded that it was not necessary to explain the characteristics of the Lg phase. Knopoff et al. (1973) and Panza and Calcagnile (1975), based on more modes extending to shorter periods, reached the same conclusion concerning the Love- and Rayleigh-type motions of the Lg phase, respectively.

Most of the investigators mentioned in this section would probably maintain that the characteristics of Lg can be explained by the anelastic attenuation of the crust-mantle layers, the frequency response of the seismograph system, and the superposition of higher mode surface waves. Ruzaikin et al. (1977), on the other hand, state that they "...remain unconvinced that normal modes will allow useful interpretation of Lg when more detailed data on its structure are obtained..." and suggest that lateral heterogeneity had a key role in shaping the characteristics of the observed Lg. Their argument was based on the discrepancy between calculations from higher mode surface waves which predicted the duration of Lg to be confined in the group velocity windows of approximately 3.5-3.1 km/sec., and observations of the Lg phase which indicated that its amplitude was significant in the group velocity window 3.5-2.8 km/sec. Oceanic Rayleigh waves of the fundamental mode ($T \geq 12$ sec) also exhibit similar "stretching" in duration. These waves have nevertheless been instrumental in shaping our present understanding concerning the oceanic structure. Thus, while we share the belief with Ruzaikin et al. that heterogeneities in the propagation path are important in shaping the waveform of Lg, we also believe that the normal mode theory, when

supplemented with theories or methods which can take heterogeneity in the path into consideration (*e.g.* the scattering theory of Aki, 1969), will serve to improve the explanation for the Lg phase.

E. Attenuation and Propagation Efficiency

This section deals with the measurement of amplitude-diminution as a function of epicentral distance; the title of the section reflects, respectively, the quantitative and qualitative aspects of it. The former refers to the rate of anelastic absorption of the wave's kinetic energy per unit distance, while the latter provides a descriptive measure for the efficiency of the medium in transmitting Lg waves.

In seismological literature, attenuation is usually measured in terms of the attenuation coefficient, γ , or the attenuation quality factor, Q. These two quantities can be related via the following equation:

$$\gamma = \frac{\pi f}{Q U} \qquad (1)$$

where f and U are the frequency and the velocity of the wave, respectively. For Lg waves, measurements of γ and Q, compiled in Table II, have been obtained by three approaches: (i) time-domain, (ii) frequency-domain, and (iii) coda.

The time domain approach entails three steps: (i) measure the wave amplitude at different epicentral distances, (ii) correct the amplitudes for the effect of geometrical spreading, and (iii) estimate the γ or Q that would explain the falloff of the amplitude in relation to distance. Nuttli (1975, 1978, 1980 a,b) and Street (1976) chose to combine steps (iii) and (ii) together, and compared the observed amplitudes directly with curves that include the effects of geometrical spreading and different degrees of attenuation. The frequency-domain approach has the advantage of being able to take the source radiation pattern into account. The procedure used by Mitchell and coworkers, who have been the primary

advocates of this approach on higher mode surface waves, is similar to that employed for the study of the fundamental mode (Tsai and Aki, 1969). Again, three steps are involved in this procedure: (i) determine the amplitude spectra for the fundamental and higher mode surface waves by applying a frequency-velocity filter (e.g. the multiple-filter technique of Dziewonski et al., 1969) (ii) calculate the attenuation coefficient that would produce the best fit between the observed amplitudes and the radiation pattern computed at each period. To date, this approach has been limited to the analysis of the fundamental and the 1st higher mode (Mitchell, 1973 a,b; Cheng and Mitchell, 1980). The coda approach, which was derived from the scattering theory of surface waves (Aki, 1969), has been applied successfully to data from narrow-band seismographs to establish (i) scaling laws for local earthquakes, and (ii) estimates of regional Q (Aki and Chouet, 1975; Chouet et al., 1978; Rautian and Khalturin, 1978). Herrmann and coworkers recently modified this method for data derived from broadband seismographs. They estimated the regional Q from Lg waves by measuring (i) the predominant frequency in the coda as a function of time, and (ii) the coda shape (Herrmann, 1980; Singh and Herrmann, 1979).

The propagation efficiency of a region is usually estimated by measuring the frequency content and wave amplitude (usually in relation to the level of the ambient noise or the amplitude of another phase); in general, three terms: clear, weak, and none are used to describe the amplitude of the Lg phase. "Clear" usually refers to an impulsive, large-amplitude, high-frequency arrival; "weak" refers to a drawn-out, small, low-frequency arrival; and "none" is indicative of completely inefficient Lg propagation. Although different authors have set their standards for clear and weak Lg somewhat differently, their conclusions concerning the propagation efficiency of a given region are, surprisingly, quite uniform. A list of regional studies on the propagation efficiency of Lg is compiled in Table III.

In interpreting the inefficient propagation of Lg in the Tibetan plateau, Ruzaikin et al. (1977) proposed two explanations which are probably applicable to most areas with major tectonic boundaries. Firstly, a disruption, termination, or vertical displacement of wave guide (which is either the entire crust or part of it) will seriously affect the propagation efficiency of Lg waves; secondly, high attenuation in the crust will also be able to affect the ability to transmit Lg. The ocean-continent boundary is probably a disruption or termination of the wave guide for Lg; disappearance of Lg waves after crossing approximately 100 km of oceanic structure is a well documented observation (e.g. Press and Ewing, 1952; Båth, 1954; etc.). This peculiar property of Lg waves to propagate only in the continental crust was used by Oliver et al. (1955) to map the continental structure in the Arctic regions.

Båth (1956) and Gutenberg (1955) report that the Lg phase was weakened or disappeared when crossing recent mountain chains. Shishkevish (1979), in his compilation of studies on Lg propagation in the Soviet Union, also notes that the Lg phase was attenuated when crossing Tien Shan, Pamir-Hindu Kush, and the Himalayas. He also point out that "...the propagation of Lg across the Tien Shan is less efficient when paths are more oblique to the trend of the range than when they are perpendicular to it...". Uniformity of the structure (Chinn et al., 1980) and the complexity of geology (Street, 1976) in the propagation path are also considered important in determining the attenuation of the Lg amplitude. In summary, the presence of a uniform, high-Q wave guide is essential for the efficient propagation of Lg; in the case of a non-uniform or low-Q wave guide, the degree of non-uniformity of the wave guide and the length of propagation in it are both important in determining the fraction of Lg-energy that will be observed.

F. Magnitude-Scale Based on Lg

Since Lg is often found to be the largest phase at regional

distances, it is natural that a magnitude-scale based on Lg amplitude would become important to studies on regional seismicity. Based on LRSM reports from 78 underground nuclear explosions, Baker (1970) proposed a general formula of the form,

$$M_{Lg} = \log_{10} (A/T) + Q(T,\Delta) + S(T) \qquad (2)$$

to calculate the magnitude-scale from Lg amplitudes. $Q(T,\Delta)$ represents a correction term for the attenuation, and $S(T)$ is a term for station correction. Baker obtained an expression for $Q(T,\Delta)$, as a sixth degree polynomial of distance, by minimizing the difference between $\log_{10}(A/T)$ and the reported m_b for each event; he also assigned tentative corrections for each station. M_{Lg} calculated by Baker indicates less scatter than the reported m_b.

Nuttli (1973) formulated a magnitude scale for Lg while studying its attenuation in the eastern United States. He assumed that the term $Q(T,\Delta)$ in equation (2) has the form $C(T,\Delta) \log_{10}\Delta$, and subsequently found two magnitude formulae, applicable at different distance ranges, for 1-sec Lg of "sustained" (3 or more cycles) amplitudes.

$$M_{Lg} = 3.75 + 0.9 \log_{10}\Delta + \log_{10} (A/T) \qquad 0.5° \leq \Delta \leq 4°$$
$$= 3.30 + 1.66 \log_{10}\Delta + \log_{10} (A/T) \qquad 4° \leq \Delta \leq 30°$$

Street (1976) and Bollinger (1979), respectively, found Nuttli's formulae to be applicable in northeastern and southeastern North America, provided that the maximum distance is limited to approximately 2000 km.

Street et al. (1976), on the other hand, assumed $C(T,\Delta)$ to be known and then specified $S(T)$ such that the magnitude scales at different periods were set equal for an m_b = 1.5 event. For an m_b = 2.5 event, the magnitude calculated at 0.1 sec. according to their formulation would be 1.8, and the discrepancy between m_b and $m_{0.1}$ increased rapidly with increasing m_b. Since there is no implicit or explicit reasoning behind the assumption of a known $C(T,\Delta)$, we are inclined towards the procedure of determining $C(T,\Delta)$ experimentally and then calculating the $S(T)$ so that a uniform magnitude would be obtained at all periods.

G. Others

Sn to Lg conversion appears to occur near the margin of the American continents. For events from the West Indies and Mexico recorded at North American stations, Isacks and Stephens (1975) identified the prominent phases which arrived after Sn as possibly a converted Lg at the continental margin. Chinn et al. (1980) observed similar conversions for events in the Nazca Plate recorded at South American stations. In neither of the studies was any Lg to Sn conversion observed.

A number of investigators have explored the possibility of using the ratio of Lg-amplitude to P-amplitude as a discriminant for the earthquake and the underground explosion populations. This possibility was tested by Pomeroy and Nowak (1979), Pomeroy (1980), Nuttli (1980 b), and Gupta et al. (1980) for propagation paths in western and central Soviet Union, and by Pomeroy and Nowak (1979) and Pomeroy (1980) for propagation paths in eastern and western United States, respectively. Their findings indicate a tendency for the Lg to P amplitude ratios to be greater than 1.0 for earthquakes and less than 1.0 for underground nuclear explosions. The ratios, however, appear to be strongly dependent on the epicentral distance and the regional attenuation in the propagation paths and therefore cannot be used reliably as a discriminant between explosions and earthquakes.

Contrary to higher-mode surface waves in continental structures, higher-mode Love waves in sediment-covered oceanic structures do not form a coherent family of arrivals at short periods (Knopoff et al., 1979). This phenomenon can serve to explain the absence of Lg waves in the oceanic structure. These authors also point out that since a large fraction of the shear energy at the stationary phases of higher-mode Love waves is concentrated in the sedimentary layer, absorption by the low-rigidity sediment and scattering due to variations in its thickness can account for the rapid attenuation of the higher-mode Love waves in oceanic structures.

TABLE I - Lg Velocity

REGION	VELOCITY	STATION (Instrument)	EVENTS	COMMENTS	REFERENCE
Africa	3.48-3.60	WWSSN and temporary SP stations	Earthquakes in Africa	Velocity higher in SE than in N part	Gumper and Pomeroy (1970)
S. Africa, Transvaal	3.68				Willmore et al. (1956)
"	3.66	SP temporary stations			Gane et al. (1956)
Australia	3.50	Riverview (Wiechert, (Galitzin)	Earthquakes in central and western Australia	Initial period $\simeq$ 3-6 seconds.	Bolt (1957)
Australia	3.44±0.04		Explosions in Australia		Bolt et al. (1958)
Eurasia	3.54±0.06	Uppsala, Kiruna, Bergen (Wiechert)	Earthquakes in Eurasia	Lg_1	Båth (1954)
"	3.37±0.04			Lg_2	"
Mediterranean region	3.40±0.02			Sg	Jeffreys (1952)
N. America	3.51±0.07			Initial period $\simeq$ 0.5 - 6 sec.	Press and Ewing (1952)
N. America, Eastern	3.57				Lehmann (1953)
Canadian Shield	3.54				Hodgson, (1953)
"	3.60-3.70	Ottawa, Resolute, Palisades Halifax (LP and SP)			Brune and Dorman (1963)
"	3.56				Horner et al. (1973)
California	3.54±0.02	SP network in California	Earthquakes from N. Calif. and Nevada		Press (1956)
Sierra Nevada	3.53±0.02	"	"		"
Central Valley & Coastal Ranges	3.55±0.03	"	"		"
U.S., Central	3.49		Earthquakes in Tenn.		Nuttli (1956)
"	3.49-3.80			Summary of previous studies	McEvilly (1964)
"	3.03-3.39	WWSSN (SP)	SALMON explosion	Velocity measured at maximum amplitude of Lg coda	Pomeroy and Nowak (1978)
"	2.18-3.72	"	Earthquakes in eastern and central N. America		"
U.S., Eastern	3.19-3.35	WWSSN (SP)	SALMON explosion	"	"
"	3.04-3.80	"	Earthquakes in eastern and central N. America	"	"
U.S., Central and SE	3.65±0.04	Saint Louis Univ. network (Wood-Anderson torsion seismometer)	New Madrid earthquakes		Stauder and Bollinger (1963)
U.S., SE	3.50±0.13	WWSSN (SP)	Earthquakes in SE United States	T $\simeq$ 0.7±0.1 sec	Bollinger (1979)
	3.52±0.10	"		T $\simeq$ 0.8±0.1 sec Vertical comp.	

TABLE II - Lg Attenuation

REGION	γ (10^{-3} km^{-1})	Q	n (Δ^{-n})	STATION	EVENTS	COMMENTS	REFERENCE
Iran	4.5 3.0			WWSSN (MSH,SHI,TAB) "	Earthquakes in Iran	1 sec Lg 3 sec Lg	Nuttli (1980a) "
N. America, Eastern	0.63 .90			WWSSN, LRSM, CNS, SLU	Earthquakes in central US	1 sec Lg(Z) 3-13 sec Rayleigh	Nuttli (1973) "
N. America, Central and eastern	0.63 0.23 0.8			WWSSN, LRSM, CNS " "	Earthquakes in SE Missouri "	1 sec 1st shear 10 sec 1st shear 4-6 sec 1st Love	Mitchell (1973a) " Mitchell (1973b)
United States		450±30		LRSM	NTS explosions	Lg	Press (1964)
U.S., NE	0.99			WWSSN, LRSM, CNS	Earthquakes in NE North America	1 sec Lg(Z)	Street (1976)
U.S., Central and eastern	0.87±0.66	1456		WWSSN (BLA)	Earthquakes in E. and central U.S.	Lg-coda	Herrmann (1980)
U.S., Eastern	0.63			WWSSN, NEUSSN	SALMON explosion and N. American earthquakes	0.3-1.0 sec Lg(Z)	Pomeroy (1979)
U.S., SE	0.63 0.90			WWSSN, LRSM "	Earthquakes in SE U.S.	1-sec Lg(Z), 100-700 km " 700 km	Bollinger (1979)
New Madrid, N.C.	6.0	1500		WWSSN	Local Earthquakes	0.1-sec Lg	Nuttli (1978)
Mississippi Valley		1500-2000				0.1-1.0 sec Lg	Nuttli and Dwyer (1978)
U.S., SE	-2.9±6.4	2190		USGS (GRT, Tenn.)	Earthquakes in eastern U.S.	Lg-coda	Herrmann (1980)
U.S., Western	4.8±1.3 2.5±1.0	229 396		WWSSN (BKS) WWSSN (DUG)	Earthquakes in western U.S.	" "	" "
U.S, W & SW of Western U.S., NW of western Colorado plateau N. Rocky Mountains		130-180 180 300-330 600-700		WWSSN " " "	Earthquakes in western U.S. " "	Lg-coda " " "	Singh and Herrmann (1979) " " "
USSR, Central Asia " , Dzhungaria " , Altai and Sayan			≃ 2 "	Network from Pamir to Lena River	Earthquakes in central and SW Asia	Lg	Nersesov and Rautian (1964)
Tien Shan W of Lake Baykal "		250 500 1200				Lg 1 sec - Lg 0.3 sec - Lg	Shishkevish (1979) " "
Near Caspian Sea USSR, S. border	1.35 3.15			WWSSN "	Earthquakes and explosions in central and western USSR	1 sec Lg(Z) "	Nuttli (1980b) "
USSR, S. " "	1.5-2.0 4.5-5.5 2.5-4.0	450-600 160-200 225-360		WWSSN (MSH, NIL, KBL, QUE, TAB) " "	Earthquakes and explosions in USSR " "	Low topographical relief High topographical relief Mixed path Both vertical and horizontal component of Lg	Springer and Nuttli (1980) " "

TABLE III Propagation Efficiency

REGION	STATION (Instrument)	COMMENTS	REFERENCE
Eurasia	Uppsala, Kiruna, Bergen (Wiechert, Galitzin)		Båth (1954)
E. Europe and Asia		Compilation	Piwinskii and Springer (1978)
Eurasia, Central			Ruzaikin et al. (1977)
USSR, Central	WWSSN		Pomeroy (1979)
USSR, E and Central		Compilation	Shishkevish (1979)
China, NW and Central		"	"
Middle East	WWSSN (EIL, IST QUE, SHI, TAB)		Kadinsky-Cade (1980)
U.S., E.	WWSSN, NEUSSN		Pomeroy (1979)
California			Gutenberg (1955)
U.S., SW and NE Mexico	Dallas		Herrin and Minton (1960)
S. America, W.	WWSSN		Chinn et al. (1980)

Part II. Seismic Discrimination Methods at Regional Distances

A. Propagation Characteristics

For propagation paths within eastern North America (ENA) Lg is commonly the phase with the largest amplitudes on conventional short-period seismograms (with peak response at less or near 1 Hz). Propagating at a group velocity of approximately 3.5 km/sec., the recorded Lg has (i) predominant frequencies of 1 to 3 Hz, (ii) particle motion in all three components: transverse, longitudinal, and vertical, and (iii) maximum amplitudes six to ten times larger than those of P waves. Works of Ruzaikin et al. (1977) and Antonova et al. (1978) indicate that Lg propagation in the eastern USSR seems comparably efficient, with Lg amplitudes significantly larger than the P amplitudes. Furthermore, Pg propagation is generally inefficient in both regions. In contrast, for propagation paths within western North America, as well as in the western and central portions of the USSR Lg is observed to have roughly equal amplitudes as P, but Pg appears relatively more prominent at regional distances. These observations: large Lg and small Pg or vice versa, seem to imply a relation between Lg- and Pg- propagation and the crustal structures along the propagation paths. Following Haskell's (1966) interpretation that (i) the attenuation of short-period, continental crustal P waves may, to a large degree, be explained as leakage of energy to the layers beneath the waveguide, and that (ii) low leakage can generally be associated with low near-surface velocities, we are in favor of explaining the relative amplitudes of Pg in terms of velocity contrasts at the lower interface of the Pg waveguide (presumably the Moho) and/or near-surface structures in the propagation paths. The amplitudes of Lg may also be related to these velocity structures in the waveguide, but the exact relation is not clear.

B. Lg- Amplitude vs. P- Amplitude

In this section, we present the quantitative relation between

the maximum amplitudes of P- and Lg- waves. Measurements of wave amplitudes were made from seismograms reocrded by the short-period instruments of World-Wide Standard Seismograph Network (WWSSN), Northeastern U.S. Seismic Network (NEUSSN) operated by Lamont-Doherty Geological Observatory, and Long Range Seismic Measurements (LRSM). The response curves for these instruments are shown in Figure 1. For the earthquakes and explosions listed in Table IV and V and plotted in Figures 2 to 3, measurements for the maximum P- and Lg- wave amplitudes were made at the stations where both waves could be identified. The ground motions were then calculated from the measured amplitudes by correcting for the instrument magnification. Comparisons of ground motions for P- and Lg- waves are presented in Figures 4 to 8 for the eastern U.S., eastern USSR, western U.S., central and western USSR, respectively. The results for the eastern USSR were taken from Ruzaikin et al. (1977) and Antonova et al. (1978). Since no scale was given for the seismograms reproduced in these two papers, the wave amplitudes in Figure 5 represents the record amplitude in millimeters.

Before we proceed to discuss the results, we would like to point out that for events located in western and central USSR the source and the receiver are, in general, separated by tectonic boundaries, whereas for eastern and western U.S. and eastern USSR the observations were usually made within the same tectonic province as the sources. The inclusion of tectonic boundaries in the propagation path may introduce significant effects on both the amplitude and the phase, or in short, the waveform of the seismic phase; consequently, we believe that direct comparisons between results from the different regions should be made with great caution.

An examination of Figures 4 through 8 indicates that (i) Lg- amplitudes are much larger than P- amplitudes in the eastern parts of the United States and the Soviet Union, (ii) for propagation paths in western U.S., western and central USSR Lg- and P- amplitudes are comparable, and (iii) the amplitude ratios of Lg to P for earthquakes are somewhat larger than those for explosions.

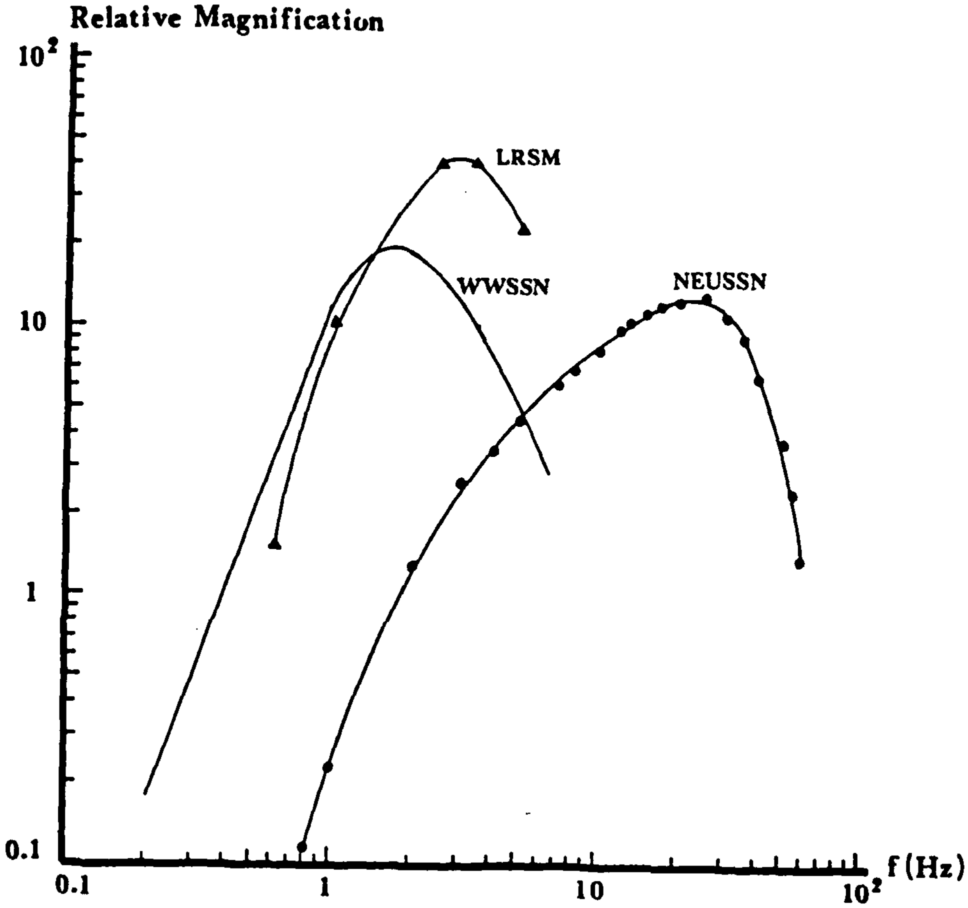

Figure 1. Response curves for the short-period instruments of World-Wide Standard Seismograph Network (WWSSN), Northeastern U.S. Seismic Network (NEUSSN), and Long Range Seismic Measurements (LRSM).

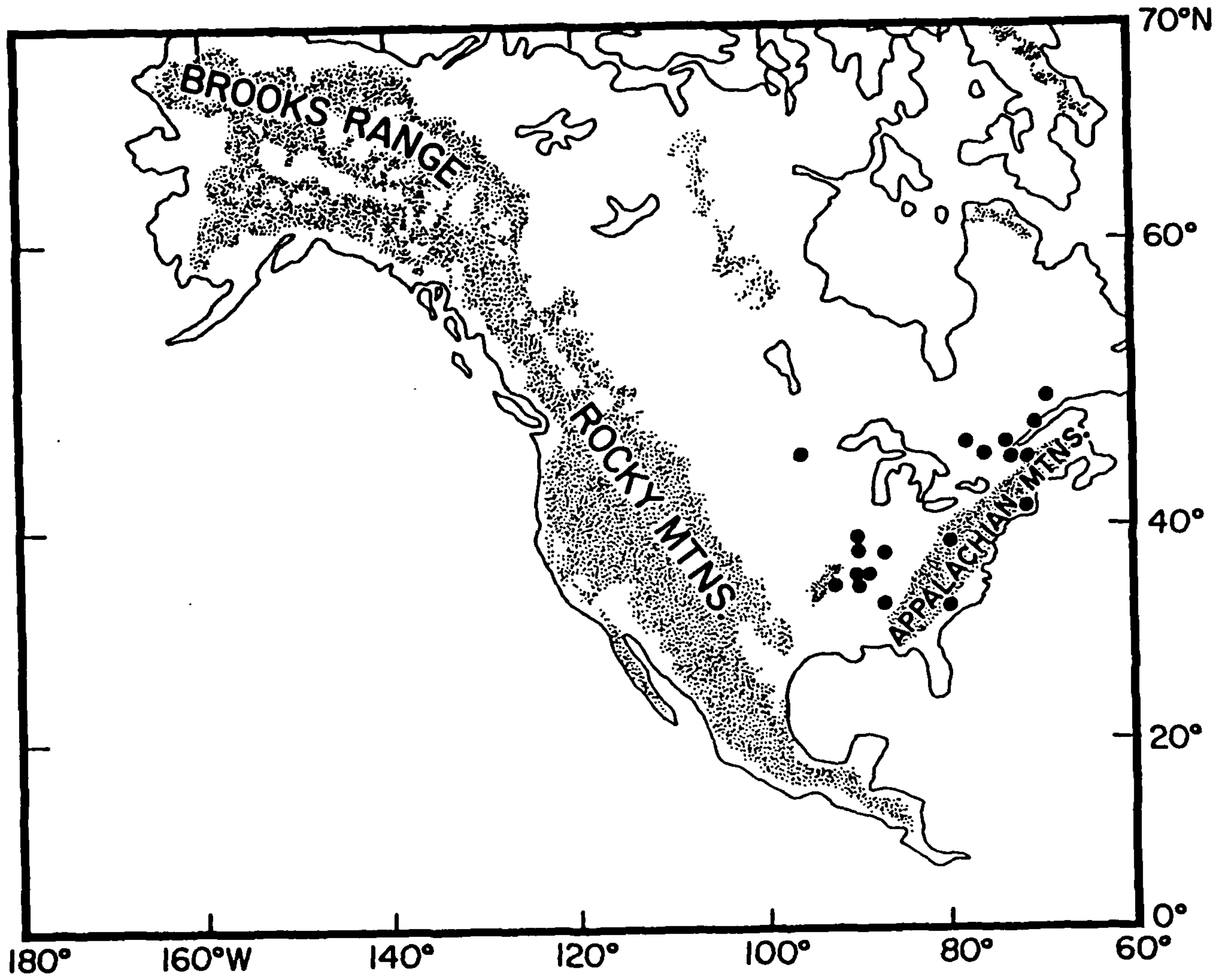

Figure 2. Location of U.S. events used in this study.

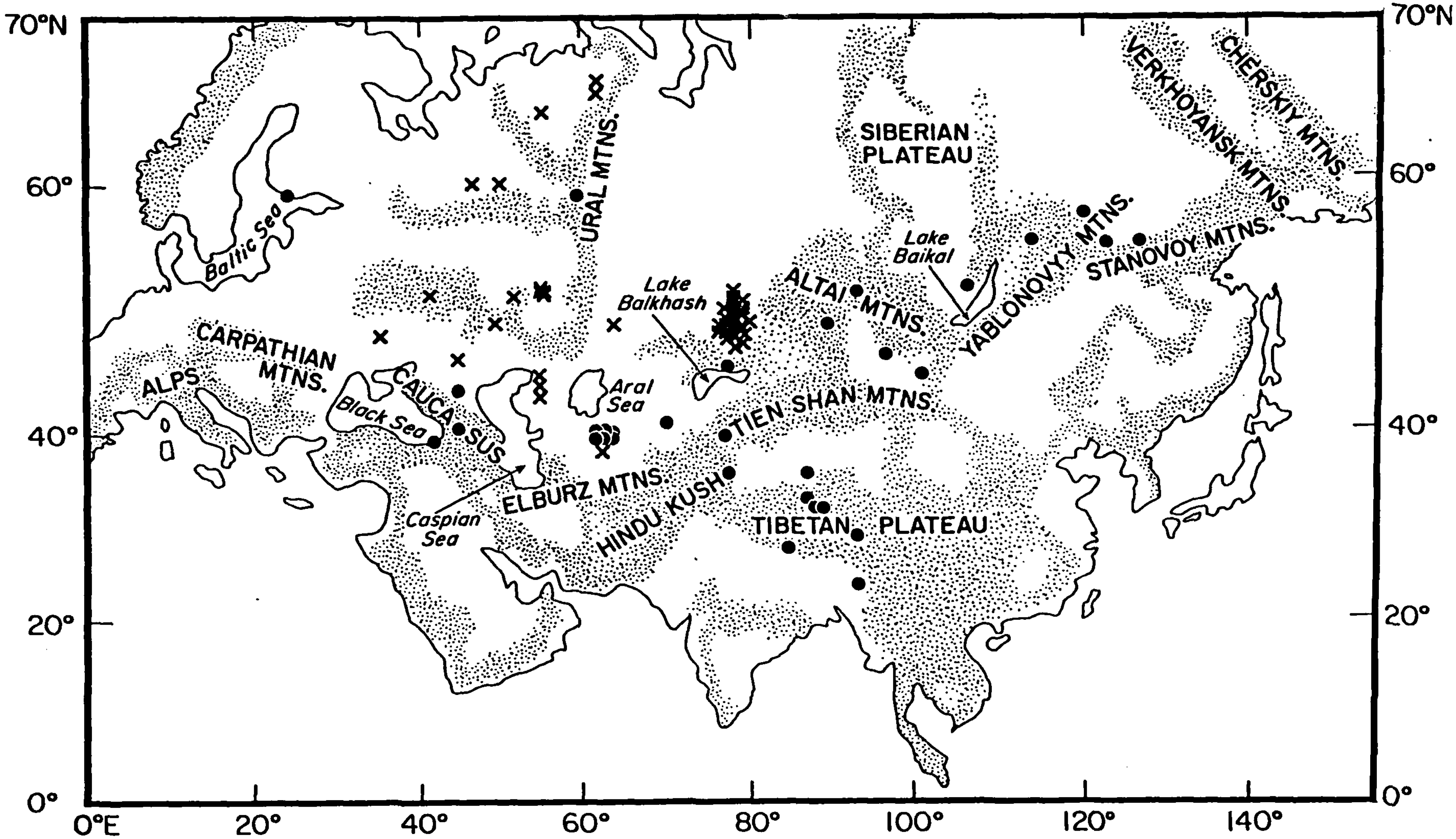

Figure 3. Location of USSR events used in this study.

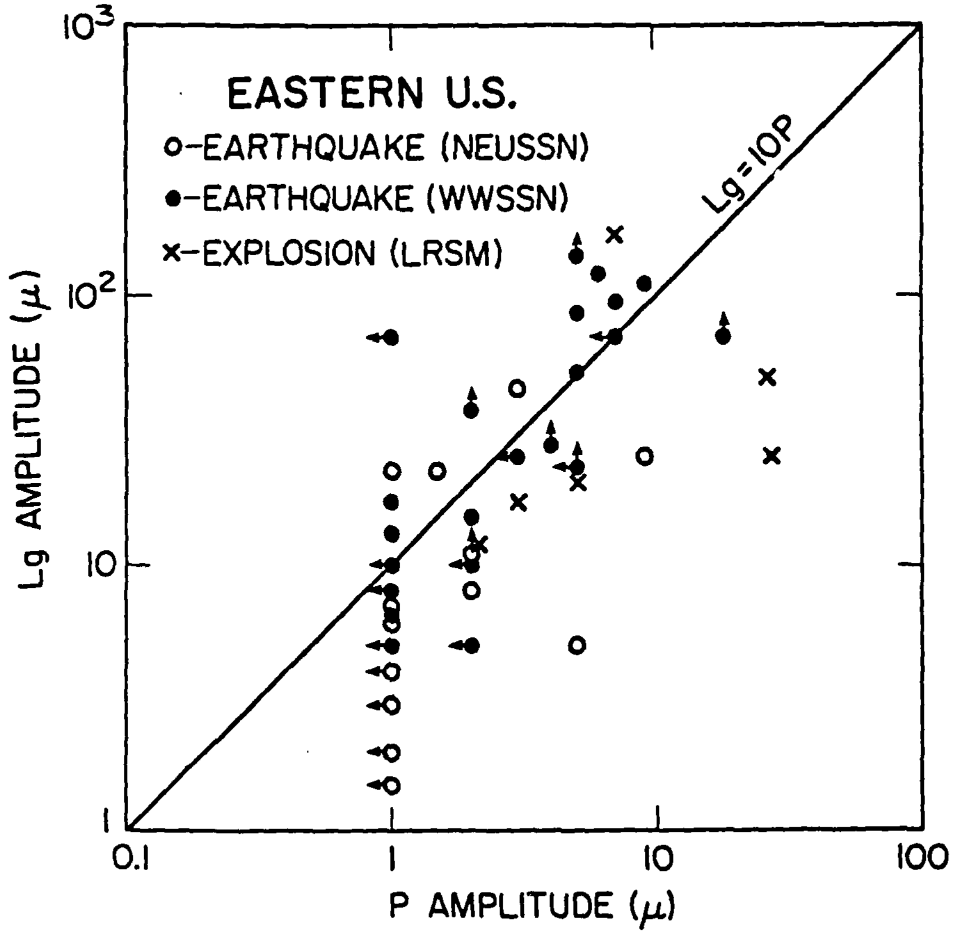

Figure 4. Lg- amplitude vs. P- amplitude in the eastern U.S.

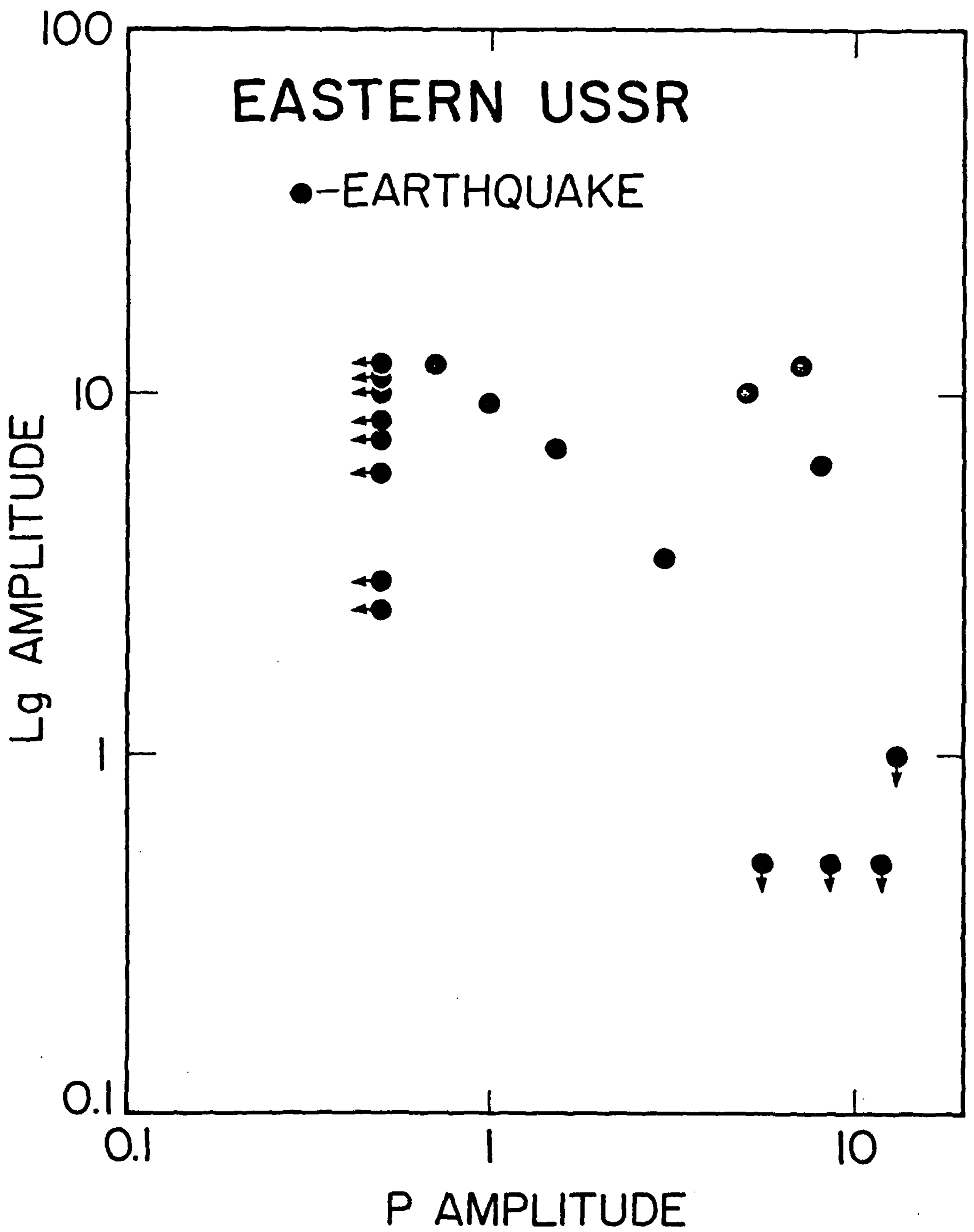

Figure 5. Lg-amplitude vs. P-amplitude in the eastern USSR.

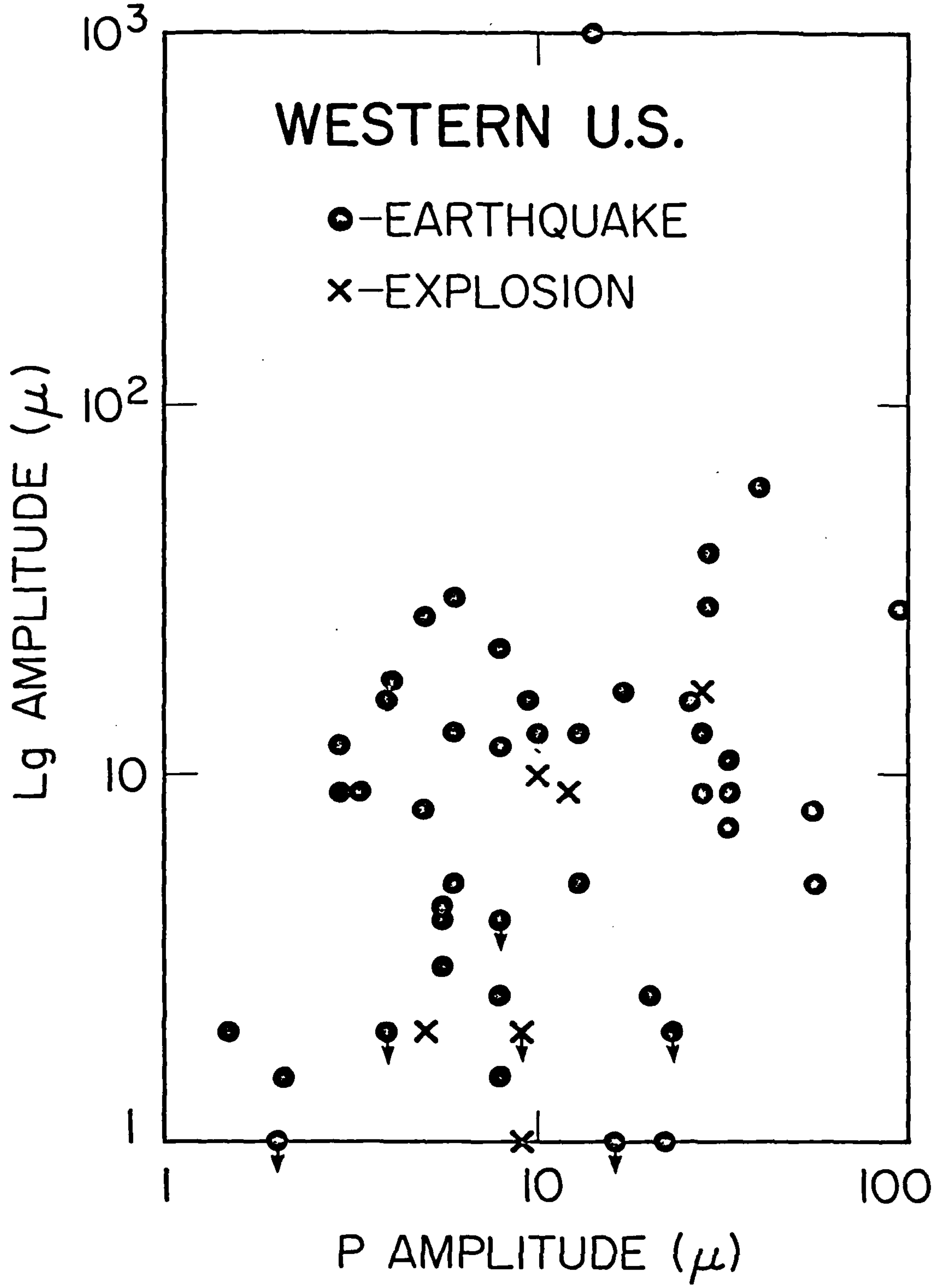

Figure 6. Lg- amplitude vs. P- amplitude in the western U.S.

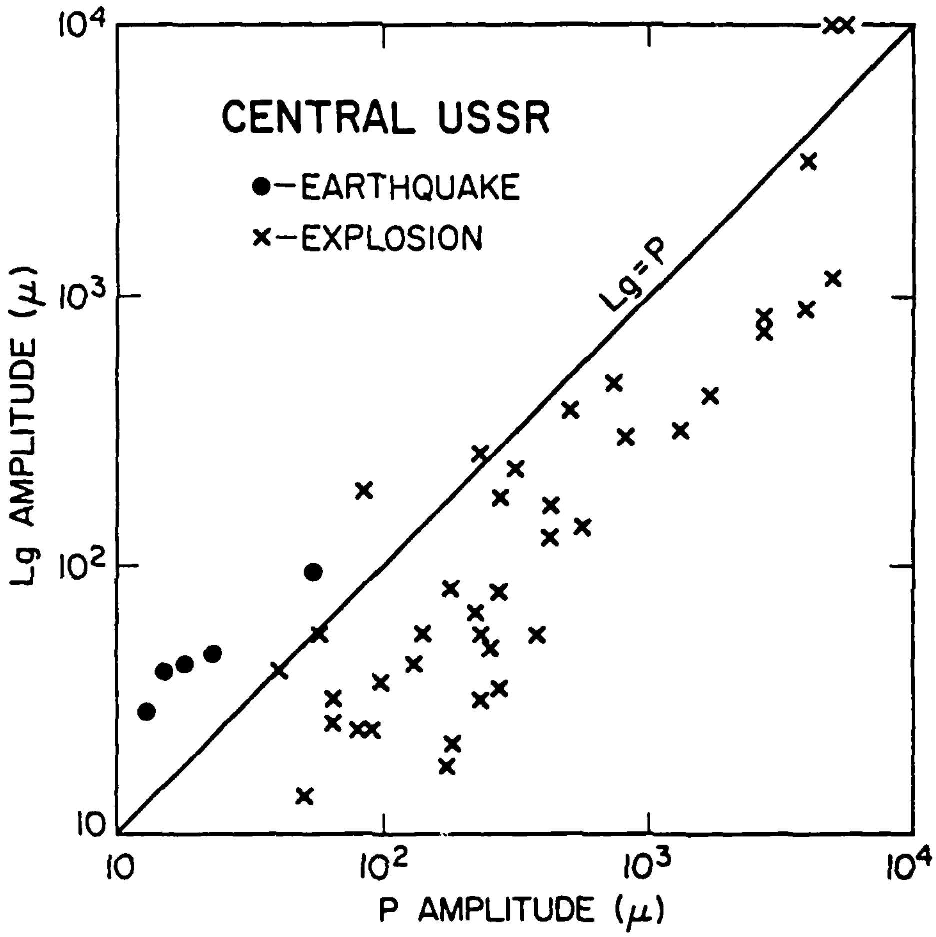

Figure 7. Lg- amplitude vs. P- amplitude in the central USSR.

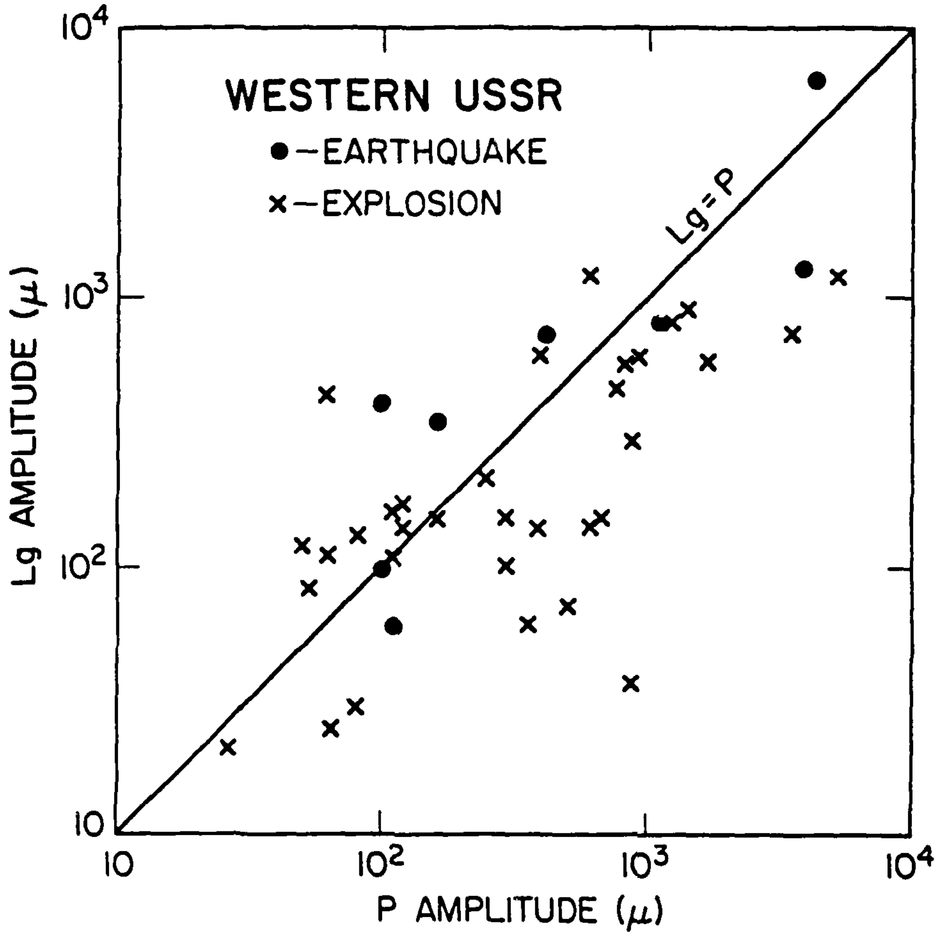

Figure 8. Lg- amplitude vs. P- amplitude in the western USSR.

Table IV

Earthquakes Used in This Study

Eastern U.S.

Date	Origin Time	Location	Latitude	Longitude	m_b	Comments
06/15/73	01:09:05	Maine-NH Quebec Border	45.390°	71.000°	5.2	m_N=4.9
01/08/74	01:12:37.4	Tennessee	36.20°	89.39°	4.1 4.3(S)	
02/15/74	22:35:44.7	Arkansas	34.05°	93.13°	4.2 3.6(S)	
04/03/74	23:05:02.5	S.Illinois	38.59°	88.09°	4.5 4.7(S)	
06/05/74	08:06:11.3	S.Illinois	38.62°	89.94°	4.0 3.6(S)	
06/13/75	22:40:27.2	Missouri	36.54°	89.68°	4.3	
07/09/75	14:54:15.1	Minnesota	45.67°	96.04°	4.6 4.3(S)	
07/12/75	12:37:16	Maniwaki	46.467°	76.222°		4.1m_N
08/29/75	04:22:51.9	Alabama	33.82°	86.60°	3.5 4.4(S)	
10/23/75	21:17:48.2	Manicouagan	49.689°	68.822°		4.0m_N
10/23/76	20:58:18	St. Simeon/ Quebec	47.492°	69.474°		4.4m_N
10/15/63	12:28:58.4	Southern Quebec	46.6°	77.6°	<3	
10/16/63	15:31:01.8	Southern New England	42.5°	70.8°	<3	
10/10/63	14:59:52.5	Virginia	39.8°	78.2°	<3	
05/04/63	21:01:35.9	S.Carolina	32.3°	79.7°	<3	
12/04/63	21:32:35.1	Northern New England	43.6°	71.5°	<3	
12/05/63	06:51:02.5	Kentucky	37.2°	87.0°	<3	
02/18/78	14:48:25.3	Canada	46.31°	74.37°	4.2	
08/14/65	13:13:56.6	S.Illinois	37.23°	89.28°	3.8	

Western USSR

Date	Origin Time	Location	Latitude	Longitude	m_b	Comments
03/02/66	02:37:03	Caucasus Mtns.	43.03°	45.71°	4.9	
02/21/70	07:09:15	Urals	59.40°	59.80°	4.0±.5	
03/21/76	22:39:40.2	Central Kazakh	42.97°	69.89°	3.9	
04/02/76	17:52:28.3	E.Caucasus	42.99°	45.09°	4.5	

Table IV

Earthquakes Used in This Study

Western USSR

Date	Origin Time	Location	Latitude	Longitude	m_b	Comments
04/08/76	22:54:17.8	Uzbek	40.487°	63.650°	4.7	
04/29/76	23:23:15.7	Turkey-USSR Border	40.977°	42.874°	4.8	
10/25/76	08:39:46.4	Europe-USSR Border	59.157°	23.725°	4.5	

Central USSR

Date	Origin Time	Location	Latitude	Longitude	m_b	Comments
04/08/76	22:54:17.8	Gazli	40.487°	63.650°		
04/12/76	16:12:58.9	Gazli	40.456°	63.610°		
04/17/76	20:21:47.2	Gazli	40.446°	63.686°		
04/18/76	22:37:39.7	Gazli	40.265°	63.812°		
04/21/76	22:33:29.8	Gazli	40.550°	63.846°		

Eastern USSR

Date	Origin Time	Location	Latitude	Longitude	m_b	Comments
05/22/73	02:15:04		52.9°	89.5°		
02/27/72	22:15:03		55.1°	93.1°		
04/30/71	15:45:12		46.4°	96.6°		
03/25/72	05:58:05		44.9°	101.0°		
02/04/72	03:34:48		53.1°	107.8°		
12/18/71	22:23:48		56.6°	114.0°		
01/15/72	18:08:04		58.2°	120.7°		
11/25/72	13:42:34		56.3°	123.6°		
08/09/72	20:51:50		56.9°	127.7°		
12/29/73	14:41:31		44.7°	82.8°		
07/07/73	11:41:25		40.0°	77.4°		
03/15/73	23:24:25		37.4°	77.8°		
02/23/73	10:45:08		37.9°	86.9°		
07/16/73	19:45:43		35.3°	86.4°		
10/13/74	21:29:47		34.8°	87.4°		
12/30/72	23:54:09		34.0°	87.6°		
02/04/72	14:08:20		30.6°	84.4°		
08/10/72	21:06:41		32.5°	93.7°		
07/17/71	15:00:53		26.2°	93.3°		

Table V

Explosions Used in This Study

Western USSR

Date	Origin Time	Location	Latitude	Longitude	Estimated Yield (kt)	Comments
03/23/71	06:59:56	Urals	61.29°	56.47°	51	
07/02/71	17:00:02	Urals	67.66°	62.00°	7	
07/10/71	16:59:59	Urals	64.17°	55.18°	27	
09/19/71	11:00:07	Urals	57.78°	41.10°	4	
10/04/71	10:00:02	Urals	61.61°	47.12°	11	
10/22/71	05:00:00	Urals	51.57°	54.54°	34	
12/30/71	06:20:58	Semi-palatinsk	49.75°	78.13°	--	
07/09/72	06:59:58	N.Black Sea	49.78°	35.04°	6	
08/20/72	02:59:58	N.Caspian Sea	49.46°	48.18°	87	
09/21/72	09:00:01	N.Caspian Sea	52.13°	51.99°	21	
10/03/72	08:59:58	N.W.Caspian Sea	46.85°	45.01°	88	
11/24/72	09:59:58	W.Kazakh-stan	51.84°	64.15°	20	
09/30/73	04:59:57	Urals	51.61°	54.58°	22	
10/26/73	05:59:58	Urals	53.66°	55.38°	7	
07/08/74	06:00:02	Urals	53.80°	55.20°	--	
08/29/74	15:00:00	Urals	67.23°	62.12°	20	
06/09/76	03:02:58	E.Kazakh	50.02°	79.08°	--	
07/04/76	02:56:58	E.Kazakh	49.91°	78.95°	--	
07/29/76	02:57:00	E.Kazakh	50.00°	78.00°	--	
03/29/77	03:56:58	E.Kazakh	49.79°	78.15°	--	

Central USSR

Date	Origin Time	Location	Latitude	Longitude	Estimated Yield (kt)	Comments
09/29/68	03:42:58	E.Kazakh	49.77°	78.19°		
11/09/68	02:53:58	E.Kazakh	49.79°	78.04°		
12/18/68	05:01:57	E.Kazakh	49.72°	78.06°		
03/07/69	08:26:58	E.Kazakh	49.81°	78.15°		
07/04/69	02:46:57	E.Kazakh	49.75°	78.19°		

Table V

Explosions Used in This Study

Central USSR

Date	Origin Time	Location	Latitude	Longitude	Estimated Yield (kt)	Comments
09/11/69	04:01:57	E.Kazakh	49.70°	78.11°		
10/01/69	04:02:58	E.Kazakh	49.81°	78.21°		
07/21/70	03:02:57	E.Kazakh	49.95°	77.75°		
11/04/70	06:02:57	E.Kazakh	49.97°	77.79°		
12/17/70	07:00:57	E.Kazakh	49.73°	78.13°		
04/25/71	03:32:58	E.Kazakh	49.82°	78.07°		
05/25/71	04:02:58	E.Kazakh	49.80°	78.21°		
10/09/71	06:02:57	E.Kazakh	50.00°	77.70°		
02/10/72	05:02:57	E.Kazakh	49.99°	78.89°		
03/28/7	04:21:57	E.Kazakh	49.73°	78.19°		
11/02/72	01:26:58	E.Kazakh	49.91°	78.84°		
02/16/73	05:02:58	E.Kazakh	49.83°	78.23°		
07/10/73	01:26:58	E.Kazakh	49.78°	78.06°		
07/23/73	01:22:58	E.Kazakh	49.99°	78.85°		
05/31/74	03:26:57	E.Kazakh	49.95°	78.84°		
12/27/74	05:46:57	E.Kazakh	49.96°	79.05°		
02/02/75	05:32:58	E.Kazakh	49.82°	78.08°		
06/08/75	03:26:58	E.Kazakh	49.76°	78.09°		
12/13/75	04:56:57	E.Kazakh	49.80°	78.20°		
12/25/75	05:16:57	E.Kazakh	50.04°	78.90°		
12/06/69	07:02:57	E.Kazakh	43.83°	54.78°		
12/12/70	07:00:57	E.Kazakh	43.85°	54.77°		
12/23/70	07:00:57	E.Kazakh	43.84°	54.85°		
04/11/72	06:00:05	E.Kazakh	37.37°	62.00°		

*Information on the earthquakes and explosions in the western North America is available on request from RAI'

Significant overlap between the two populations, however, prevents the amplitude-ratio method from becoming an effective discriminant. The last observation is in agreement with Nuttli (1980 b) for events in western and central Asia, but contrary to the conclusion of Gupta et al. (1980) for propagation paths in western Russia.

Additional results on the amplitude ratios of Lg to P waves as a function of distance are presented in Figures 9a to 9e. These plots were taken from the published results of Soviet investigators as compiled by Shishkevish (1979). The data were obtained from the recordings of the Pamir-Lena River seismic array for earthquakes in the Baikal region, Sinkiang, the Gobi desert, southwestern China, and the Himalayas. Except for Figures 9d and 9e which contain propagation paths in the tectonically active mountain-belts of Central Asia, the short-period Lg/P ratios are generally greater than 6 for propagation paths in the stable region of central and eastern USSR.

C. Logarithmic Ratios of Amplitude/Period (A/T) for Lg to A/T for P vs. Distance

Since the results from the last section did not take the epicentral distances into consideration, in this section we plot the amplitude/period ratios of Lg- to P- waves vs. distance in Figures 10 and 11 to see if this approach may improve the separation between the explosion- and earthquake- populations. We have included the period of the observed wave in the calculation to the determination of body- or surface-wave magnitudes, in the hope of reducing the scatter introduced by the period differences of the observed waves.

For the western USSR, as shown in Figure 10, the logarithmic rations of A/T at epicentral distances less than 10°, although sparse, are approximately equal to zero, i.e. $(A/T)_{Lg}$ is approximately the same as $(A/T)_P$. For epicentral distances greater than 10°,

Figure 9a

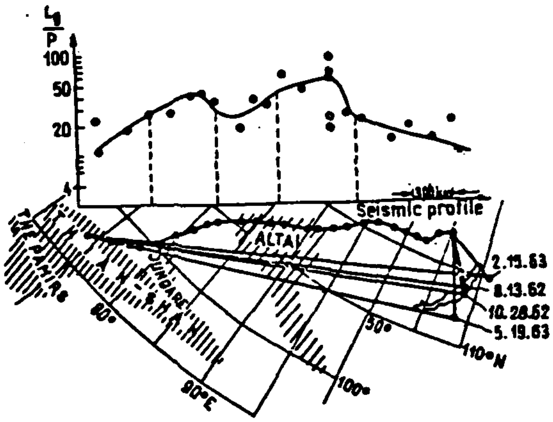

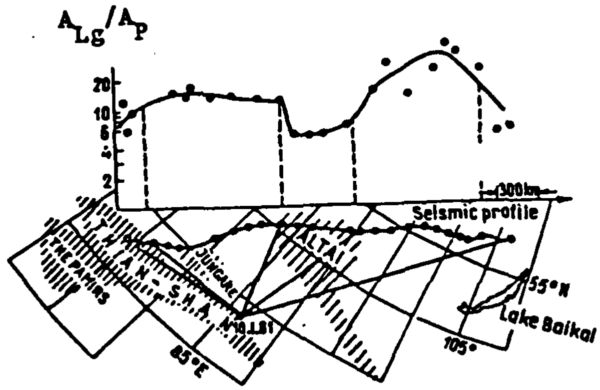

Figure 9b

Figure 9c

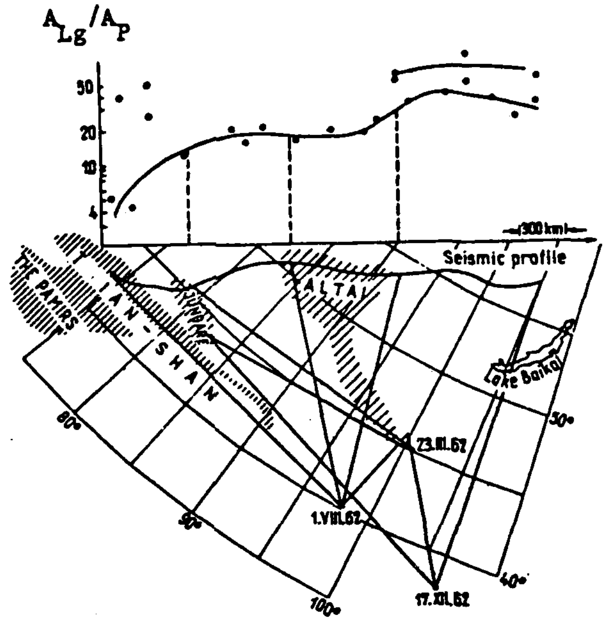

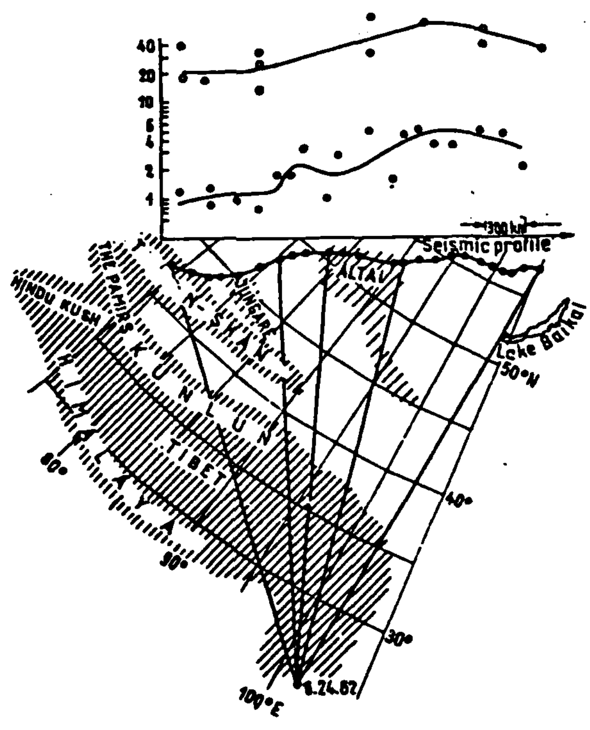

Figure 9d

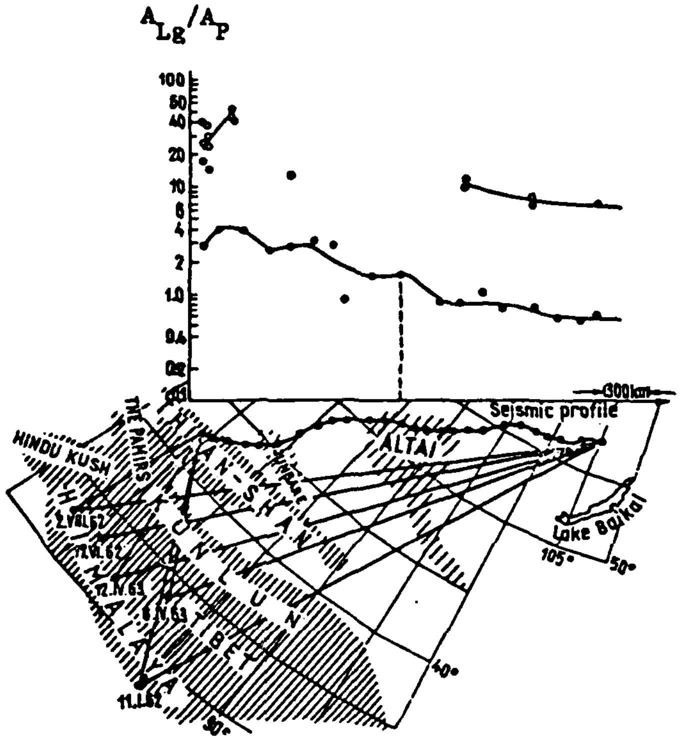

Figure 9e

Figures 9a-9e. The logarithmic ratios, A_{Lg}/A_p, vs. epicentral distance for earthquakes in (a) the Cisbaykal region, (b) Sinkiang, (c) Gobi desert, (d) southwestern China, and (e) the Himalayas as recorded by the seismic stations of the Pamir-Lena River profile. Solid circles represent data obtained from the short-period SKM-3 seismographs; solid circles, from unspecified long-period (probably SKD) seismographs; and shaded regions, mountain belts. The date of the earthquakes is also specified on the plot.

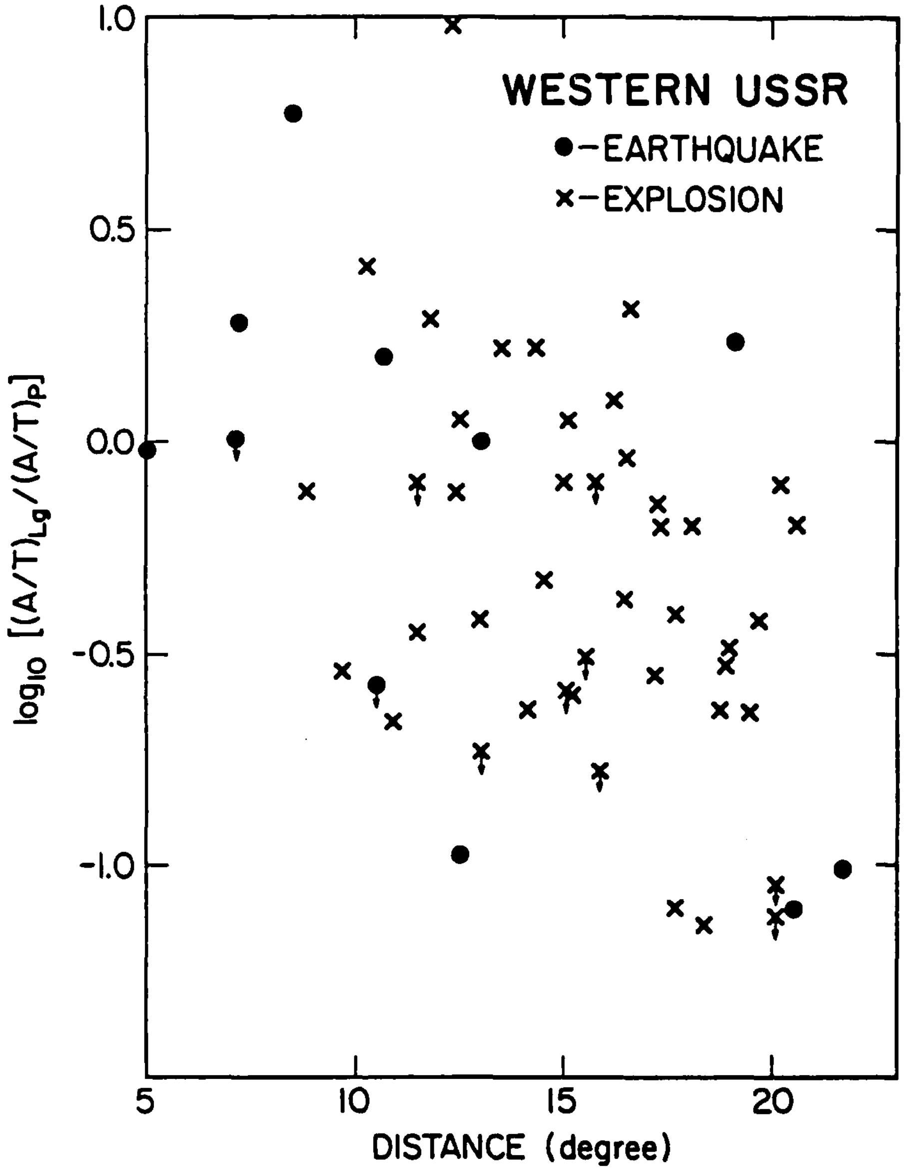

Figure 10. Logarithmic ratios of A/T for Lg to A/T for P vs. epicentral distance in western USSR.

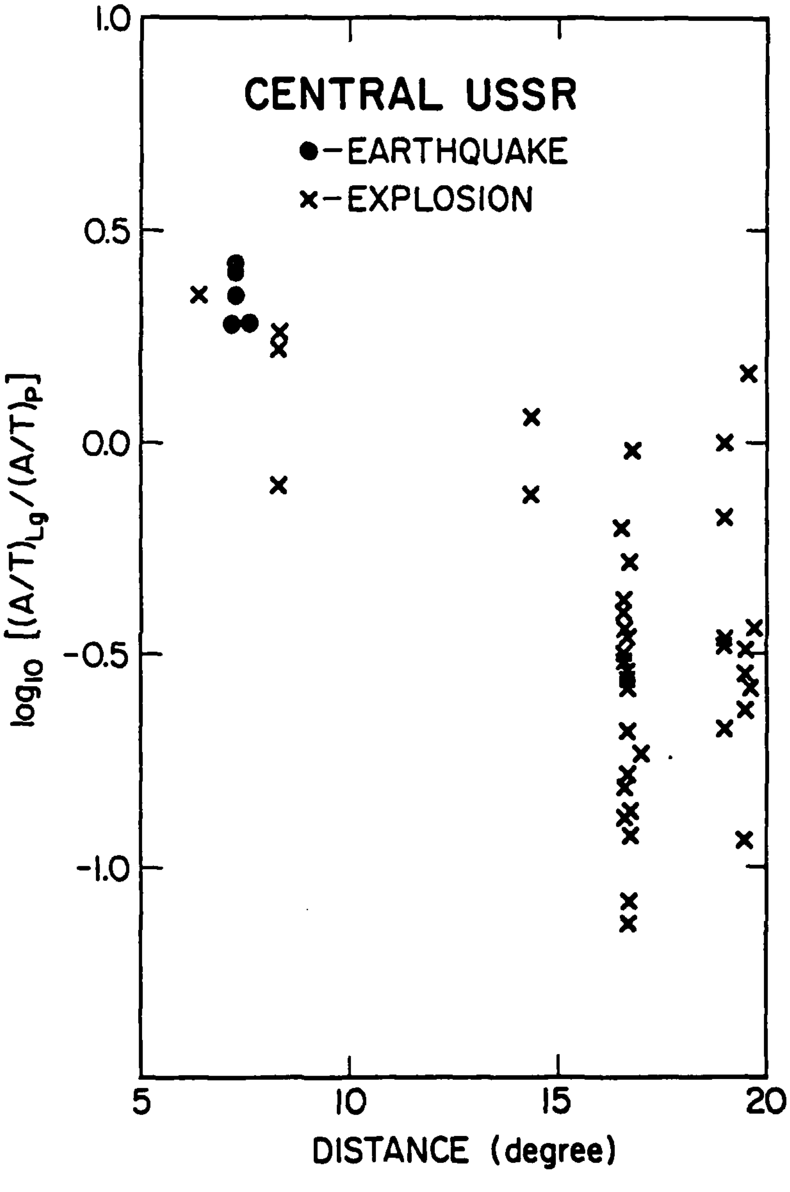

Figure 11. Logarithmic ratios of A/T for Lg to A/T for P vs. epicentral distance in central USSR.

the logarithmic ratios show large scatter and, in general, have negative values. In Figure 11, the logarithmic ratios obtained at the WWSSN stations KBL and MSH are shown for 25 presumed explosions at the East Kazakh test site (~ 49.8°n, 78.2°E) and five Gazli earthquakes. Since the presumed explosions occurred in the same region, the epicentral distances tend to cluster at 16.5°-17.0° for KBL and 19.0°-19.5° for MSH. Considering the relative similarity in the source function and the proximity of the propagation paths, the wide variation in the logarithmic ratios at a single station is most striking. In contrast to the scatter of the explosion data, the logarithmic ratios for the Gazli earthquakes seem to lie closely together.

Although the A/T ratios of Lg to P in these two figures show large scatter, two general patterns can be discerned. Firstly, the logarithmic ratios are on the average larger at near distances than farther away. Secondly, the earthquake population apparently cannot be separated from the explosions based on this method. The falloff of the logarithmic ratios with distance is probably a result of differences in the geometrical spreading and attenuation characters of P and Lg waves. [In a homogeneous sphere, the geometrical spreading would introduce a factor of r^{-1} to P waves but only $(\sin\Delta)^{-1/2}$ to Lg waves, where r and Δ are the epicentral distances in km and radians, respectively. In a spherically layered earth the spreading factor for P waves would depend on the cross section of the ray-pencil at the source and the receiver, which depend on the elastic parameters at the source and the receiver as well as the layers above the turning point of the ray (cf. Aki and Richards, 1980); but the spreading factor for Lg waves would remain the same. Similarly, the differences in the propagation path would affect the attenuation of P- and Lg- amplitudes differently.] If we assume that the effects of the geometrical spreading and attenuation can be combined at regional distances--again, similar to the correction term used in calculating the body- or surface-wave magnitude--then the falloff of the logarithmic ratios with distance implies a faster diminution of Lg- amplitude than P- amplitudes: a factor

that should be taken into account quantitatively in future studies. Also, since the usage of amplitude/period ratios do not improve the separation between the earthquakes and explosions over the amplitude ratios noticeably, we would recommend using the latter which is simpler than the former, in conjunction with some other methods.

D. Group Velocity at Amplitude Maxima

Since the comparison between the amplitudes of short-period P waves to those of Lg waves at regional distances did not prove to be as useful a discriminant as the m_b - M_S method at teleseismic distances, we directed our efforts to the search of depth information from the coda which arrives after the direct S. The coda generally contains the largest amplitudes at regional distances and includes the multiply-reflected S waves as well as Lg waves. The description in the first part of this final report indicates that the waveform of Lg is probably a superposition of higher-mode surface waves (both Love- and Rayleigh-type), the relative excitation of which depends on the focal depth and the source mechanism, modified by the anelastic and scattering properties of the propagation path. Also, several studies (e.g. Knopoff et al., 1973; Panza and Calcagnile, 1975; etc.) indicate that (i) shallow events tend to excite the fundamental and the lower-order modes more efficiently than the higher-order modes, and (ii) for waves with the same period, fundamental and lower-order modes generally have lower group velocities than the higher-order modes. Thus, if the effects of the propagation path are neglected, then shallow events would tend to contain larger amplitudes at lower group-velocity window than deep events. With this theoretical possibility in mind, we measured the group velocity at amplitude maxima as a function of distance.

For events in the eastern U.S., the group velocities at amplitude maxima vs. distance shown in Figure 12 were obtained at stations of the NEUSSN; Figure 13 from stations of the WWSSN and the

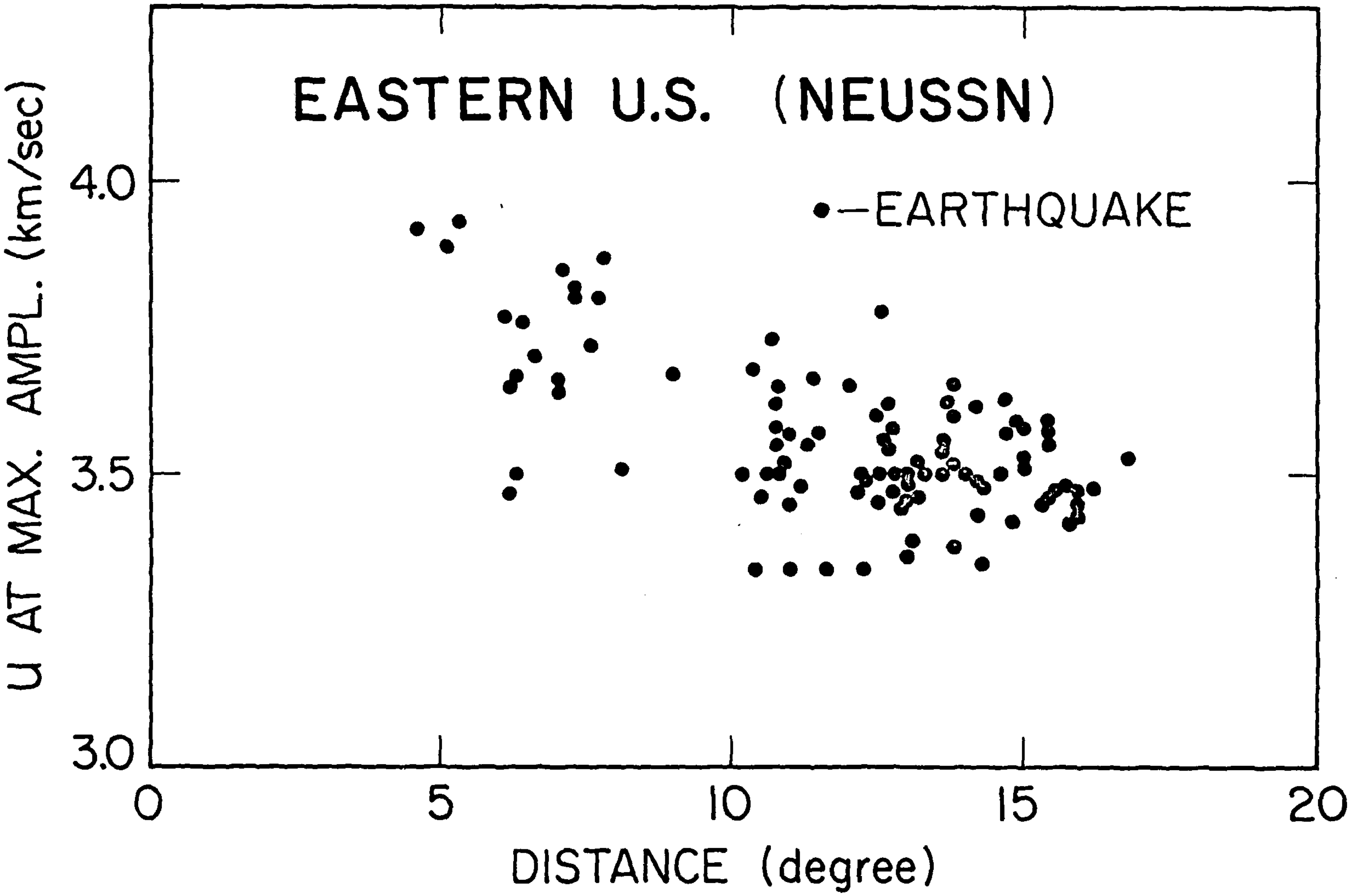

Figure 12. Group velocities measured at amplitude maxima vs. distance for propagation paths in the eastern U.S. as recorded by the NEUSSN.

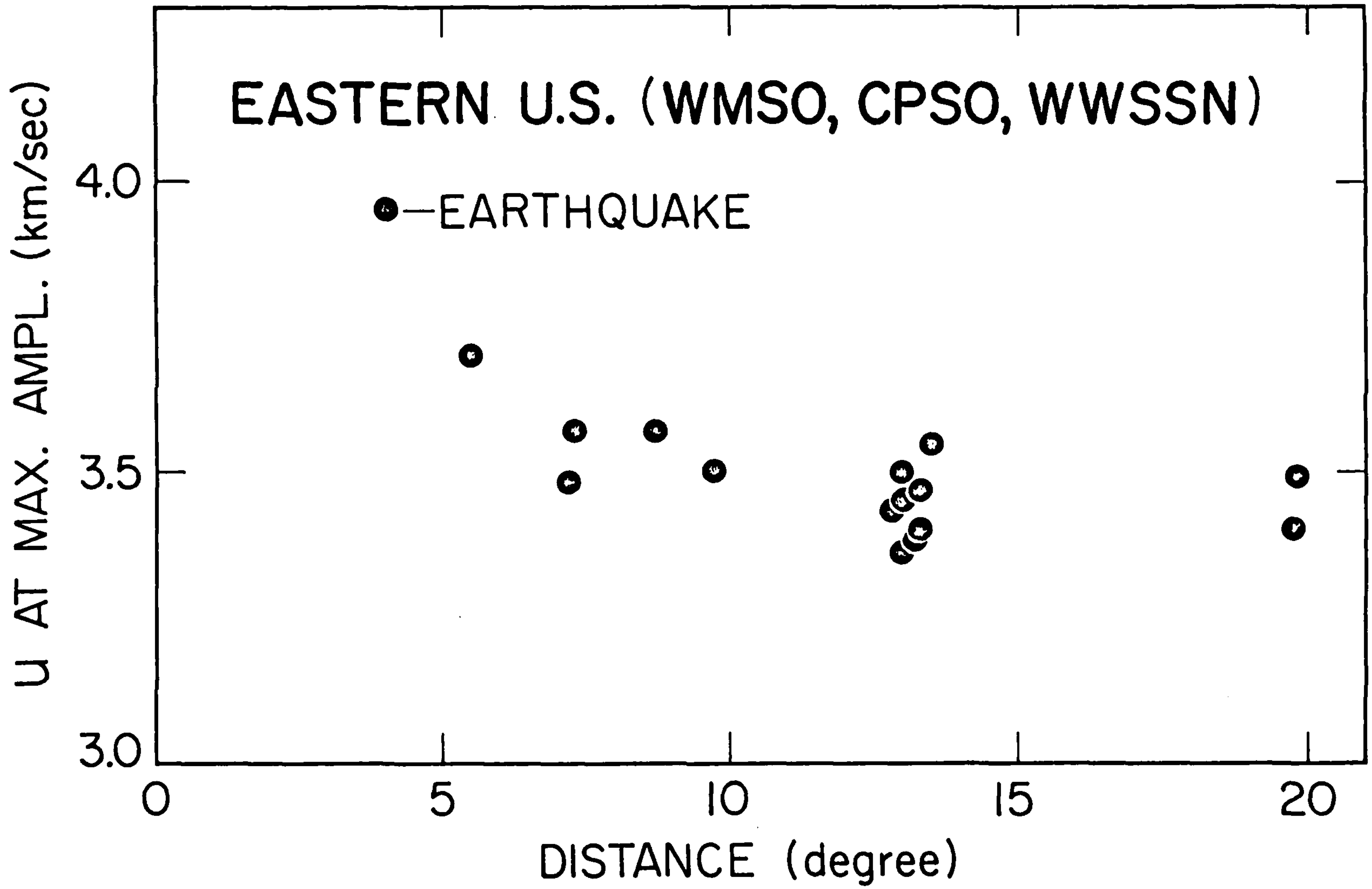

Figure 13. Group velocities measured at amplitude maxima vs. distance for propagation paths in the eastern U.S. as recorded by the stations of the WWSSN and the University of Minnesota array.

University of Minnesota array (the Wichita Mountain and Cumberland Plateau Seismic Observatories, abbreviated as WMSO and CPSO); and Figure 14, from WWSSN and LRSM stations. Similarly, measurements in Figures 15 and 16 were derived from WWSSN stations for propagation paths mostly in the western and central USSR, respectively. An examination of these figures indicate that except for central USSR, the group velocities at the amplitude maxima for explosions seem to be less than those for earthquakes. This observation would support our hypothesis if the earthquakes are located deeper than the explosions. In general, the burial depths for underground explosions are less than 1 km, whereas the focal depths for the earthquakes used in this study are poorly known. [Using the travel times of P waves, the depth resolution for shallow teleseismic events is probably no better than ± 25 km.] Tectonic considerations, however, can constrain the focal depths of earthquakes in the eastern U.S. and the western USSR to be less than 35 km. The proximity of the Gazli earthquakes to the Alpine-Himalayan orogenic belt would probably increase this uncertainty even further. The only conclusion which we can safely draw from the above discussion is that the focal depths of the earthquakes were probably deeper than those of the explosions. A lack of more stringent constraints on their focal depths prevents us from testing our hypothesis quantitatively. For central USSR, the large spatial separation between the East Kazakh test site and Gazli and/or the inclusion of major tectonic boundaries in the propagation may also explain the disparity in the observed group velocities.

E. Energy-Ratio Method

During the initial stage of the group velocity study described above, it was noted that for earthquakes in the eastern U.S. the energy in the coda with the largest amplitude, which normally arrives after the direct S-phase, was distributed roughly equally about a group velocity of 3.4 km/sec. That is,

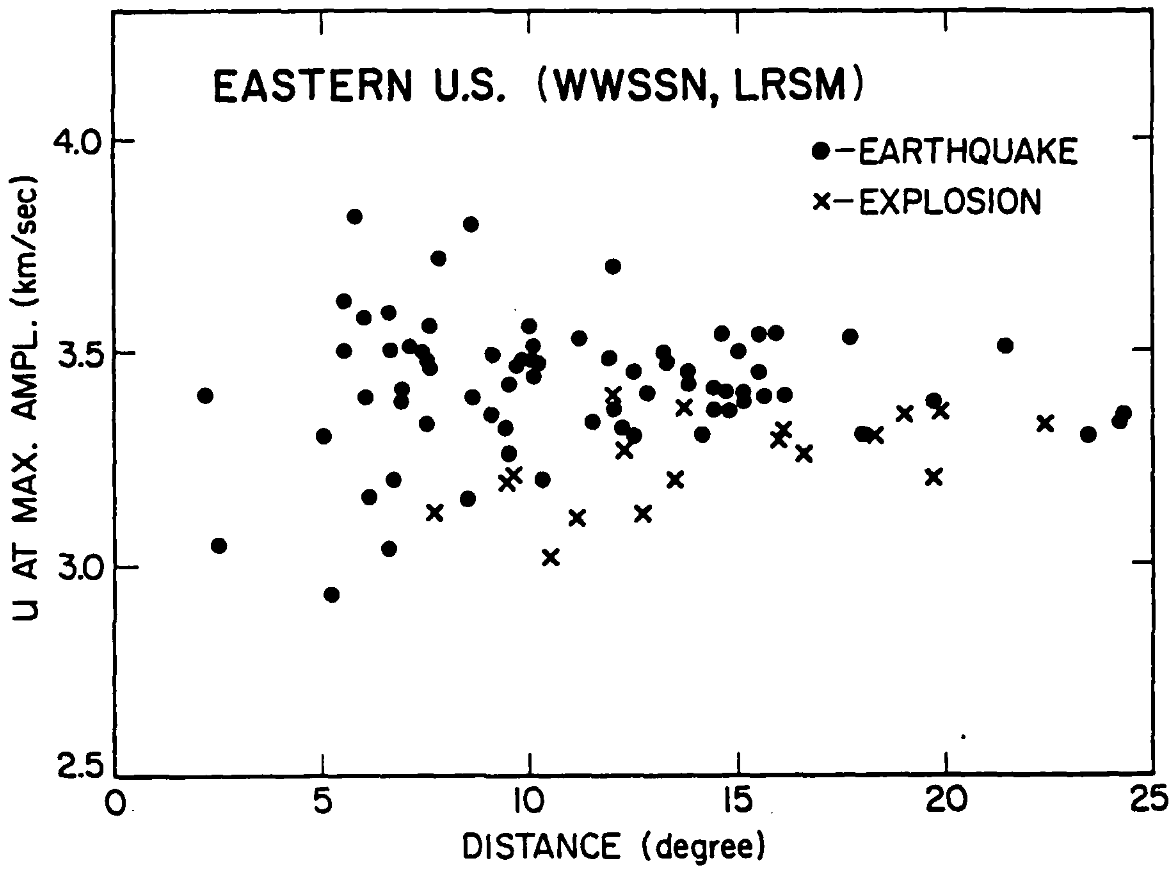

Figure 14. Group velocities measured at amplitude maxima vs. distance for propagation paths in the eastern U.S. as recorded by the WWSSN and LRSM stations.

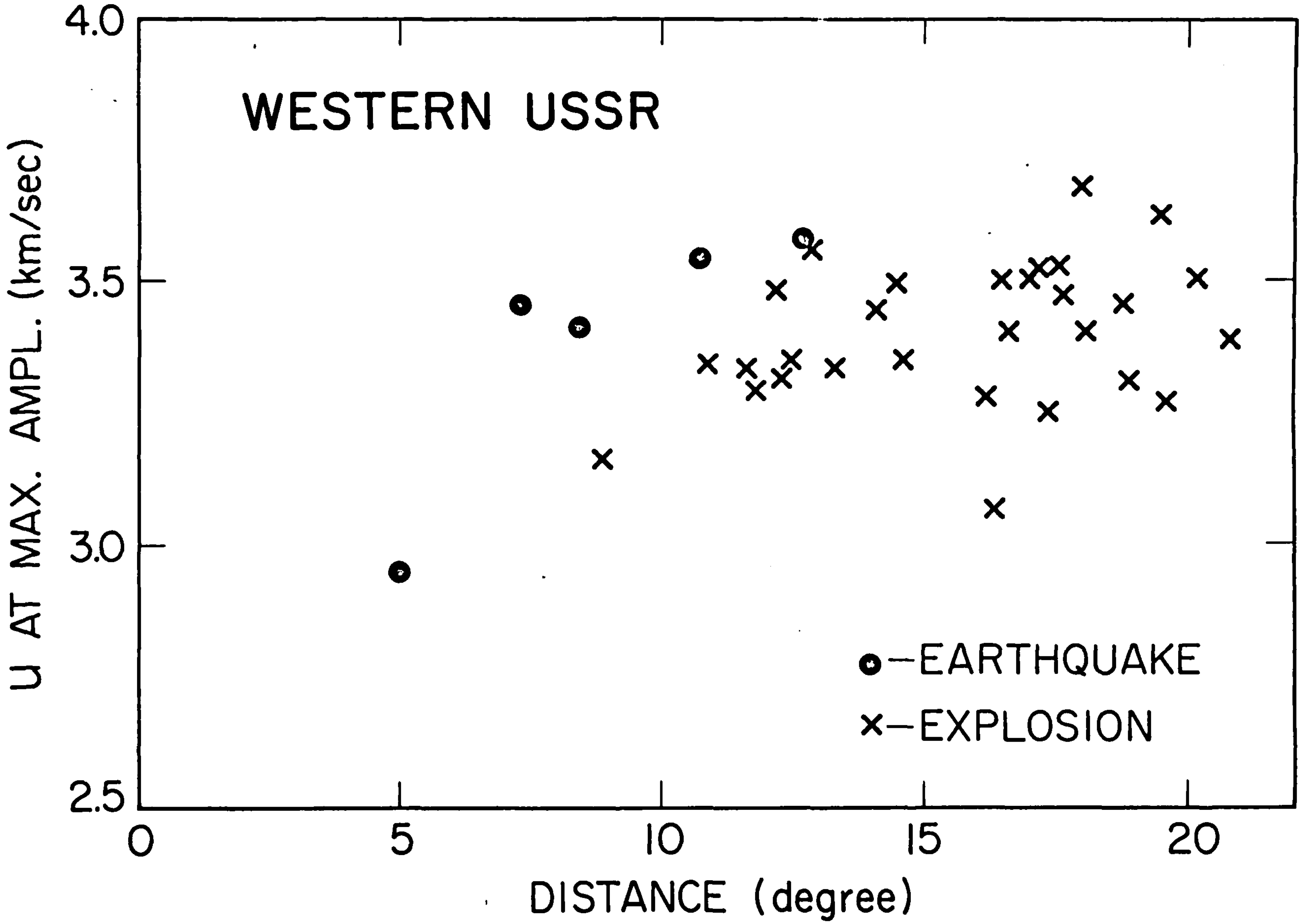

Figure 15. Group velocities measured at amplitude maxima vs. distance for propagation paths mostly in the western USSR as recorded by the stations of WWSSN.

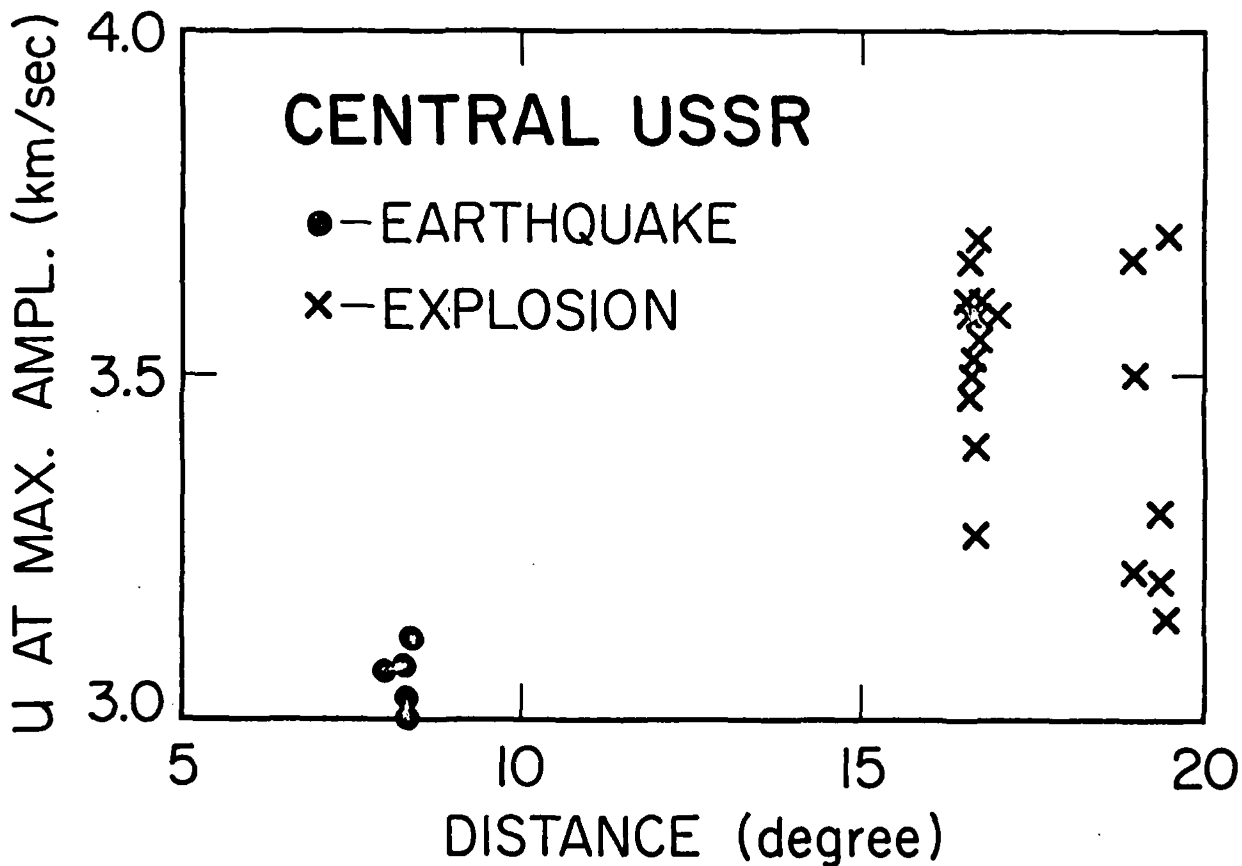

Figure 16. Group velocities measured at amplitude maxima vs. distance for propagation paths mostly in the central USSR as recorded by the stations of WWSSN.

about half of the energy in the coda propagated at a group velocity greater than 3.4 km/sec , while the other half, at a group velocity of less than 3.4 km/sec. As a result of this observation, two group-velocity windows were selected: 3.4-4.0 km/sec and 2.8-3.4 km/sec , to see if the energy distribution in these two windows differs between earthquakes and underground explosions. The motivation behind this approach is similar to that of the previous section on group velocity, i.e. shallow events presumably contain more energy in the 2.8-3.4 km/sec window, during which the fundamental and lower-order modes arrive, than comparably-sized deep events. Thus, instead of measuring the group velocity of the amplitude maxima at a single point, the energy-ratio approach averages the amplitude spectra of two band-limited, group-velocity windows and compares them. Moreover, since our measurements were taken from the vertical-component seismograms, only waves of the Rayleigh-, P-, and SV-types are of interest to us.

To quantify the amount of energy within each group-velocity window, we measured the area enclosed by the envelope of the waveform in the selected group-velocity windows with a planimeter. This technique is analogous to the AR-method used by Brune et al. (1963) on long-period surface waves. Since the area measured is proportional to the energy contained in the group-velocity window, we have designated the areas in the 3.4-4.0 km/sec and 2.8-3.4 km/sec windows by E_{HIGH} and E_{LOW}, respectively. The subscripts high and low refer to the relative group velocity in the two windows.

Figure 17 shows E_{HIGH} vs. E_{LOW} for events in the eastern U.S. Results from this figure seem to indicate that the underground nuclear explosion, SALMON, contained relatively more energy in the low group-velocity window than the earthquakes. Although this observation may not be independent of the lower group velocity observed for SALMON, the technique had nonetheless improved the separation between the earthquake- and explosion-populations in this case.

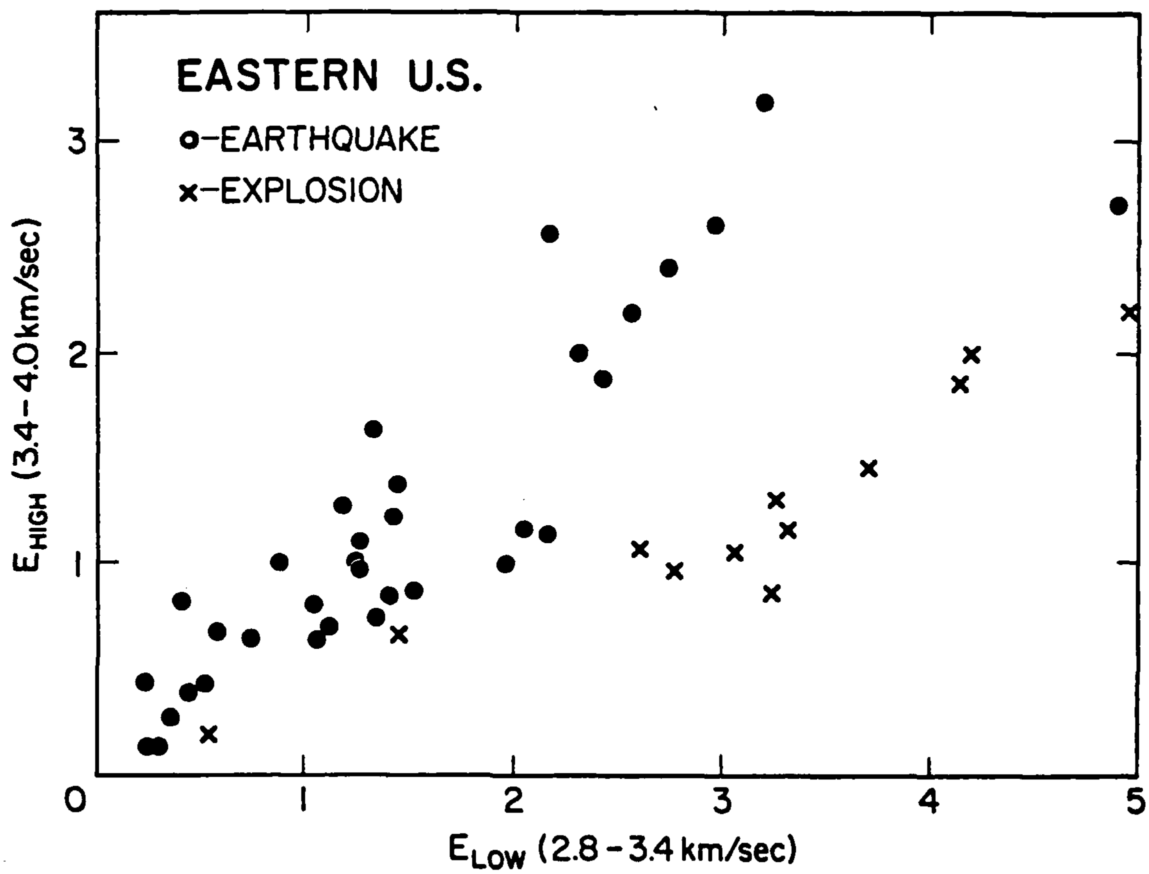

Figure 17. Energy in the 3.4-4.0 km/sec window (E_{HIGH}) vs. energy in the 2.8-3.4 km/sec window (E_{LOW}) for events in the eastern U.S.

Figures 18-20 show the ratios of E_{HIGH} to E_{LOW} as a function of epicentral distance for the eastern U.S., and the western and central portions of the USSR, respectively. An inspection of these figures show that the energy ratios exhibit a clear separation between earthquakes and explosions in the eastern U.S., but not in the western USSR. (The plot for central USSR did not contain any earthquake data; consequently, no comparison was possible.) The difference in the discrimination ability may be explained in several ways. Firstly, the data from SALMON was anomalous because of the effects of the unusual burial medium, salt, and the propagation through the thick sedimentary wedge of the Mississippi Embayment. Secondly, the peaceful nuclear explosions (PNE's) conducted in western USSR may, for engineering purposes, have been designed or deployed differently from the non-PNE's. Thirdly, the great-circle paths from these events in the western USSR to the recording stations generally include one or several large-scale, lateral heterogeneities (e.g. the Gulf of Finland, Gulf of Bothnia, Baltic Sea, or the Alpine-Himalayan belt) which may affect the energy distribution in the coda by frequency-dependent absorption, scattering, and changes in group velocity. Lastly, the selected group-velocity windows may have to be modified in different regions to optimize the potential of extracting depth information from the Lg coda. Other or a combination of these explanations is, of course, also quite possible.

This paragraph expands on the optimization of the energy-ratio method mentioned above. According to the study of Herrmann (1974), the excitation function of higher-mode surface waves depends primarily on the focal depth. Thus, if we know the average structure of the source and the propagation path, then we can calculate the relative importance of the lower-order to higher-order modes for sources at a certain depth, say, 5 km. Since we can also calculate the group-velocity curves for the higher-mode surface waves, we should be able to define a threshold group velocity at which the difference in the energy ratio for the given hypocentral depth is maximized. This approach will be pursued in future studies on regional-distance discrimination.

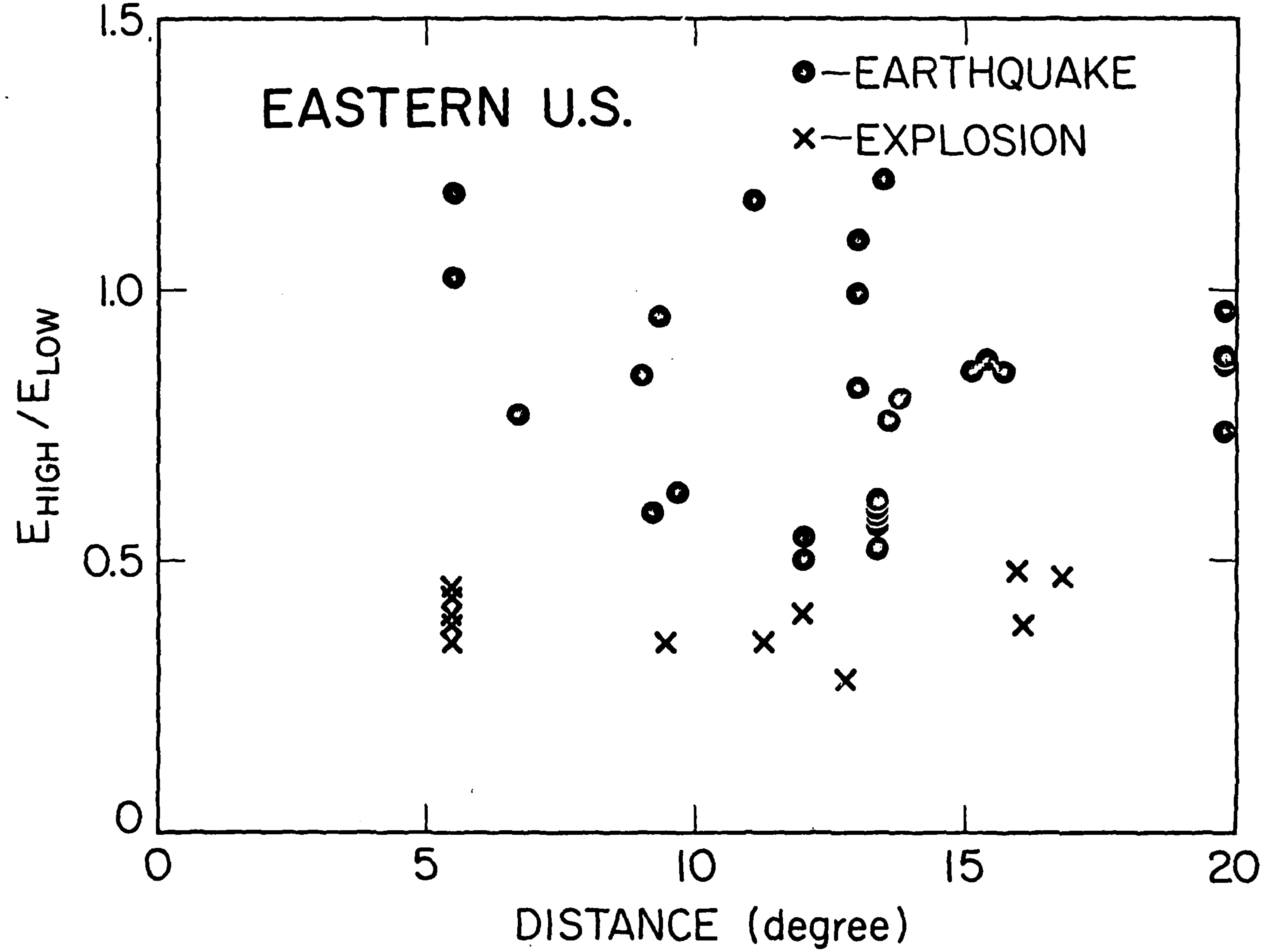

Figure 18. Ratios of E_{HIGH} to E_{LOW} as a function of epicentral distance for propagation paths in the eastern U.S.

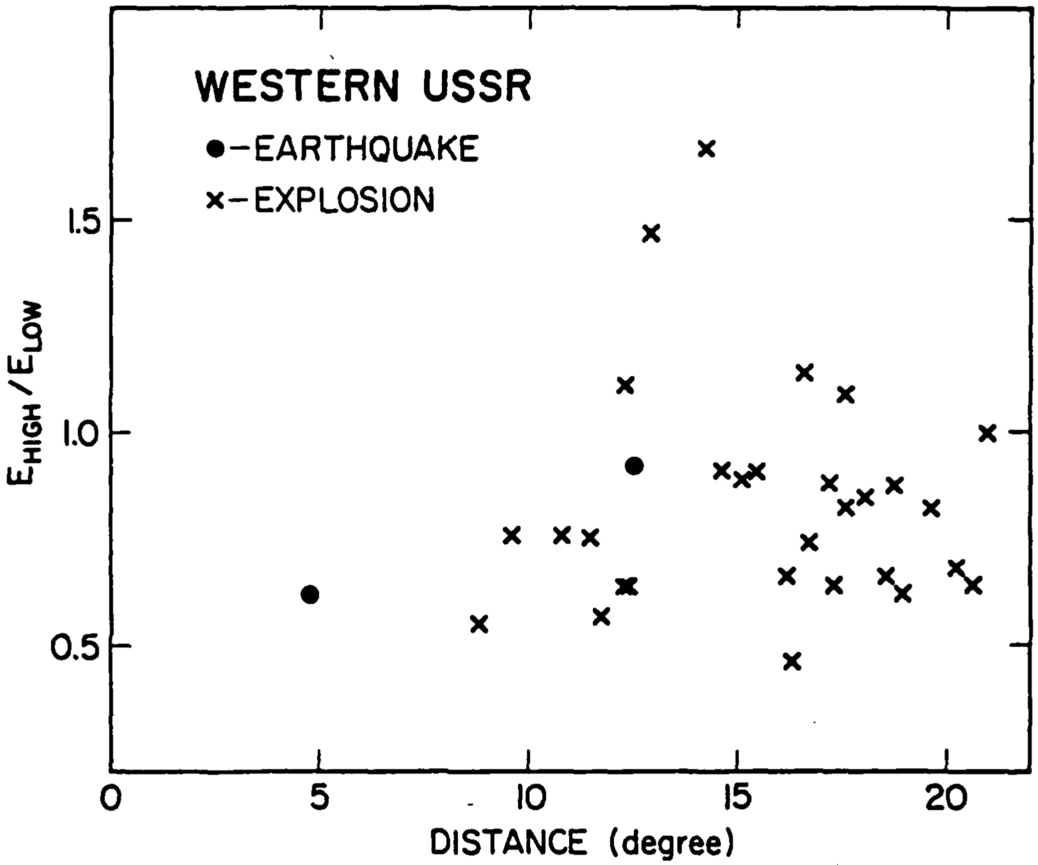

Figure 19. Ratios of E_{HIGH} to E_{LOW} as a function of epicentral distance for propagation paths in the western USSR.

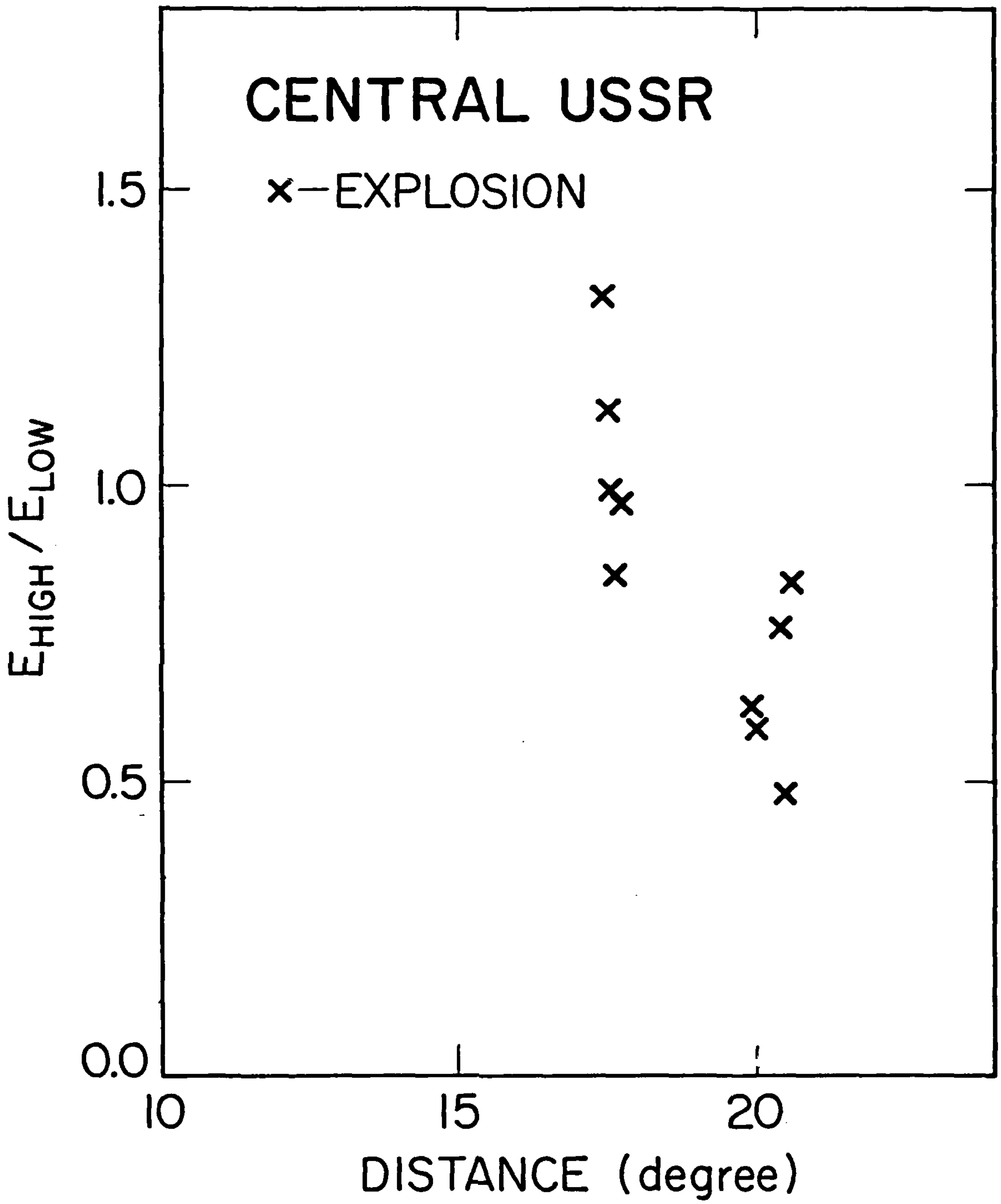

Figure 20. Ratios of E_{HIGH} to E_{LOW} as a function of epicentral distance for propagation paths in the central USSR.

The various discrimination methods discussed in this section all seem to indicate that significant discrepancies exist in the results derived from the different regions. Differences in the propagation characteristics of the various regions can explain most of the observed discrepancies. Thus, we will need to improve our understanding on the propagation characteristics of seismic waves on a regional basis so that we may (i) assess the feasibility of the methods discussed above with more confidence, and (ii) devise some other discrimination methods.

Part III. Preliminary Studies

As part of our program on the seismic wave propagation at regional distances we have initiated several studies, the preliminary results of which are reported below.

A. Attenuation of Lg Waves

Studies on the attenuation of Lg waves were carried out for the eastern U.S., as well as western and central USSR. In the eastern U.S., readings on the amplitude and the period of Lg were made from the short-period seismograms of WWSSN and NEUSSN. The amplitudes were normalized relative to the assigned magnitude (by USGS, NOAA, or St. Louis University) of the event and the ratios of normalized amplitude to period vs. epicentral distances were then plotted on Figure 21. Since the assigned magnitude was probably derived from averaging a limited number of readings, measurements at different stations would inevitably deviate from this mean. Moreover, since these deviations are propagated into the normalization process, the scaled amplitudes would not only be subject to the modulating effects at the recording site but also to those from which the assigned magnitude was based on. If our normalized-amplitude/period ratios can approximate statistically the unbiased values, then the data shown in Figure 21 suggests a slightly higher attenuation rate for the eastern U.S. than that derived by Nuttli (1973) for the central U.S.

The data from the western and central USSR were obtained somewhat differently since most of the events were presumed explosions. The procedure used to obtain the amplitude vs. epicentral distance relation is as follows: (i) The estimated yields from Dahlman and Israelson (1977) were converted to body-wave magnitudes via the relation

$$m_b = 0.93 \log_{10} Y + 3.49.$$

This empirical relation was derived by Ericsson (1971) for data from the NTS explosions. Ericsson claimed that this relation is

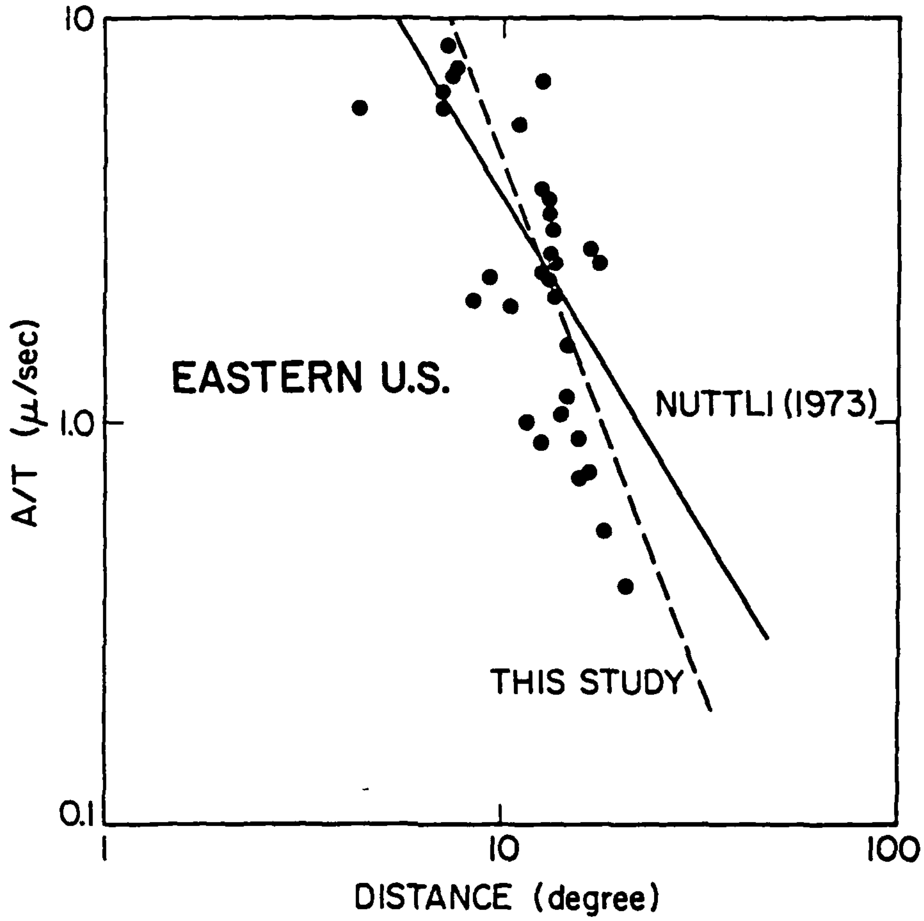

Figure 21. Ratios of normalized amplitude to period of Lg waves vs. epicentral distance in the eastern U.S. See text for a discussion of the normalization procedure.

also representative for tests in the USSR. The validity of this claim, however, remains to be demonstrated. (ii) We then normalized the observed amplitudes corresponding to an $m_b = 4.4$ event by using the following formula

Normalized Amplitude = Observed Amplitude X $10^{(4.4-m_b)}$

(This second step is similar to the procedure used to normalize the events in eastern U.S.). Since the magnitude used in the above calculation was estimated, the uncertainties in the normalized amplitudes would probably exceed the ones for earthquakes. The procedure nevertheless provides a first-order estimate for the attenuation of Lg waves.

Explosion data from the western and central USSR, earthquake data from the western USSR, as well as the normalized amplitude-mean at 500, 1000, 1500, and 2000 km taken from Antonova et al. (1978) in Figure 22. The earthquake data from the western USSR, was normalized similar to that from the eastern U.S. The results from Antonova et al. (1978) were recorded at the Pamir-Lena River seismic array for earthquakes in the Central Asia. Antonova et al. concluded that (i) at epicentral distances less than 700 km, the amplitudes of Lg are proportional to $\Delta^{-1.4}$, and (ii) the exponent decreases, i.e. becomes more negative, as distance increases such that at 2000 km the exponent is approximately between -2.2 and -2.5. Despite the large scatter, our data is not inconsistent with curves having slopes between -2 and -3 at these epicentral distances. In comparison to the results from the eastern U.S., the attenuation rate in the western and central USSR appears rather high. But, if we take the propagation paths, which straddle one or several major tectonic boundaries (most of the Soviet data was derived from earthquakes outside the USSR, while our data was obtained from presumed Soviet explosions as recorded outside the USSR), into consideration then the higher attenuation rates are not unreasonable.

B. Attenuation and Magnitude-Scale for Intermediate-Period Rayleigh Waves

For propagation paths in the eastern North America, Rayleigh

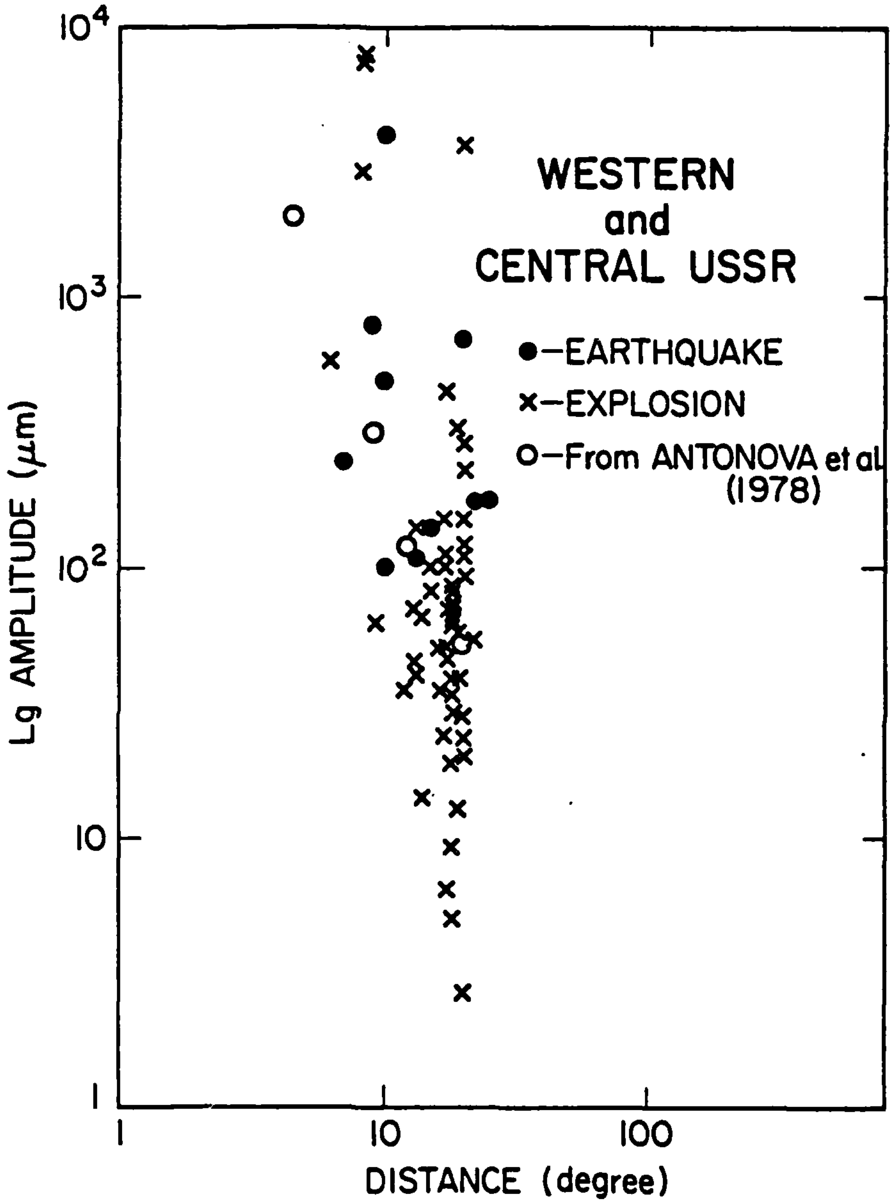

Figure 22. Ratios of normalized amplitude to period of Lg waves vs. epicentral distance in the western and central USSR. Amplitude data from Antonova et al. (1978) are also included in this plot.

waves with periods between 8 to 14 seconds are the most prominent feature on the long-period seismograms of WWSSN (T_o=15 sec, T_g=100 sec).

(a) Attenuation

To measure the anelastic properties of intermediate-period Rayleigh waves, we measured the amplitudes and periods at the amplitude maxima and plotted the ratios of amplitude to period as a function of epicentral distances in Figure 23. In a study on the surface-wave attenuation of central U.S., Nuttli (1973) showed that in the distance range 2° to 20° the falloff of wave amplitude with propagation distance, due to the effects of geometrical spreading and anelastic attenuation, can be approximated by a straight line on a log-log plot. Following Nuttli's example, we found that the data in Figure 23 can be fitted by a straight line with a slope of -1.66, which corresponds to an attenuation coefficient of 0.10 deg^{-1}. This attenuation rate is the same as that derived by Nuttli for the central U.S. but different from those of Basham (1971) and Evernden et al. (1971). We concur with Nuttli's (1973) interpretation that the discrepancy arises from the phase Rg, instead of the fundamental-mode Rayleigh waves, measured by Basham and Evernden et al. (Nuttli also notes that Rg is "...prominent on the seismograms of North American stations for earthquakes or underground explosions in the western United States. However, it is not well developed for earthquakes in the central United States recorded at eastern stations..."). The magnitude-scale derived by Vanek et al. (1962) indicates that the amplitudes of surface waves, at periods near 10 sec , are attenuated at the same rate as in the eastern and central U.S. This observation together with our findings in Part II on Lg-propagation in the U.S. and the USSR seem to imply a close similarity between the crustal structure in the eastern U.S. and that in the eastern and central USSR.

(b) Magnitude Scale

Based on the attenuation rate derived above, we obtained a magnitude-scale formula for regional distances

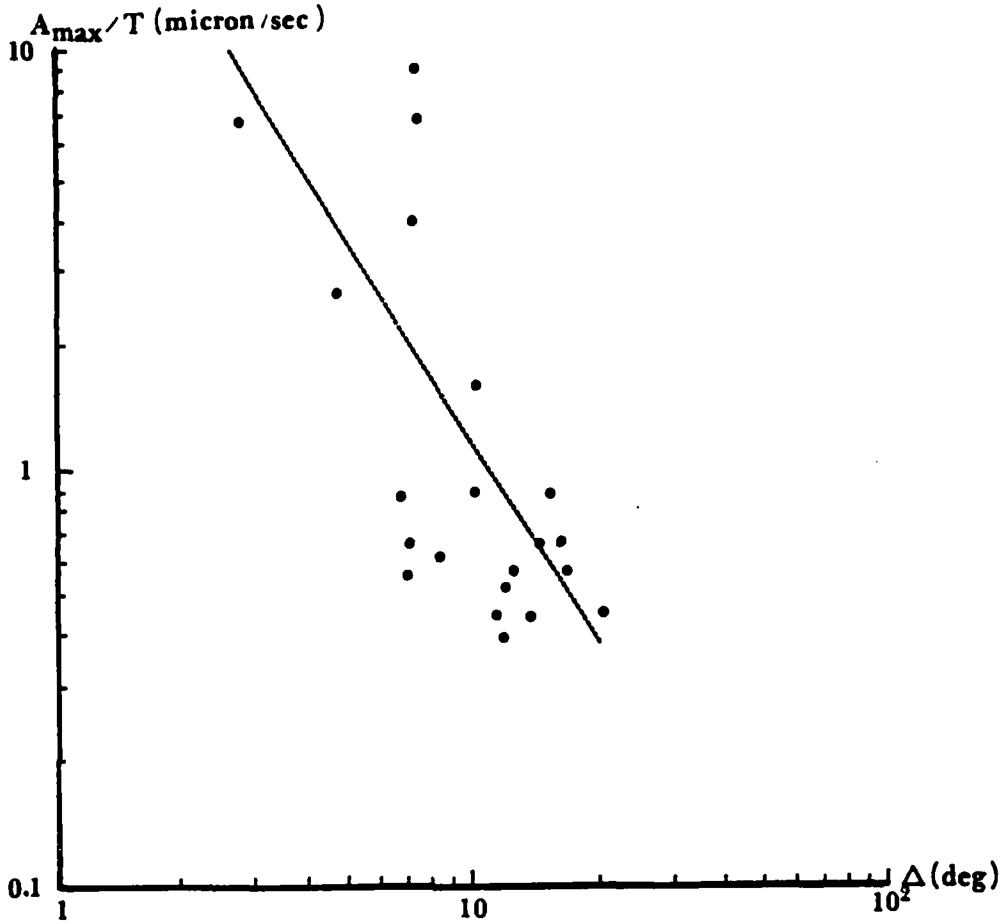

Figure 23. Ratios of amplitude to period of intermediate-period (8-14 sec) Rayleigh waves vs. epicentral distance in the eastern U.S. The dotted line represents an approximation of $\gamma = 0.1\ \mathrm{deg}^{-1}$ in the distance range of 2° to 20°.

$$M_S = \log_{10} (A_{max}/T) + 1.66 \log_{10} \Delta + 2.60$$

This formula was slightly modified from Equation (4) of Nuttli (1973), where he used $(A/T)_{max}$ and wave periods of 3-12 seconds instead of (A_{max}/T) and 8-14 seconds used in this study. In both cases, the range of applicability is between 2° and 20° in eastern North America.

C. Intermediate-Period M_S vs. M_{Lg} in Eastern and Central U.S.

Having determined the magnitude-scale formulae for Lg waves (M_{Lg} at 0.3-1.0 sec) and intermediate-period Rayleigh waves (M_S at 8-14 sec) appropriate for the eastern and central U.S., we became interested in investigating (i) the relationship between M_S and M_{Lg}, and (ii) the possibility of using them as a discriminant. The magnitudes M_S and M_{Lg} for four earthquakes and one underground nuclear explosion (SALMON) in the eastern U.S. were measured and plotted in Figure 24; also shown in this figure are the data points for four central U.S. earthquakes taken from a study by Nuttli (1973). An inspection of this figure shows that (i) all the data points can be approximated by a linear relation of the form: $M_S = 1.69\ M_{Lg} - 4.08$; and (ii) the explosion data cannot be discriminated from the earthquake population. Since there is only one explosion used in this preliminary study, we would like to examine more data from eastern and central U.S. explosions (e.g. RULISON, GAS BUGGY, RIO BLANCO, etc.) in the future.

D. Usefulness of High-Frequency Waves at Regional Distances

Although many of the NEUSSN stations operate with peak magnifications in the 10-20 Hz range, the seismograms for earthquakes within regional distances, as examined by us, did not show frequencies higher than 5 Hz. This observation is quite different from the efficient propagation of Lg and intermediate-period surface waves in the eastern and central U.S.; consequently, we suspect that waves at frequencies higher than 5 Hz are attenuated rapidly by scattering at small-scale heterogeneities so that they may not be very useful at regional distances in certain regions.

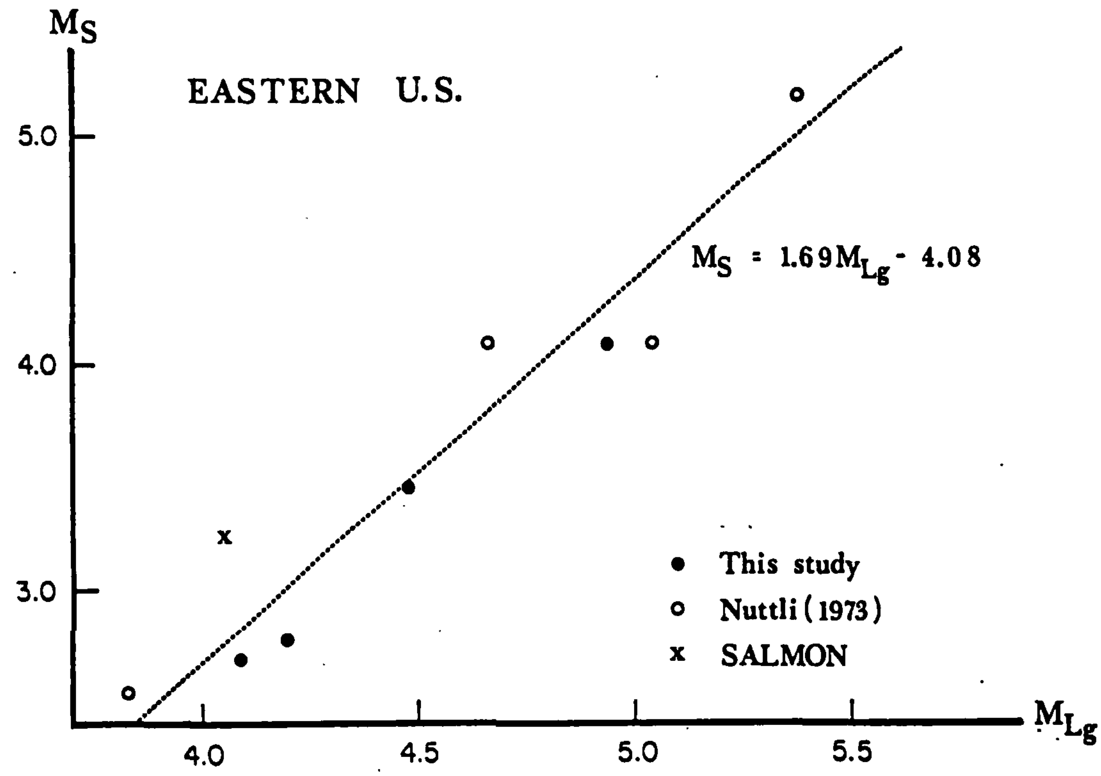

Figure 24. M_S (from 8-13 sec Rayleigh waves) vs. M_{Lg} (from 0.3-1.0 sec Lg waves) for events in the eastern and central U.S.

Part IV. Magnitude-Yield Relation and Others

An accurate determination of the magnitude-yield relation is an important geophysical problem. Aside from its obvious application for estimating the yield of unknown nuclear tests by measuring the amplitudes of the observed seismic waves, a well-determined magnitude-yield relation may become one of the most useful tools for calibrating the seismic energy (especially at short periods) radiated by earthquakes. The task of casting this relation into a well defined form, however, is not an easy one. Difficulties can be traced to both the magnitude and the yield ends of the relation. Below we will describe some of the difficulties involved.

The amplitudes of the observed seismic waves can be significantly affected by several factors, such as (i) the medium and the burial depth of the source, (ii) the degree of seismic coupling between the source and the surrounding medium, and (iii) the local structures beneath the source and the receivers. The first and third factors have plagued seismologists for years, but these problems are currently being solved. To our knowledge, the second factor has not been studied extensively, its effects are therefore not well understood.

Several investigators have attempted to establish the magnitude-yield relation based on magnitudes that are determined from local/regional networks and/or a relatively small number of events. In view of the lack of completeness of these studies and the importance of this problem, we have decided to (i) undertake a comprehensive compilation of available published results that are relevant to the problem of yield-estimation, (ii) present the results from our compilation in a useful form, and (iii) improve the determination of body-wave magnitudes, in a statistical sense, by increasing the number of amplitude measurements at various epicentral distances. [ISC determines its body-wave magnitudes only if three or more stations report their amplitudes. It then applies the

unified magnitude of Gutenberg (1956) to the amplitudes to determine the m_b. Few stations, however, have the habit of reporting their amplitudes to the ISC.]

Data

Because of the large number ($\geq$ 400) of nuclear tests in the United States and the Soviet Union, we have limited most of our data base to those underground nuclear explosions for which reports on their estimated yield exist. The U.S. data used is derived from Springer and Kinnaman (1971, 1975), and the Soviet data, from Bolt (1976) and Dahlman and Israelson (1977). The magnitude determinations used are from Bolt (1976) and the International Seismological Centre (ISC) Bulletins. There are some doubts concerning the source reference of the estimated yield for the Soviet tests, compiled by Dahlman and Israelson, as well as the magnitude of the Soviet tests as reported by Bolt; we are in the process of uncovering these uncertainties.

Table VI represents a compilation of the U.S. explosion data used in this report. The table contains the name, data, origin time, location, and burial depth of the event; it also describes the rock-type surrounding the buried source (e.g. tuff, alluvium, rhyolite, etc.), the dimensions (volume, diameter, and height) of the collapse cavity, the body-wave magnitude (ISC), and the announced or estimated yield. Except for the magnitude, all the information was provided to Springer and Kinnaman (1971, 1975) by the U.S. Atomic Energy Commission (AEC). A compilation of the available Soviet data is outlined in Table VII. A compilation of the of the date, computed origin time and location (Bolt, 1976), the body-wave magnitudes (from ISC and Bolt's compilation), and the estimated yield for these events (Dahlman and Israelson, 1977).

Based on the compilations in Table VI and VII, we have made the following plots:

From the Soviet data: m_b (ISC and Bolt's) vs. estimated yield (Figure 25 and 26, respectively)

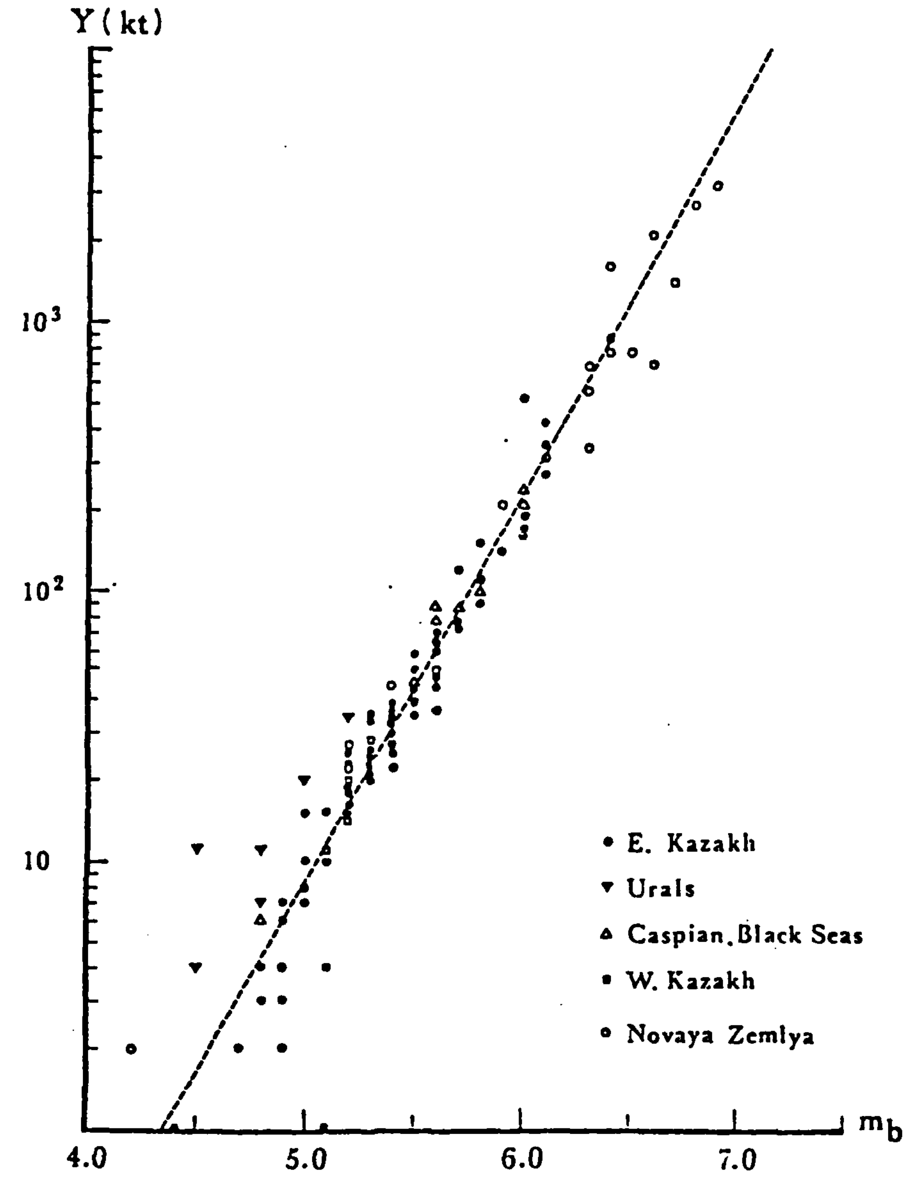

Figure 25. Body-wave magnitude (ISC) vs. yield for events in the USSR. The dashed line, $m_b = 0.75 \log_{10} Y + 4.345$, represents our preliminary, best-fitting relation between these two quantities.

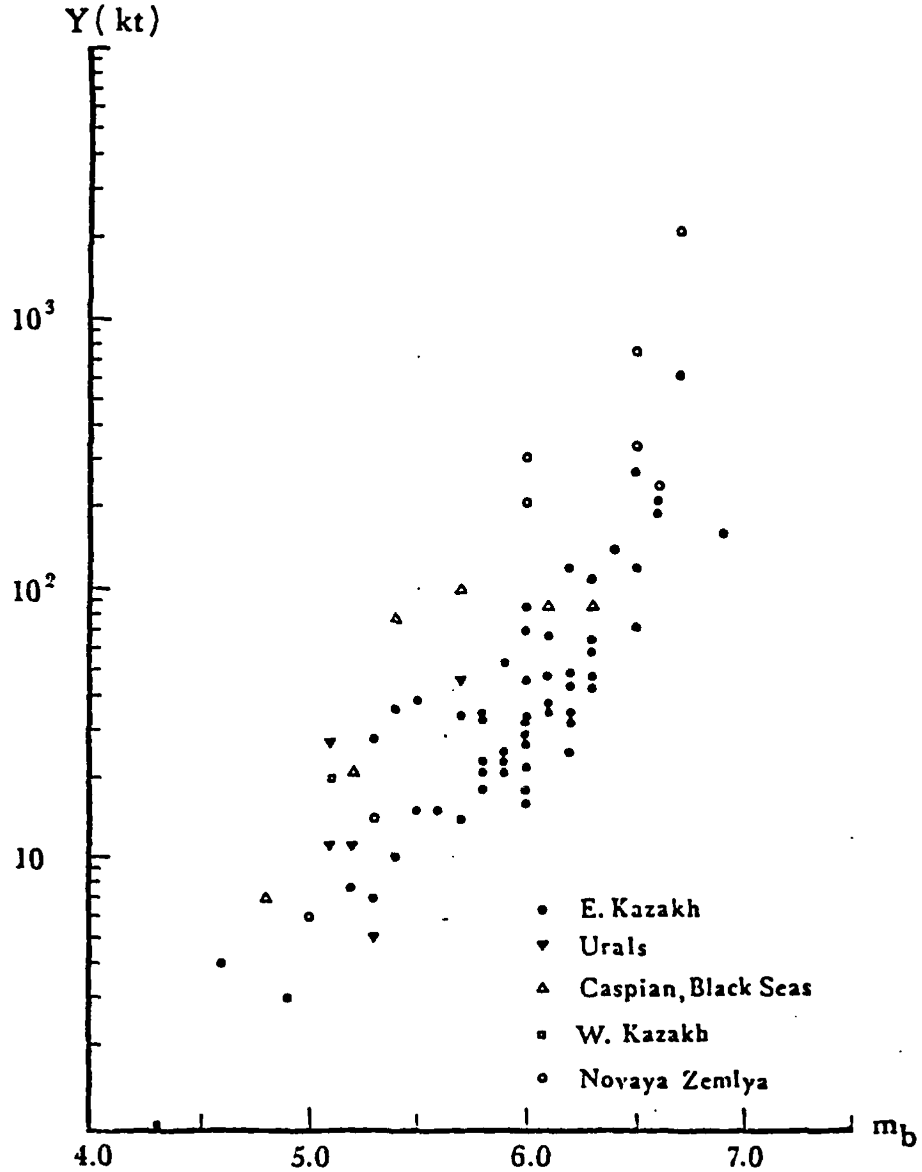

Figure 26. Body-wave magnitude (from Bolt's compilation) vs. yield for events in the USSR.

From the U.S. data:

a. m_b (ISC) vs. estimated yield (Figure 27)

b. volume of collapse vs. estimated yield (Figure 28)

c. diameter and height of collapse center vs. estimated yield (Figures 29 and 30 respectively)

d. volume of collapse vs. depth of burial (Figure 31)

Information on the locality and the rock-type of the test-site are also included whenever available.

Results and Discussion

A comparison between the empirically determined and computed magnitude-yield relations in different media (cf. Figures 7-8 of Bolt, 1976) and the data points in Figure 25 and 27 shows that the U.S. data can be approximated closely by the curve for granite, whereas the Soviet data lies roughly between the curves for granite and water. Body-wave magnitudes taken from Bolt, on the other hand, show larger scatter than m_b (ISC) when plotted as a function of estimated yield (Figures 25 and 26). There is some indication that (i) events in the East Kazakhstan are more efficient in generating seismic waves than the other test sites of the Soviet Union, and (ii) events situated in tuff and rhyolite generate waves more efficiently than those located in alluvium at the Nevada Test Site (NTS).

In plotting the collapse volume vs. the estimated yield (Figure 28), we divided the data into three groups: the first two groups (open and closed symbols) refer to events presented in Figure 27, while the third group (semi-filled symbols) consists of events that contain information on the collapse volume and the estimated yield but not on the body-wave magnitude. The first two groups are divided, somewhat arbitrarily, into normal

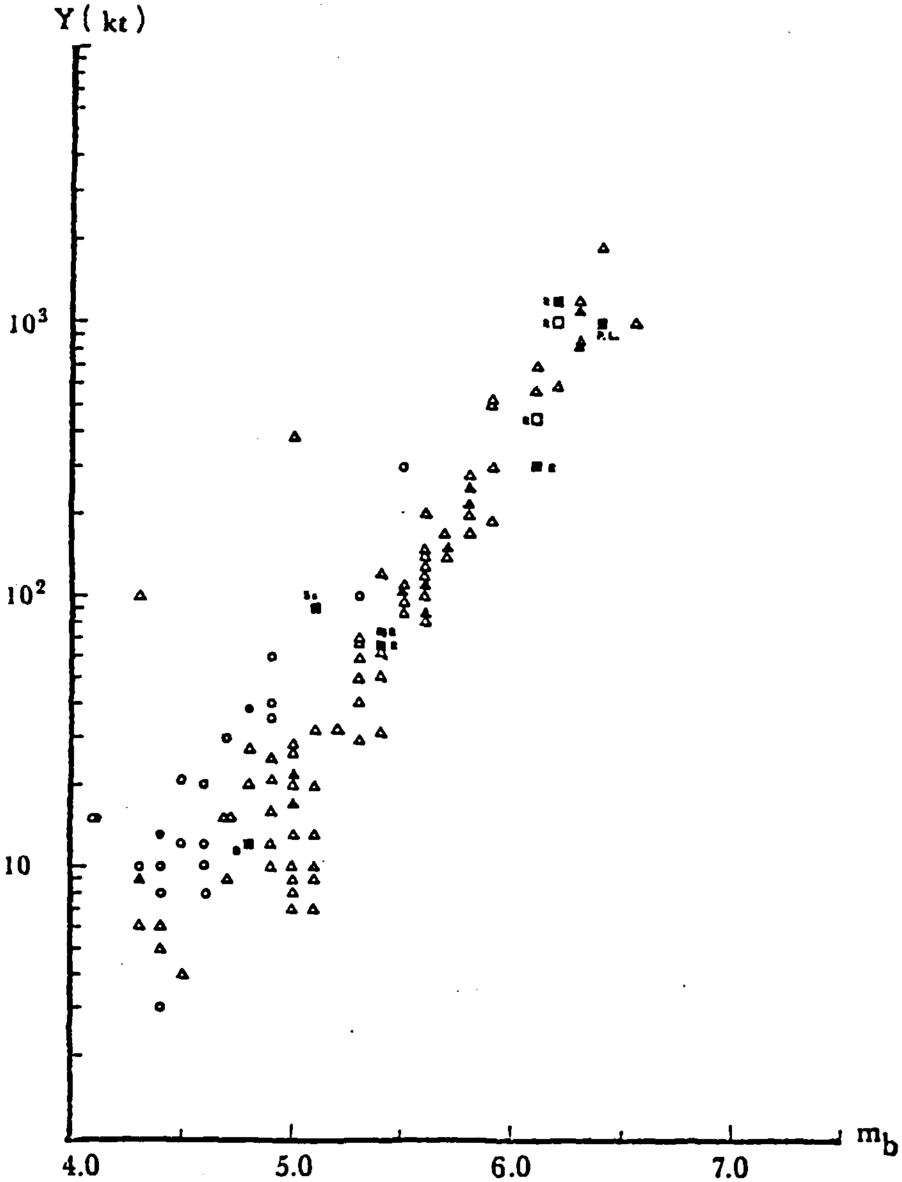

Figure 27. Body-wave magnitude (ISC) vs. yield for events in the U.S. Circles denote tests in alluvium; triangles, tests in tuff; and rectangles, tests in rhyolite (R), sandstone (Ss), or pillow lava (P.L.). The announced and estimated yields are indicated by filled and open symbols, respectively.

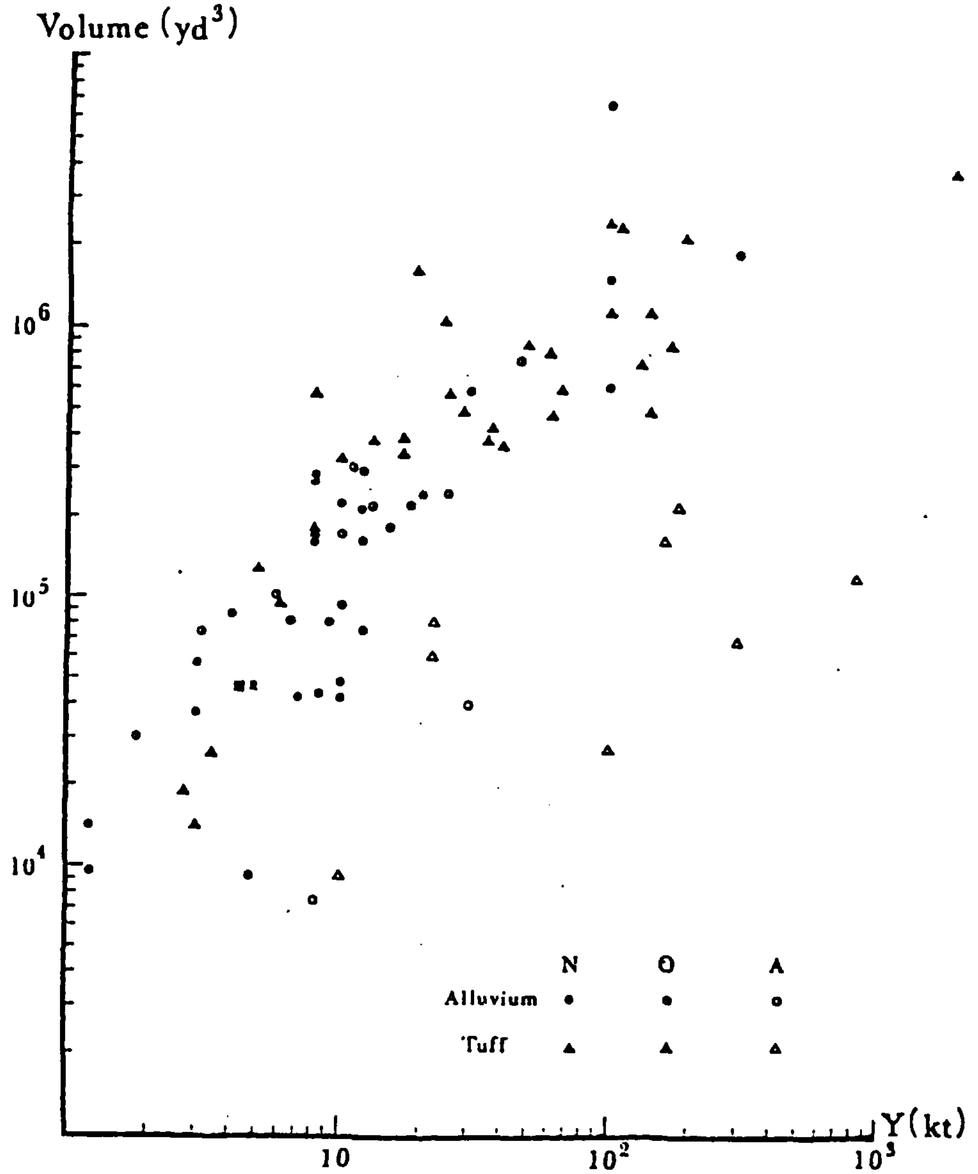

Figure 28. Volume of collapsed crater vs. estimated yield for events in the U.S. Open and filled symbols refer to events presented in Figure 3, whereas semi-filled symbols refer to events that contain information on the collapse volume and the estimated yield but not on the body-wave magnitude and therefore not plotted in Figure 3. Filled symbols denote normal (N) events which lie closely together as a group; open symbols, anomalous (A) events which appear to have unusually small collapse volumes for their estimated yields.

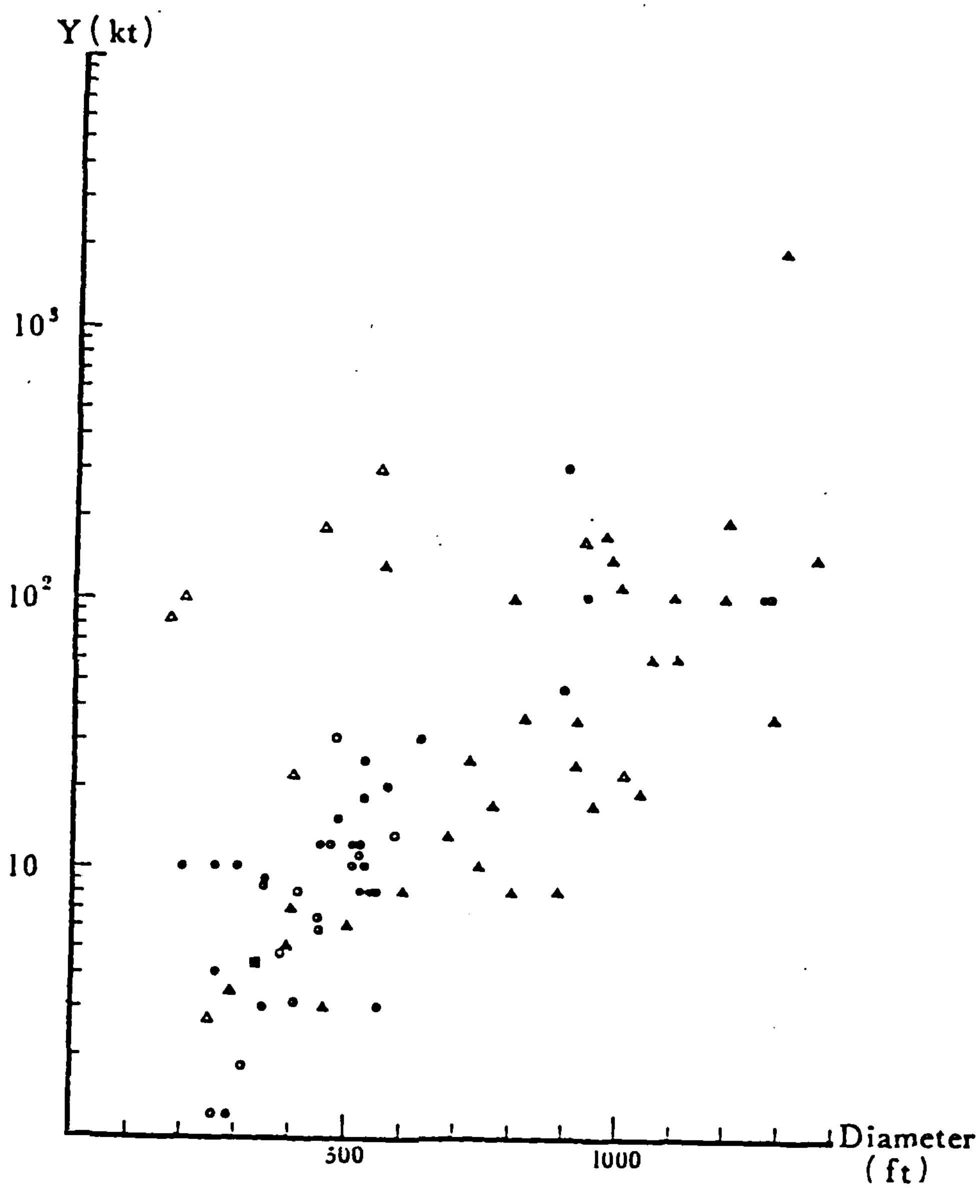

Figure 29. Diameter of the collapsed crater vs. estimated yield for events in the U.S. Except for the semi-filled symbols, the legends are similar to those in Figure 4.

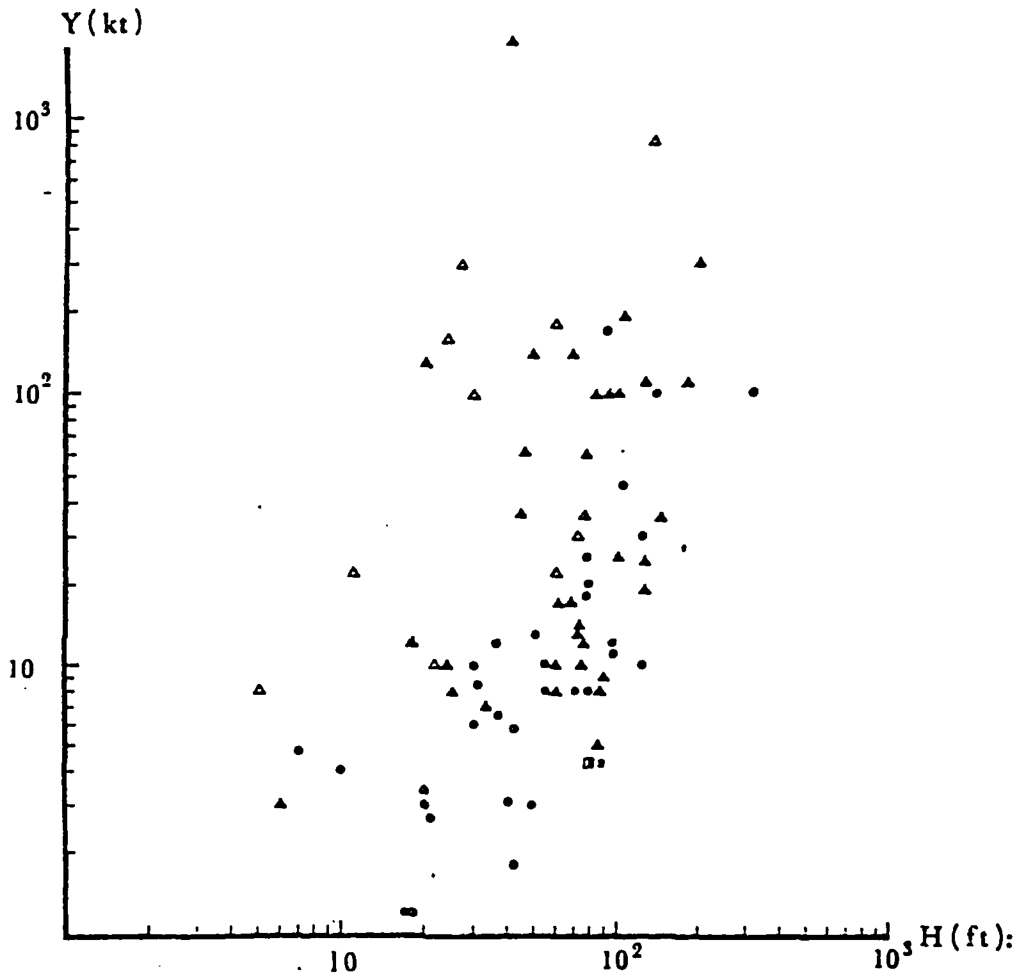

Figure 30. Height of the collapsed crater vs. estimated yield for events in the U.S. Except for the semi-filled symbols, the legends are similar to those in Figure 4.

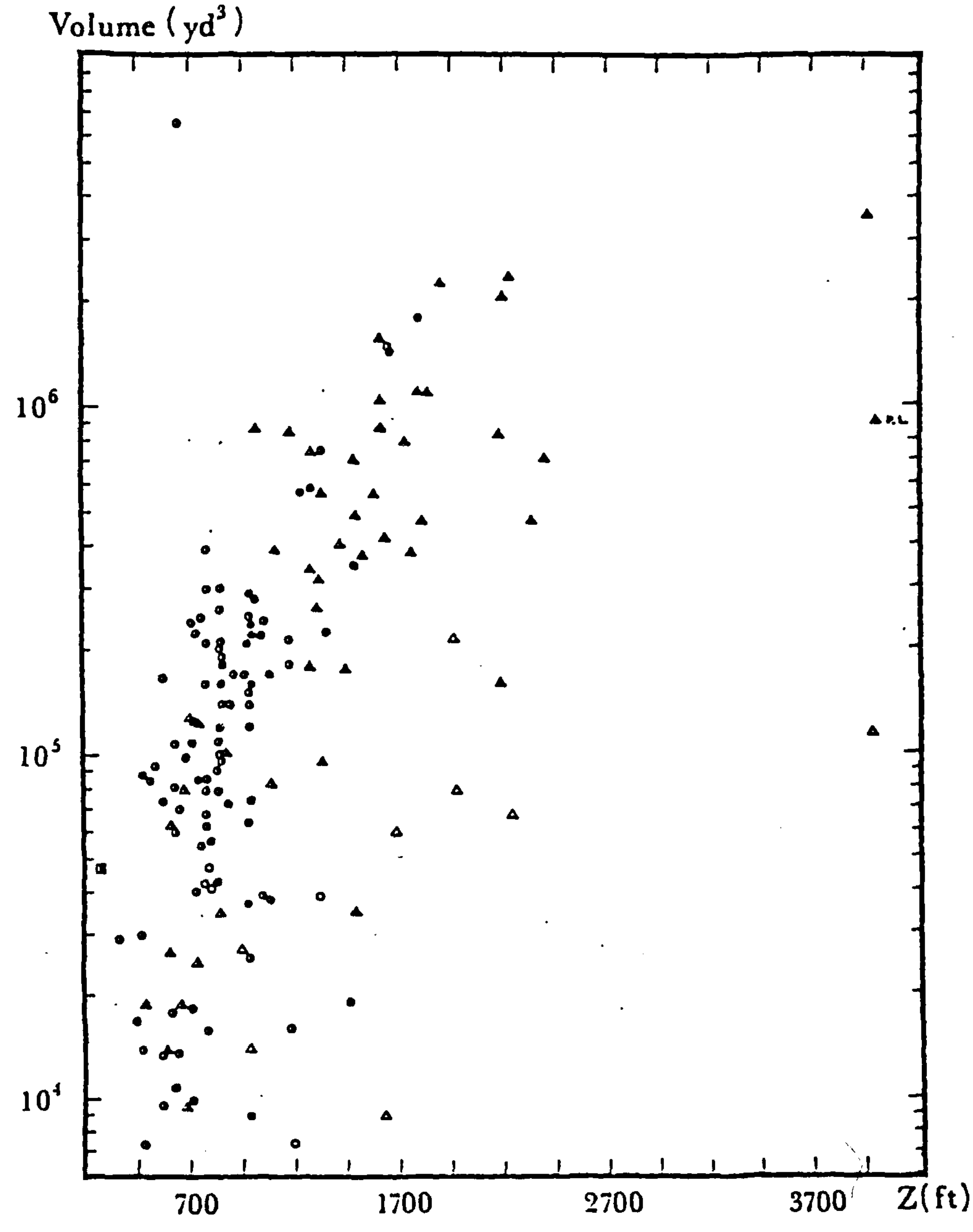

Figure 31. Volume of the collapsed crater vs. burial depth of the device for events in the U.S. Except for the semi-filled symbols, the legends are similar to those in Figure 4.

(closed symbols) and anomalous (open symbols) events. The normal events lie closely together as a group, while the anomalous events appear to have unusually small collapse volumes for their estimated yields. Figures 29 and 30 (the diameter and depth, respectively, of the collapse crater vs. estimated yield) were plotted from the same data set. It is quite interesting that except for the anomalous events, the diameter of the collapse crater can be approximated as being linearly proportional to the logarithm of the yield; the height of the crater, however, appears to be independent of the yield. Figure 31, which relates the collapse volume to the burial depth, is composed of the events found in Figure 29 (or 30 as well as events without reports on their magnitude and yield. This figure seems to indicate three depth-dependent distributions: (i) the volume of collapse is independent of burial depth when the latter is less than about 900 feet, (ii) at depths between 900 and 2500 feet, the logarithm of the collapse volume is approximately linearly proportional to the burial depth, and (iii) for the three events at deeper than 4000 feet, the volume of collapse is again unpredictable. A cautionary remark is deemed necessary at this point: the burial depth of the test charge is usually commensurate with its size; consequently, the collapse volume is probably a complex function of the local rock type, burial depth, and the actual yield.

Table VI

U.S Underground Nuclear Explosions

			Device	Epicenter			Collapse Crater						
Year	Date	Shot Time	Depth (ft)	Latitude (°N)	Longtitude (°W)	Medium	Volume (yd^3)	Diam X Ht. (ft)	Announced	Estimated	M_b (ISC)	Type	Name
1961	1203	230500	1191	37.05	116.03	A	2.16 E05	584 X 50	13			0	Fisher
1962	0109	163000	992	37.06	116.04	A	9 E03	380 X 7	4.7			0	Stoat
	0118	180000	856	37.05	116.03	A	1 E05	452 X 42	5.8			0	Agouti
	0130	180000	1191	37.05	116.04	A	1.6 E04	570 X 14				0	Dormouse
	0208	180000	595	37.13	116.05	A	7.35 E04	406 X 40	3.1			0	Stillwater
	0209	163000	786	37.04	116.04	A	8 E04	446 X 37	6.5			0	Armadillo
	0219	163000	492	37.05	116.03	A	3 E04	314 X 42	1.8			0	Chinchilla
	0219	175000	696	37.13	116.04	T	9.54 E03	296 X 11				0	Codsaw
	0223	180000	1000	37.13	116.05	A	7.39 E04	464 X 36	12			0	Cimarron
	0301	191000	1191	37.04	116.03	A	1.8 E05	620 X 40				0	Pampas
	0305	181500	110	37.11	116.37	Basalt		265 X 84	0.43				Danny Boy
	0308	180000	841	37.12	116.05	A	4.31 E04	350 X 31	8.4			0	Brazos
	0315	163000	784	37.04	116.03	A	1.6 E05	484 X 67				0	Hognose
	0328	180000	614	37.12	116.03	T	2.65 E04	294 X 20	3.4			0	Hoosic
	0331	180000	448	37.05	116.04	A	1.7 E04	260 X 24				0	Chinchilla
	0405	180000	856	37.04	116.02	A	3 E05	520 X 97	11			0	Dormouse Prime
	0406	180000	766	37.12	116.04	A	2.47 E05	500 X 70				0	Pasaic
	0421	184000	634	37.12	116.03	A	1.78 E04	310 X 17				0	Dead
	0427	180000	714	37.12	116.04	A	1.09 E05	394 X 72				0	Black
	0507	193300	848	37.05	116.03	A	1.1 E05	454 X 62				0	Paca
	0512	190000	1424	37.07	116.03	T	4 E05	820 X 75	36			0	Aardvark
	0519	150000	714	37.12	116.05	A	9.8 E03	250 X 13				0	Eel
	0525	150000	632	37.13	116.05	A	1.06 E05	460 X 51				0	White
	0601	170000	539	37.05	116.03	A	1.6 E04	300 X 26				0	Raccoon
	0606	170000	860	37.05	116.04	A	9.7 E04	530 X 44				0	Packrat
	0621	170000	854	37.04	116.03	A	2.6 E05	558 X 92				0	Daman I
	0627	180000	1340	37.04	116.04	A	7.5 E05	896 X 103	46			0	Haymaker
	0630	213000	489	37.12	116.05	A	8.7 E04	360 X 70				0	Sacramento
	0706	170000	635	37.18	116.05	A	6.5 E06	1280 X 320	100			0	Sedan
	0713	160000	1356	37.06	116.03	A	2.24 E05	680 X 50				0	Merrimac
	0727	210000	493	37.13	116.06	A	6.5 E03	340 X 58				0	Wichita
	0824	150000	744	37.12	116.04	A	2.26 E05	500 X 79				0	York
	0824	170000	676	37.05	116.02	A	7 E04	400 X 44				0	Bobac
	0914	171000	711	37.04	116.02	A	2.4 E05	510 X 97				0	Hyrax
	0920	170000	792	37.06	116.03	A	3 E05	560 X 92				0	Peba
	1005	170000	1622	37.14	116.05	T	8.76 E05	850 X 125	110			0	Missis-sippi
	1019	180000	792	37.04	116.02	A	3.9 E05	606 X 125				0	Bandicoot
	1027	150000	1048	37.15	116.05	A	3.9 E04	400 X 21				0	Santee
	1127	180000	747	37.12	116.03	T	1.25 E05	460 X 61				0	Anacostia
	1207	190000	993	37.05	116.03	A	2.5 E05	510 X 81				0	Tendrac
	1212	184500	761	37.05	116.02	A	1.4 E05	560 X 50				0	Numbat
1963	0208	160000	994	37.15	116.05	A	1.52 E05	446 X 73				0	Casselman
	0208	183000	856	37.05	116.02	A	2.1 E05	514 X 78				0	Acushi
	0329	154900	917	37.04	116.02	A	1.7 E05	550 X 48				0	Gerbil
	0405	175200	793	37.04	116.02	A	2.1 E05	474 X 114				0	Ferret Prime
	0522	154000	1289	37.11	116.04	T	7.35 E05	852 X 88				0	Stones
	0614	141000	642	37.05	116.02	A	6 E04	302 X 58				0	Mataco
	0812	234500	992	37.04	116.02	A	1.4 E05	496 X 61				0	Pekan
	0815	130000	738	37.15	116.08	A	4.0 E04	300 X 40				0	Satsop
	1011	140000	857	37.04	116.02	A	2.0 E05	480 X 100				0	Grunion
	1114	160000	854	37.04	116.02	A	2.1 E05	520 X 69				0	Anchovy
	1122	173000	987	37.12	116.04	A	6.4 E04	400 X 42				0	Greys
	1204	163830	860	37.04	116.03	A	1.9 E05	490 X 78				0	Sardine
	1212	160200	540	37.13	116.04	A	9.3 E04	400 X 60				0	Eagle
1964	0116	160000	1610	37.14	116.05	T	1.59 E06	1040 X 125		19	5.2	N	Fore
	0123	160000	868	37.13	116.04	T	1.01 E05	960 X 39				0	Oconto
	0220	153000	1616	37.15	116.04	T	1.03 E06	920 X 126		24	5.1	N	Klickitat
	0313	160200	376	37.05	116.01	A	2.9 E04	240 X 46				0	Pike
	0414	144000	668	37.13	116.03	T	1.89 E04	295 X 22				0	Hook
	0415	143000	491	37.04	116.02	A	1.4 E04	236 X 19				0	Sturgeon
	0424	201000	1663	37.15	116.05	A	1.44 E06	1265 X 93		100	5.2	0	Turf
	0429	204700	859	37.04	116.03	A	1.8 E05	480 X 72		15	4.1	N	Pipe Fish
	0514	144000	536	37.12	116.04	A	8.5 E04	400 X 55				0	Backswing
	0515	161500	792	37.04	116.01	A	6.3 E04	416 X 28				0	Minnow

Table VI

U.S. Underground Nuclear Explosions

Year	Date	Shot Time	Device Depth (ft)	Epicenter Latitude (°N)	Epicenter Longtitude (°W)	Medium	Collapse Crater Volume (yd^3)	Collapse Crater Diam X Ht. (ft)	Announced	Estimated	M_b (ISC)	Type	Name
1964	0625	133000	673	37.11	116.03	T	7.93 E04	416 X 47				0	Fade
cont.	0630	133300	847	37.17	116.06	A	7.88 E04	347 X 90		9		A	Dub
	0716	131500	1277	37.18	116.04	T	1.79 E05	536 X 65				0	Bye
	0904	181500	856	37.02	116.02	A	1.6 E05	450 X 74		12		N	Guanay
	1002	200300	1484	37.08	116.01	T				12	4.0	N	Auk
	1009	140000	1325	37.15	116.08	A	3.89 E04	475 X 72	38	30	4.0	A	Par
	1016	155930	849	37.04	116.02	A	1.2 E05	472 X 50				0	Barbel
	1105	150000	1319	37.17	116.07	Dolomite			12	9	4.8		Handcar
	1205	211500	1323	37.11	116.05	T	3.2 E05	740 X 60		10	4.8	N	Crepe
	1216	200000	592	37.03	116.01	A	1.4 E04	260 X 18	1.2			N	Parrot
	1216	201000	498	37.18	116.07	T	1.9 E04	254 X 21	2.7			N	Mudpack
1965	0114	160000	706	37.12	116.02	T	1.28 E05	450 X 60				0	Wool
	0204	153000	762	37.13	116.06	A	5.41 E04	360 X 45				0	Cashmere
	0216	173000	972	37.05	116.02	A	1.7 E05	510 X 55	10			N	Merlin
	0218	161847	588	36.82	115.95	A	1.66 E05	300 X 100				0	Wishbone
	0303	191300	2459	37.06	116.04	T				65			Wagtail
	0326	153408	1761	37.15	116.04	T	3.8 E05	920 X 185		35		N	Cup
	0405	210000	1466	37.03	116.02	A	1.9 E04	450 X 8				0	Kestrel
	0414	131400	280	37.28	116.52	R	4.69 E04	338 X 79	4.3			0	Palanquin
	0421	220000	1000	37.01	116.20	T				8	5.0		Gumdrop
	0507	154711	624	37.14	116.07	A	6.25 E04	385 X 30				0	Tee
	0521	130852	922	37.12	116.03	T	8.92 E05	630 X 148				0	Tweed
	0611	194500	593	37.04	116.02	A	9.5 E03	290 X 17	1.2			0	Petrel
	0723	170000	1741	37.10	116.03	T	7.9 E05	1055 X 77		60	5.4	N	Bronze
	0806	172330	1053	37.02	116.04	A	2.2 E05	526 X 77		18		N	Mauve
	0901	200800	990	37.02	116.01	A	2.1 E05	506 X 72		12	4.2	N	Screamer
	0910	171200	1494	37.08	116.02	T	3.5 E05	978 X 40				0	Charcoal
	1112	180000	791	37.05	116.02	A	8.6 E04	456 X 39				0	Sepia
	1203	151302	2236	37.16	116.05	T	2.33 E06	800 X 100				N	Corduroy
	1216	191500	1642	37.07	116.03	T	4.2 E05	1284 X 44		36	5.3	N	B[illegible]
										32	5.2		Lampblack
1966	0118	183500	1842	37.09	116.02	T							
	0121	182800	1093	37.03	116.02	A	3.8 E04	464 X 16				0	Dovekie
	0203	181737	836	37.13	116.07	A	2.57 E04	260 X 27				0	Plaid II
	0224	155507	2204	37.27	116.43	T			16	7	5.0		Rex
	0307	184100	642	37.04	116.03	A	8.07 E04	408 X 58				0	Finfoot
	0318	190000	1092	37.01	116.01	T	8.3 E04	458 X 39				0	Purple
	0406	135717	739	37.14	116.14	T	1.25 E05	386 X 85		5	4.4	N	Stutz
	0407	222730	742	37.02	115.99	T	2.5 E04	440 X 14				0	Tomato
	0414	141343		37.24	116.43	R			65	31	5.4	N	Duryea
	0425	123800	970	36.89	115.94	T				4	4.5		Pin Stripe
	0504	133217	646	37.14	116.14	A	1.09 E04	190 X 17				0	Traveler
	0505	140000	1001	37.05	116.04	A	1.6 E05	548 X 55	13	8	4.4	N	Cyclamen
	0512	193726	810	37.13	116.07	A	4.14 E04	300 X 24		10	4.3	A	Tapestry
	0513	133000	1800	37.09	116.03	T	1.1 E06	1196 X 83		100	5.6	N	Piranha
	0519	135628	2200	37.11	116.06	T	2.03 E06	1200 X 105		190	5.9	N	Dumont
	0527	200000	1106	37.18	116.10	T	3.9 E05	954 X 67	21	17	5.0	N	Discus Thrower
	0602	153000	1518	37.23	116.06	Granite			56		5.6		Pile Driver
	0603	140000	1839	37.07	116.03	T	1.1 E06	1362 X 69		140	5.7	N	Tan
	0615	180247	1494	37.17	116.05	D	7.01 E05	1300 X 60				0	Kankakee
	0625	171300	1057	37.15	116.07	A	2.41 E05	526 X 77	25			N	Vulcan
	0630	221500	2688	37.32	116.30	R		1300 X 35	300	450	6.1	N	Halfbeak
	0912	153001	835	36.88	115.95	A				12	4.6	0	Derringer
	0929	144530	750	37.17	116.05	A	8.54 E04	264 X 10		4		N	Newark
	1105	144500	650	37.17	116.05	A	1.36 E04	190 X 15				0	Simms
	1111	120000	782	37.13	116.05	A	6.33 E04	400 X 45				0	Ajax
	1118	150200	693	37.04	116.01	A	9.9 E04	452 X 50				0	Cerise
	1213	210000	800	36.88	115.94	A	4.74 E04	200 X 125		10	4.6	A	New Point
	1220	153000	825	37.30	116.41	T	(cylindrical)	170 X 135	825	830	6.3	A	Greeley
1967	0119	164500	1194	37.14	116.13	Dolomite	8.52 E05	500 X 180		49	5.3		Nash
	0120	174003	1836	37.16	116.00	Limestone		35 X 135		29	5.3		Bourbon
	0208	151500	844	37.17	116.05	A	9.07 E04	260 X 30		10	4.6	A	Ward
	0223	188400	981	37.02	116.02	A	3.7 E04	560 X 20		3	4.4	A	Persimmon
	0223	185000	2400	37.13	116.07	T	7.12 E05	900 X 40		130	5.6	N	Agile
	0302	150000	890	37.17	116.05	A	7.24 E04	460 X 12				0	River III
	0407	150000	899	37.05	116.02	A	1.4 E05	510 X 52				0	Fawn
	0421	150900	789	37.02	116.06	A	4.2 E04	400 X 33		7		A	Chocolate
	0427	144500	719	37.14	116.06	A	1.84 E04	114 X 12				0	Effendi
	0510	134000	1639	37.08	115.99	T	9 E03	184 X 22		10	4.9	A	Mickey
	0520	150000	2449	37.13	116.06	T		1120 X 148	250	230	5.8		Commodore
	0523	140000	3207	37.27	116.37	T			150	140	5.7		Scotch
	0526	150002	2069	37.25	116.48	R			71	47	5.4		Knickerbocker

Table VI

U.S. Underground Nuclear Explosions

Year	Date	Shot Time	Device Depth (ft)	Epicenter Latitude (°N)	Epicenter Longitude (°W)	Medium	Collapse Crater Volume (yd³)	Collapse Crater Diam X Ht. (ft)	Announced	Estimated	M_b (ISC)	Type	Name
1967	0626	160000	1230	37.20	116.21	T				9	5.1		Midi Mist
cont.	0629	112500	1018	37.03	116.62	A	2.8 E05	542 X 79		8	4.6	N	Umber
	0727	130000	1587	37.15	116.05	T	5.6 E05	890 X 60		8	5.0	N	Stanley
	0818	201230	1089	37.01	116.04	A	1.7 E05	522 X 71		8	4.6	N	Bordeaux
	0831	163000	1463	37.18	116.21	T				9	5.0		Door Mist
	0907	134500	1700	37.15	116.05	T		1156 X 72		13	5.0		Yard
	0921	204500	572	37.17	116.04	A	1.33 E04	153 X 28	2.2			O	Marvel
	0927	170000	2188	37.10	116.05	T	8.3 E05	967 X 92		170	5.7	N	Zaza
	1018	143000	2343	37.12	116.06	T	4.74 E05	980 X 49		140	5.7	N	Lampher
	1025	143000	992	37.03	116.03	A	1.2 E05	525 X 48				O	Sazerac
	1108	150000	2200	37.09	116.04	T				7	5.1	N	Cobbler
1968	0119	181500	3200	38.63	116.21	T				1200	6.3		Faultless
	0221	153000	2116	37.12	116.05	T				200	5.8		Knox
	0229	170830	1345	37.18	116.21	T				20	5.0		Dorsal Fi
	0615	14000	2242	37.26	116.31	T	6.7 E04	548 X 27		300	5.9	A	Rickey
	0628	122200	1992	37.24	116.48	T				58	5.3		Chateau-gay
	0827	163000	794	36.88	115.93	A	1.6 E04	332 X 17				O	Diana Moo
	0906	140000	1909	37.14	116.05	T	2.24 E06	1000 X 182		110	5.5	N	Noggin
	0917	140000	1535	37.12	116.13	T	3.74 E05	682 X 72		13	5.1	N	Stoddard
	0924	170500	1092	37.20	116.21	T				10	5.0		Hudson Seal
	1003	142900	989	37.03	115.99	T	1.4 E04	460 X 6		3		A	Knife C
	1104	151500	1980	37.13	116.09	T	7.9 E04	400 X 60		22		A	Crew
	1115	154500	1191	37.03	116.03	A	7.2 E03	412 X 5		8		A	Knife B
	1120	180000	1010	37.01	116.21	T				12	4.9	N	Ming Vase
	1219	163000	4600	37.23	116.47	T			1100	1000	6.3		Benham
1969	0115	190000	810	37.15	116.07	A	5.64 E04	350 X 49		3			Packard
	0115	193000	1700	37.21	116.22	T				40	5.3		Wineskin
	0130	150000	1490	37.05	116.03	A		880 X 10		40	4.9		Vise
	0320	181200	998	37.02	116.03	A	2.2 E05	532 X 74		10	4.4	N	Barsac
	0321	143000	1525	37.13	116.09	A				35	4.9		Coffer
	0507	134500	1964	37.28	116.50	T	2.14 E05	450 X 60		180	5.5	A	Purse
	0527	141500	1689	37.07	115.99	T	6 E04	1004 X 11		22	5.0	A	Torrido
	0612	140000	994	37.01	116.03	A	2.9 E05	520 X 96		12	4.5	N	Tapper
	0716	130230	1346	37.12	116.05	T	9.57 E04	500 X 30		6		N	Ilurim
	0716	145500	1800	37.14	116.09	A	1.78 E06	898 X 201		300	5.5	N	Hutch
	0827	134500	784	37.02	116.04	A	6.8 E04	402 X 48				O	Pliers
	0916	143000	3800	37.31	116.46	T			1000	700	6.1		Jorum
	1002	220600	4000	51.42	-179.18	Pillow Lava	9.0 E05	2002 X 15	1000		6.4	O	Milrow
	1008	143000	2025	37.26	116.44	T		380 X 20		82	5.6		Pipkin
	1029	220151	2050	37.14	116.06	T		1000 X 75	110	140	5.6		Calabash
	1121	145200	1292	37.03	116.00	T				17	5.0	N	Picalilli
	1205	170000	1375	37.18	116.21	T				16	4.9		Diesel Train
	1217	150000	1807	37.08	116.00	T	4.7 E05	1102 X 46		61	5.4	N	Grape A
	1217	151500	1240	37.01	116.02	A	5.7 E05	632 X 123		30	4.7	N	Lovage
	1218	190000	1500	37.12	116.03	T	4.83 E05			28		N	Terrine
1970	0123	163000	998	37.14	116.04	T	2.36 E05	574 X 79		20		N	Ajo
	0204	170000	1819	37.10	116.03	T		1450 X 70		120	5.6		Grape B
	0205	150000	1450	37.16	116.04	T	1.74 E05	800 X 25	25	8		N	Labis
	0225	142838	1340	37.04	116.00	T	5.64 E05	720 X 100		25		N	Cumarin
	0226	153000	1287	37.12	116.06	A	5.91 E05	938 X 140		100	5.3	N	Yannigan
	0306	142401	950	37.02	116.09	T	2.7 E04	200 X 30	9.0	100	4.3	A	Cyathus
	0319	140330	988	37.00	116.02	A		455 X 35		6		O	Jal
	0323	230500	1839	37.09	116.02	T		1100 X 65		93	5.5		Shaper
	0326	190000	3957	37.30	116.53	T	3.54 E06	1300 X 40	1000	1900	6.4	N	Handley
	0421	143000	1125	37.05	115.99	T				6	4.4		Snubber
	0421	150000	1310	37.12	116.08	T	2.63 E05	600 X 85		8	4.6	N	Can
	0501	144000	870	37.13	116.03	T		515 X 43		6	4.3		Hod
	0505	153000	1330	37.22	116.18	T				28	5.0		Mint Lea
	0515	133000	1455	37.16	116.04	T		790 X 157		39			Cornice
	0521	141500	1580	37.05	116.01	T				20	5.1		Morrones
	0526	150000	1743	37.11	116.06	T		975 X 160	105	110	5.5		Flask
	1014	143000	1839	37.07	116.00	T		1010 X 175		94	5.5		Tijeras
	1105	150000	1291	37.03	116.01	T		729 X 95		11			Abeytas
	1217	160500	2171	37.13	116.08	T		1100 X 100	220	170	5.8		Carpetba
	1218	153000	994	37.17	116.10	T		500 X 80	10	32	5.1		Banenerr
1971	0623	153000	1493	37.02	116.02	T		616 X 21		10			Laguna
	0624	140000	1702	37.15	116.07	T		1000 X 78		40	4.9		Harebell
	0706	14000	1735	37.11	116.05	T		810 X 103	80	100			Miniata
	0818	140000		37.06	116.04	T		857 X 33		[illegible]	[illegible]		[illegible]

Table VI

U.S. Underground Nuclear Explosions

Year	Date	Shot Time	Device Depth (ft)	Epicenter Latitude (°N)	Epicenter Longtitude (°W)	Medium	Collapse Crater Volume (yd^3)	Collapse Crater Diam X Ht. (ft)	Announced	Estimated	M_b (ISC)	Type	Name
1971 cont.	1008	143000	1240	37.11	116.04	T		840 X 26		7			Cathay
	1106	220000	5875	51.47	-179.11	Basalt		3600 X 55	5000		6.6		Cannikin
	1214	210959	1085	37.12	116.09	A		372 X 41		24			Chaenacti
1972	0517	14100	1059	37.12	116.09	A		336 X 48		8			Zinnia
	0720	171600	1391	37.21	116.18	T				21	4.9		Diamond Sculls
	0921	153000	1838	37.08	116.04	T		1350 X 90		130	5.6		Oscuro
	0926	143000	970	37.12	116.09	A		388 X 51	15	15	4.1		Delphinia
	1221	201500	2258	37.14	116.08	T		584 X 97		27	4.8		Flax
1973	0308	161000	1866	37.10	116.03	T		1116 X 41		67	5.3		Miera
	0425	222500	1486	37.00	116.03	A				21	4.5		Angus
	0426	171500	1850	37.12	116.06	T		1150 X 125	85	120	5.6		Starwort
	0517	160000		39.79	108.37	Sandstone			90		5.1		Rio Blanc
	0605	170000	1284	37.18	116.21	T				26	5.0		Dido Quee
	0606	130000	3490	37.24	116.35	T				570	6.1		Almendro
	0628	191512	1530	37.15	116.09	A				60	4.9		Portulaca
	1012	170000	1350	37.20	116.20	T				9	4.7		Husky Ace
1974	0227	170000		37.10	116.05					150	5.6		Latir
	0619	160000		37.20	116.19					20	4.8		Ming Blad
	0710	160000		37.07	116.03					170	5.7		Escabosa
	0830	150000		37.15	116.08					200	5.6		Portmanteau
	0926	150500		37.13	116.07					100	5.5		Stanyan
1975	0228	151500		37.11	116.06					185	5.6		Topgallan
	0307	150000		37.13	116.08					120	5.4		Cabrillo
	0405	194500		37.19	116.21					20	4.9		Dining Ca
	0424	141000		37.12	116.09					9	4.5		Edam
	0514	140000	2510	37.22	116.47					380	5.0		Tybo
	0603	142000	2398	37.34	116.52					275	5.8		Stilton
	0603	144000	2090	37.09	116.04					160	5.6		Mizzen
	0619	130000	2992	37.35	116.32					520	5.9		Mast
	0626	123000	4301	37.28	116.37					750	6.1		Camembert
	1024	171126	440	37.22	116.18					15	4.7		Husky Pup
	1028	143000	4150	37.29	116.41					1200	6.2		Kasseri
	1120	150000	2680	37.22	116.37					500	5.9		Inlet
	1220	200000	2349	37.13	116.06					160	5.6		Chiberta
1976	0103	191500	4761	37.30	116.33					600	6.2		Muenster
	0204	142000	2100	37.07	116.03					200	5.6		Keelson
	0204	144000	2149	37.11	116.04					150	5.6		Esrom
	0212	144500	3999	37.21	116.49					900	6.1		Fontina
	0214	113000	3229	37.24	116.42					350	5.8		Cheshire
	0309	140000	2851	37.31	116.36					350	5.8		Estuary
	0314	123000	4177	37.31	116.47					900	6.2		Colby
	0317	141500	2884	37.26	116.31					500	6.0		Pool
	0317	144500	2559	37.11	116.05					200	5.8		Strait

Table VII

Presumed USSR Underground Nuclear Explosions

Year	Date	Origin Time	Latitude (°N)	Longitude (°E)	m_b (Bolt's)	Announced	Estimated	m_b (ISC)	Location
1964	0315	75958	49.70	78.00	6.2		49	5.6	
	0516	60058	49.90	78.30	6.2		44	5.6	
	0719	55959	49.90	78.10	6.0		29	5.4	
	0918	75955	72.90	55.20			2	4.2	N.Z.
	1025	75959	73.50	53.70	5.3		14	5.1	N.Z.
	1116	55957	49.70	78.00	6.1		49	5.6	
1965	0115	55959	49.89	78.97	7.0	125	110	5.8	
	0303	61457	49.82	78.07	6.0		34	5.5	
	0511	63958	49.79	77.92			6	4.9	
	0617	24458	49.97	78.07	5.8		21	5.2	
	0917	35958	49.81	78.05	5.5		15	5.2	
	1008	55959	49.89	78.05	5.8		34	5.4	
	1121	45758	49.77	78.06	6.1		47	5.6	
	1224	45958	49.88	78.04			7	5.0	
1966	0213	45758	49.82	78.13	6.5		270	6.1	
	0320	54958	49.70	78.00			170	6.0	
	0421	35758	49.81	78.05	5.3		28	5.3	
	0507	35758	49.74	77.90			4	4.8	
	0629	65758	49.93	78.01			36	5.6	
	0721	35758	49.70	78.00	5.9		24	5.3	
	0805	35758	49.90	78.00	6.1		29	5.4	
	0819	35301	50.40	77.90	4.6		4	5.1	
	0907	35158	49.90	78.00			4	4.8	
	0930	55953	38.80	64.50	5.3	30			Uzbekistan
	1019	35758	49.75	78.03	6.3		65	5.6	
	1027	55758	73.44	54.75	6.5		770	6.4	N.Z.
	1218	45758	49.93	77.73	6.5		120	5.8	
1967	0226	35758	49.78	78.12	6.6		210	6.0	
	0325	55759	49.77	78.08	5.9		21	5.3	
	0420	40758	49.74	78.12	6.3		58	5.5	
	0528	40758	49.81	78.11	6.2		32	5.4	
	0629	25658	49.87	78.10			27	5.3	
	0715	32657	49.83	78.11	6.0		27	5.4	
	0804	65758	49.82	78.05	5.8		23	5.3	
	0916	40358	50.01	77.82	6.0		22	5.3	
	0922	50358	50.03	77.61	6.0		16	5.2	
	1017	50358	49.82	78.10	6.1		67	5.6	
	1021	45958	73.37	54.81	6.0		210	5.9	N.Z.
	1030	60358	49.84	78.11	6.0		33	[illegible]	
	1122	40357	49.90	77.30			3	4.8	
	1208	60357	49.84	78.22			22	5.4	
1968	0107	34658	49.81	78.02			10	5.1	
	0424	103557	49.83	78.08			7	5.0	
	0611	30558	49.84	78.16	5.8		18	5.2	
	0619	50557	49.96	79.09	6.5		35	5.4	
	0701	40202	47.92	47.95	5.7		46	5.5	N. Caspian Sea
	0712	120757	49.67	78.12	5.9		23	5.3	
	0820	40558	50.00	78.00			4	4.8	
	0905	40557	49.76	78.14	6.2		35	5.4	
	0929	34258	49.77	78.19	6.3		110	5.8	
	1107	100205	73.40	54.86	6.0		310	6.1	N.Z.
	1109	25358	49.79	78.04			4	4.9	
	1218	50157	49.72	78.06	5.7		14		
1969	0307	82658	49.81	78.15	6.3		47	5.6	
	0516	40257	49.77	78.15	6.0		18	5.2	
	0531	50157	49.98	77.73	6.2		25	5.3	
	0704	24657	49.75	78.19	6.0		22	5.2	
	0723	24658	49.87	78.32	6.1		38	5.4	
	0902	45957	57.41	54.86	5.2	8	11	4.8	Urals
	0908	45956	57.36	55.11	5.2	8	11	4.6	Urals
	0926	65956	45.89	42.47	5.4		78	5.6	N. Caspian Sea
	1001	40258	49.81	78.21	5.9		21	5.2	
	1014	70006	73.40	54.81	6.5		340	6.3	N.Z.
	1130	33257	49.92	79.00	6.9		160	6.0	
	1206	70257	43.83	54.78	5.7		100	5.8	E. Caspian Sea
	1228	34658	50.00	77.82	6.5		72	5.7	
	1229	40158	49.73	78.15			1	5.1	
1970	0129	70258	49.80	78.21	5.9		52	5.5	
	0327	50257	49.76	78.01	5.4		10	5.0	
	0625	45952	52.20	55.69	5.3		5		Urals
	0628	15758	49.83	78.25	6.2		120	5.7	
	0721	30257	49.95	77.75	6.0		29	5.4	
	0724	35657	49.80	78.17	5.8		21	5.3	
	0906	40257	49.77	78.09	6.0		46	5.4	
	1014	55957	73.31	55.15	6.7	6000	2100	6.6	N.Z.
	1104	60257	49.97	77.79	6.0		34	5.4	
	1212	70057	43.85	54.77	6.6		190	6.0	
	1217	70057	49.73	78.13	6.1		35	5.4	
	1223	70057	43.83	54.85	6.6		240	6.0	E. Caspian Sea
1971	0322	43258	49.74	78.18	6.0		26	5.7	
	0323	65956	61.29	56.47	5.9	45	51	5.5	Urals
	0425	33258	49.82	78.09	6.4		140	5.9	
	0606	40257	49.98	77.77	5.5		39	5.5	
	0619	40358	50.01	77.74	5.4		36	5.4	

Table VII

Presumed USSR Underground Nuclear Explosions

	0630	35657	49.97	79.05	5.9		25	5.2	
	0710	165959	64.17	55.18	5.1		27	5.2	Urals
	0919	110007	57.78	41.10			4	4.5	Urals
	0927	55955	73.39	55.10			770	6.5	N.Z.
	1009	60257	50.00	77.70			24	5.3	
	1021	66257	49.99	77.65			44	5.5	
	1022	50000	51.57	54.54			34	5.2	Urals
	1129	60257	49.76	78.13			34	5.4	
	1215	75259	49.98	77.90			3	4.9	
	1222	65956	47.87	48.22			210	6.0	N. Caspian Sea
	1230	62058	49.75	78.13			90	5.7	
1972	0210	50257	49.99	78.89	6.3		43	5.4	
	0310	45657	49.75	78.18	5.8		33	5.4	
	0328	42157	49.73	78.19	5.6		15	5.1	
	0411	60005	37.37	62.00	4.8		7		Turkman
	0607	12757	49.76	78.17	5.7		34	5.4	
	0706	10258	49.72	77.98	4.8		1	4.4	
	0709	65958	49.78	35.40	5.0		6	4.8	N. Black Sea
	0714	145949	50.00	46.40	3.6		0.2		N. Caspian Sea
	0816	31657	49.76	78.15	5.6		15	5.0	
	0820	25958	49.46	48.18	6.3		87	5.7	N. Caspian Sea
	0826	34657	49.99	77.78	5.8		35	5.3	
	0828	55957	73.34	55.08		1000	690	6.3	N.Z.
	0902	85658	49.96	77.73	5.3		7	4.9	
	0921	90001	52.13	51.99	5.2		21		N. Caspian Sea
	1003	85958	46.85	45.01	6.1		88	5.6	NW Caspian Sea
	1102	12658	49.91	78.84			350	6.1	
	1124	90008	52.78	51.07	5.1		11	4.5	Urals
	1124	95958	51.84	64.15	5.1		20	5.2	W. Kazakh
	1210	42658	49.85	78.18	6.0		70	5.6	
	1210	42708	50.11	78.81	6.7		620	6.0	
	1228	42713	51.70	79.20	4.9		3		
1973	0216	50258	49.83	78.23	5.5		48	5.5	
	0419	43258	50.01	79.72			27	5.4	
	0710	12658	49.78	78.06			28	5.2	
	0723	12258	49.99	78.85			420	6.1	
	0815	15958	42.71	67.41			28	5.3	Uzbekistan
	0828	25958	50.55	68.39			14	5.2	W. Kazakh
	0912	65954	73.30	55.16			2700	6.8	N.Z.
	0919	25957	45.63	67.85			11	5.1	W. Kazakh
	0927	65958	70.76	53.87			210	5.9	N.Z.
	0930	45957	51.61	54.58			22	5.2	Urals
	1026	42658	49.76	78.20			19	5.2	
	1026	55958	53.66	55.38			7	4.8	Urals
	1027	65957	70.78	54.18			3200	6.9	N.Z.
	1214	74657	50.04	79.01			150	5.8	
1974	0130	45658	49.89	77.99			2	4.9	
	0130	45702	49.83	78.08			23	5.2	
	0416	55302	49.99	78.82			3	4.9	
	0516	30257	49.74	78.15			23	5.2	
	0531	32657	49.95	78.84			140	5.9	
	0625	35658	49.89	78.11			2	4.7	
	0710	25657	49.79	78.14			16	5.2	
	0814	145958	68.91	75.90			45	5.4	N.Z.
	0829	95956	73.37	55.09			870	6.4	N.Z.
	0829	150000	67.23	62.12			20	5.0	Urals
	0913	30258	49.82	78.09			15	5.2	
	1016	63257	49.97	78.97			43	5.5	
	1102	45957	70.82	54.06			1600	6.4	N.Z.
	1207	55957	49.91	77.65			2	4.1	
	1216	62302	49.75	78.06			8	5.0	
	1216	64102	49.82	78.12			6	4.8	
	1227	54657	49.96	79.05			51	5.6	
1975	0220	53258	49.82	78.08			77	5.7	
	0311	54258	49.79	78.25			30	5.4	
	0427	53657	49.99	78.98			60	5.6	
	0608	32658	49.76	78.09			35	5.5	
	0807	35658	49.81	78.24			14	5.2	
	0823	85958	73.37	54.64			550	6.3	N.Z.
	0929	105958	69.59	90.40			6	4.8	W. Siberia
	1018	85956	70.84	53.69			1400	6.7	N.Z.
	1021	115957	73.35	55.08			700	6.6	N.Z.
	1029	44658	49.98	78.97			90	5.8	
	1213	45657	49.80	78.20			10	5.1	
	1225	51657	50.04	78.90			90	5.7	
1976	0115	44658	49.87	78.25			14	5.2	
	0421	50257	49.93	78.82			20	5.3	
	0704	25658	49.91	78.95			90	5.8	
	0723	23258	48.79	78.05			10	5.1	

REFERENCES

Aki, K. (1969), Analysis of the seismic coda of local earthquakes as scattered waves, J. Geophys. Res., 74, 615-631.

Aki, K. and B. Chouet (1975), Origin of coda waves: source, attenuation and scattering effects, J. Geophys. Res., 80, 3322-3342.

Aki, K., and P.G. Richards (1980), Quantitative Seismology-Theory and Methods, W.H. Freeman and Co., San Francisco, 932 p.

Antonova, L.V., F.F. Aptikayev, R.I. Kurochkina, I.L. Nersesov, A.V. Sitnikov, F.S. Tregub, L.D. Fedorskaya and V.I. Khalturin (1978), Experimental seismic investigations of the Earth's interior, Inst. of Phys. of the Earth, Nauka, Moscow, 155 p.

Baker, R.G. (1970), Determining magnitude from Lg, Bull. Seism. Soc. Am., 60, 1907-1920.

Barley, B.J. (1979), On the use of seismometer arrays to locate sources of higher mode Rayleigh waves, AWRE Report No. 0 54178.

Basham, P.W. (1971), A new magnitude formula for short-period continental Rayleigh waves, Geophys. J. Roy. Astr. Soc., 23, 255-260.

Båth, M. (1954), The elastic waves Lg and Rg along Euroasiatic paths, Arkiv. Geofys., 2, 295-324.

Båth, M. (1956), Some consequences of the existence of low velocity layers, Ann. Geofis., 9, 411-450.

Båth, M. (1958), Channel waves, J. Geophys. Res., 63, 583-587.

Bollinger, G.A. (1979), Attenuation of the Lg phase and the determination of m_b in the southeastern United States, Bull. Seism. Soc. Am., 69, 45-63.

Bolt, B.A. (1957), Velocity of the seismic waves Lg and Rg across Australia, Nature, 180, 495.

Bolt, B.A. (1976), Nuclear explosions and earthquakes - the parted veil, W.H. Freeman and Co., San Francisco, 309 p.

Bolt, B.A., H.A. Doyle, and D.F. Sutton (1958), Seismic observations from the 1956 atomic explosions in Australia, Geophys. J.R. astr. Soc., 1, 135-145.

Brune, J. and J. Dorman (1963), Seismic waves and earth structure in the Canadian Shield, Bull. Seism. Soc. Am., 53, 167-210.

Brune, J., A. Espinosa, and J. Oliver (1963), Relative excitation of surface waves by earthquakes and underground explosions in California and Nevada, J. Geophys. Res., 68, 3501-3513.

Cheng, C.C. and B.J. Mitchell (1980), Crustal Q. structure in the United States from multi-mode surface waves, Semi-Annual Technical Report No. 3, Saint Louis University, St. Louis, Missouri.

Chinn, D.S., B.L. Isacks, and M. Barazangi (1980), High-frequency seismic wave propagation in western South America along the continental margin, in the Nazca Plate, and across the Altiplano, Preprint.

Chouet, B., K. Aki, and M. Tsujiura (1978), Regional variation of the scaling law of earthquake source spectra, Bull. Seism. Soc. Am., 68, 49-79.

Dahlman, O. and H. Israelson (1977), Monitoring underground nuclear explosions, Elsevier Scientific Publishing Co., Amsterdam, 440 p.

Dziewonski, A.M., S. Bloch, and M. Landisman (1969), A technique for the analysis of transient seismic signals, Bull. Seism. Soc. Am., 59, 427-444.

Ericsson, U. (1971), Seismometric estimates of underground nuclear explosion yields, National Defense Research Institute, Stockholm, Report C, 4464-26.

Evernden, J.F. and J. Filson (1971), Regional dependence of surface-wave versus body-wave magnitudes, J. Geophys. Res., 76, 3303-3308.

Gane, P.G., A.R. Atkins, J.P.F. Sellschop, and P. Seligmann (1956), Crustal structure in the Transvall, Bull. Seism. Soc. Am., 46, 293-316.

Gumper, F. and P.W. Pomeroy (1970), Seismic wave velocities and earth structure on the African continent, Bull. Seism. Soc. Am., 60, 651-668.

Gupta, I.N., B.W. Barker, J.A. Burnetti, and Z.A. Der (1980), A study of regional phases from earthquakes and explosions in western Russia, Bull. Seism. Soc. Am., 70, 851-872.

Gutenberg, B. (1955), Channel waves in the Earth's crust, Geophys., 20, 283-294.

Haskell, N.A. (1966), The leakage attenuation of continental crustal P waves, J. Geophys. Res., 71, 3955-3967.

Herrin, E. and P.D. Minton (1960), The Velocity of Lg in the Southwestern United States and Mexico, Bull. Seism. Soc. Am., 50, 35-44.

Herrin, E. and J. Richmond (1960), On the Propagation of the Lg Phase, Bull. Seism. Soc. Am., 50, 197-210.

Herrin E. (1961), On $\bar{P}$ and Lg, J. Geophys. Res., 66, 334-335.

Herrmann, R.B. (1974), Surface wave generation by central United States earthquakes, Ph.D. dissertation, Saint Louis University.

Herrmann, R.B. (1980), Q estimates using the coda of local earthquakes, Bull. Seism. Soc. Am., 70, 447-468.

Herrmann, R.B. and O.W. Nuttli (1975), Ground-motion modelling at regional distances from earthquakes in a continental interior, I. Theory and observations, Earthq. Engin. and struc. dyn., 4, 49-58.

Hodgson, J.H. (1953a), A seismic survey in the Canadian Shield I: Refraction studies based on rock-bursts at Kirtland Lake, Ontario, Pub. Dominian Observatory, Ottawa, 16, 113-163.

Hodgson, J.H. (1953b), A seismic survey in the Canadian Shield II: Refraction studies based on timed blasts, Pub. Dominian Observatory, Ottawa, 16, 167-181.

Horner, R.B., A.E. Stevens, and H.S. Hasegawa (1973), The Bengough, Saskatchewan earthquake of July 26, 1972, Can. J. Earth Sci., 10, 1805-1821.

Isacks, B.L. and C. Stephens (1978), Conversion of Sn to Lg at a continental margin, Bull. Seism. Soc. Am., 65, 234-244.

Jeffreys, H. (1952), The times of P up to 30°, Mon. Notices of the R. astr. Soc., Geophys. Suppl., 6, 348-364.

Jeffreys, H. (1976), The Earth, Its Origin, History and Physical Constitution, Cambridge University Press, Cambridge, 6th Edition, 547 p.

Kadinsky-Cade, K. (1980), Short-period seismic wave propagation in the Middle East, Annual Technical Report No. 1, Cornell University, Ithaca, New York.

Knopoff, L., F. Schwab, and E. Kausel (1973), Interpretation of Lg, Geophys. J. R. astr. Soc., 33, 389-404.

Knopoff, L., F. Schwab, K. Nakanishi, and F. Chang (1974), Evaluation of Lg as discriminant among different continental crustal structures, Geophys. J. R. astr. Co., 39, 41-70.

Knopoff, L., R.G. Mitchel, E.G. Kausel, and F. Schwab (1979), A Search for the Oceanic Lg Phase, Geophys. J. R. astr. Soc., 56, 211-218.

Kovach, R.L. and D.L. Anderson (1964), Higher mode surface waves and their bearing on the structure of the Earth's mantle, Bull. Seism. Soc. Am., 54, 161-182.

Lehmann, I. (1953), On the short-period surface wave 'Lg' and crustal structure, Bul. d'Information, U.G.G.I., 2, 248-251.

McEvilly, T.V. (1964), Central U.S. crust - upper mantle structure from Love and Rayleigh wave phase velocity inversion, Bull. Seism. Soc. Am., 54, 1997-2015.

Mitchell, B.J. (1973a), Radiation and attenuation of Rayleigh waves from the southeastern Missouri earthquake of October 21, 1965, J. Geophys. Res., 78, 886-899.

Mohorovicic, A. (1914), Das Beben vom 8 X 1909, Gerlands Beitrage zur Geophysik, 13, 217-240.

Nersesov, I.L. and T.G. Rautian (1964), Kinematics and dynamics of seismic waves to distances of 3500 km from the epicenter, Akad. Nauk SSSR, Trudy Inst. Fiziki Zemli, 32, 63-87.

Nurmagambetov, A. (1974), Attenuation of seismic waves and energy classification of earthquakes from observations acquired with ChISS seismographic systems, Magnitude and Energy Classification of Earthquakes, Vol. 2, Moscow, 1974, 164-173.

Nuttli, O.W. (1973), Seismic wave attenuation and magnitude relations for eastern North America, J. Geophys. Res., 78, 876-

Nuttli, O.W. (1978), A time-domain study of the attenuation of 10-Hz waves in the New Madrid seismic zone, Bull. Seism. Soc. Am., 68, 343-355.

Nuttli, O.W. (1980a), The excitation and attenuation of seismic crustal phases in Iran, Bull. Seism. Soc. Am., 70, 469-485.

Nuttli, O.W. (1980b), On the attenuation of Lg waves in western and central Asia and their use as a discriminant between earthquakes and explosions, Semi-Annual Technical Report No. 3, Saint Louis University, St. Louis, Missouri.

Oliver, J.E., M. Ewing and F. Press (1955), Crustal structures of the Arctic regions from Lg phase, Geol. Soc. Am., 66, 1063-1074.

Oliver, J. and M. Ewing (1957), Higher modes of continental Rayleigh waves, Bull. Seism. Soc. Am., 47, 187-204.

Oliver, J. and M. Ewing (1958), Normal modes of continental surface waves, Bull. Seism. Soc. Am., 48, 33-49.

Panza, G.F., F.A. Schwab, and L. Knopoff (1972), Channel and crustal Rayleigh waves, Geophys. J. R. astr. Soc., 30, 273-280.

Panza, G.F., G. Calcagnile (1975), Lg, Li and Rg from Rayleigh modes, Geophys. J. Roy. astr. Soc., 40, 475.

Piwinskii, A.J. and D.L. Springer (1978), Propagation of Lg waves across eastern Europe and Asia, Lawrence-Livermore Laboratory, U. California.

Pomeroy, P.W. and T. Nowak (1978), An investigation of seismic wave propagation in western USSR, Semi-Annual Technical Report No. 2, Rondout Associates, Inc., Stone Ridge, New York.

Pomeroy, P.W. (1979), Regional seismic wave propagation, Semi-Annual Technical Report No. 3, Rondout Associates, Inc., Stone Ridge, New York.

Pomeroy, P.W. (1980), Regional seismic wave propagation, Semi-Annual Technical Report No. 4, Rondout Associates, Inc., Stone Ridge, New York.

Press, F. (1956), Velocity of Lg waves in California, Trans. Am. Geophys. Union, 37, 615-618.

Press, F. (1964), Seismic wave attenuation in the crust, J. Geophys. Res., 69, 4417-4418.

Press, F. and M. Ewing (1952), Two slow surface waves across North America, Bull. Seism. Soc. Am., 42, 219-228.

Rautian, T.G. and V.I. Khalturin (1978), The use of the coda for determination of the earthquake source mechanism, Bull. Seism. Soc. Am., 68, 923-948.

Richter, C.F. (1958), Elementary Seismology, W.H. Freeman and Co., San Francisco, 768 p.

Romney, C., B.G. Brooks, R.H. Mansfield, D.S. Carder, J.N. Jordan, and D.W. Gordan (1962), Travel times and amplitudes of principal body phases recorded from GNOME, Bull. Seism. Soc. Am., 52, 1057-1074.

Ruzaikin, A.I., I.L. Nersesov, V.I. Khalturin, and P. Molnar (1977), Propagation of Lg and lateral variations in crustal structures in Asia, J. Geophys. Res., 82, 307-316.

Shishkevish, C. (1979), Propagation of Lg seismic waves in the Soviet Union, Rand Note, Santa Monica, California.

Singh, S. and R.B. Herrmann (1979), Q. Regionalization of western United States, Earthquake Notes, 50, No. 4, 27.

Springer, D.L. and R.L. Kinnaman (1971), Seismic source summary for U.S. underground nuclear explosions, 1961-1970, Bull. Seism. Soc. Am., 61, 1073-1098.

Springer, D.L. and R.L. Kinnaman (1975), Seismic-source summary for U.S. underground nuclear explosions, 1971-1973, Bull. Seism. Soc. Am., 65, 343-349.

Springer, D.L. and O.W. Nuttli (1980), Some characteristics of short-period seismic waves in southern Soviet Union, Semi-Annual Technical Report No. 3, Saint Louis University, St. Louis, Missouri.

Stauder, W. and G. Bollinger (1963), Pn velocity and other seismic studies from the data of recent southeast Missouri earthquakes, Bull. Seism. Soc. Am., 53, 661-679.

Street, R.L. (1976), Scaling Northeastern United States/Southeastern Canadian Earthquakes by their Lg Waves, Bull. Seism. Soc. Am., 66, 1525.

Street, R.L., R.B. Herrmann and O.W. Nuttli (1975), Spectral characteristics of the Lg wave generated by central United States earthquakes, Geophys. J. Roy. astr. Soc., 41, 51-64.

Sutton, G.H., W. Mitronovas, and P.W. Pomeroy (1967), Short-period seismic energy radiation patterns from underground nuclear explosions and small-magnitude earthquakes, Bull. Seism. Soc. Am., 57, 249-267.

Tsai, Y.B. and K. Aki (1969), Simultaneous determination of the seismic moment and attenuation of seismic surface waves, Bull. Seism. Soc. Am., 59, 275-287.

Vanek, J., A. Zatopek, V. Karnik, N.V. Kondorskaya, Y.V. Riznichenko, E.F. Savarensky, S.L. Solov'ev, and N.V. Shebalin (1962), Standardization of magnitude scales, Izo. Acad. Sci. USSR Phys. Solid Earth, 2, 108-111.

END 3-81